STUDIES ON MARINE NATURAL PRODUCTS

A thesis submitted

under the requirements

for the Degree of

Doctor of Philosophy in Chemistry

in the

University of Canterbury

by

David J. Stirling

University of Canterbury
Christchurch
New Zealand
1996

CONTENTS

ABSTRACT

An investigation of the marine sponge *Halisarca* sp. was carried out following the discovery of strong activities in antiviral and P388 murine leukaemia assays of an extract from this sponge. A polyether type of compound is suspected as the cause of this activity. The investigation of *Halisarca* sp. made a significant contribution to the development of a chemical screening process.

The absolute configuration of pateamine has been elucidated by a combination of degradative and synthetic chemistry utilising formation of diastereoisomers with Mosher's acid. Several other derivatives of pateamine are reported.

The algal metabolite thyrsiferol has been isolated from the digestive gland of the marine mollusc *Aplysia parvula*. The egg masses of *A. parvula* have also been examined.

The NMR characterisation of the thyrsiferol has been extended through the extensive use of one- and two- dimensional spectroscopic experiments.

I would like to thank my supervisors, Dr. Murray H. G. Munro and Dr. John W. Blunt, for the time, enthusiasm and patience they have directed towards my research efforts.

The assistance of the technical staff at the Department of Chemistry and the staff and students at the Edward Percival Field Station is gratefully acknowledged. Special thanks must go to Gill Barns for performing the antiviral, antimicrobial and P388 murine leukaemia assays and to Bruce Clark for mass spectrometric analysis. I would also like to thank Lewis Pannell (NIDDK, NIH, USA) for additional mass spectrometric analysis, Mike Page and Ron Thow for sponge collection and identification.

I would like to express my gratitude to my co-workers in the laboratory for their advice and continual amusement over the years, especially Drs Peter Northcote, Nigel Perry, Laurent Ettouati, Marc Litaudon, and Eric Dumdei and also to Patrick Fell, Julie Rae, Joanne Hart, Michael Stewart, Jackie Wood, Gill Nicholas, Rachel Lill, Li Shangxiao, Sarah Hickford, Kevin Mitchell, Shane Blincoe and the many honours' students that have passed through the lab.

I would also like to thank my parents and family for their support and encouragement, even though they still wonder what I really do.

Chapter 1

Introduction

1.1 Natural Products as Potential Drug Sources

As the human population has developed and expanded, the demands for food, space and good health have increased. The increasing importance of treating new or sedentary diseases has outstripped the capabilities of empirical ethnobotanical knowledge, traditionally derived from terrestrial flora and fauna, to provide new treatments and cures for diseases that were not critical to those cultures developing natural remedies. The increasing demand for good health has also led to the problem of supply for existing herbal or naturally based remedies. This is compounded by the destruction of habitat and loss of cultures capable of disseminating or adding to the present ethnobotanical store of knowledge. The use of crude preparations from plants and animals can have several disadvantages[1] such as climatic, ecological, morphological and geographical variations in the quantities of the active constituent(s). Other drawbacks include the possible co-occurrence of undesirable components with detrimental side effects and the loss of biological activity due to the variability of preparation or storage of the crude material. It is therefore desirable to isolate the individual natural products which give rise to the observed biological activity.

Williams *et al.*[2] define a natural product as "a substance that has no known role in the internal economy of the producing organism" and that the function of natural products is to "...confer any survival advantage on the producing organism due to the structure of the natural product itself." This contrasts with other natural organic products such as sugars, amino acids, and nucleic acids, which are primary metabolites and are both essential and ubiquitous.

The metabolic cost of producing bioactive natural products can be justified by having a protective role in the organism: protection from overgrowth, protection from predation, protection from competition for space, light and nutrients, and protection from infection by micro-organisms. Williams *et al.*[2] point out that natural products are sparse in those organisms possessing an immune system and are common in those lacking an immune system such as plants, fungi, micro-organisms and invertebrate animals. Natural compounds isolated from species that lack an immune system are therefore a rich source of biologically active compounds. The origin of biologically active natural products associated with an organism can be obscure as they may be synthesised *de novo* by the organism itself, or they may be sequestered from a dietary or symbiotic source, or be a product of joint metabolism.

1.1.1 Marine Natural Products

The seas and oceans of the world cover a vast area of the earth and contain a huge diversity of relatively unexplored flora and fauna. It has been estimated that four-fifths of the Earth's animal life live in or on the water.[3] Coupled with the growing accessibility of the marine environment, such as by SCUBA diving, marine organisms now represent a valuable, and largely intact, resource for the discovery of novel bioactive natural products with pharmaceutical potential.

Data from the National Cancer Institute (NCI) in the USA, compiled by Dr. Peter Murphy of the Australian Institute of Marine Sciences (AIMS) in 1992,[4] further illustrates the utility of screening marine natural products as potential

drug sources. Figure 1.1 displays the number of anticancer leads from various sources in the NCI *in vitro* preclinical antitumour drug screen. It can be seen that although, relative to terrestrial sources, a low number of compounds of marine origin have been screened, there is a high proportion of anticancer leads originating from marine animal sources.

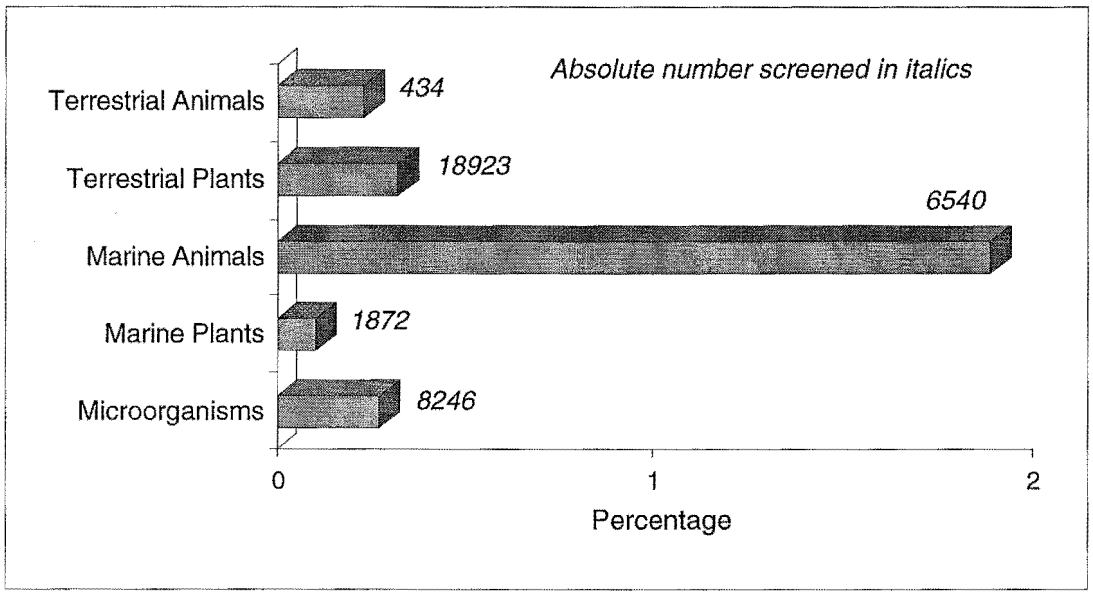

Figure 1.1 Anticancer Leads with Significant Cytotoxic Activity in the NCI Preclinical Antitumour Drug Discovery Screen.[4]

Australian results from AIMS[4] indicate more specifically, that the marine invertebrate phylum Porifera (sponges) provides a rich source of cytotoxic marine natural products, with over 11 % of specimens in this phylum displaying significant cytotoxicity (*viz* IC_{50} <4 μg/mL). The marine world is a very competitive and hostile environment. Therefore it is not surprising that so many marine species have diverted greater amounts of resources to the development of secondary metabolic pathways, as part of their chemical survival strategy, than those species of the terrestrial world.

1.1.2 Sponges[5]

Sponges belong to the phylum Porifera and there are in excess of 5000 living species ranging is size from around 5 mm to as large as 2 metres across. Sponges are sessile animals (although larvae can be crawling or free swimming entities) permanently attaching themselves to hard surfaces, such as rocks or mollusc shells. These are usually found in relatively shallow salt water but they are also found in deep ocean water, or in fresh water lakes and streams. Sponges are hollow filter feeders and extract food particles such as bacteria, algae and dinoflagellates from a flow of water that is pumped through their bodies by flagella. This flow of water enters the sponge through perforations called incurrent pores, the water is strained of food particles and exits the atrium or body cavity through excurrent pores called osculi. Sponge cells face different environments according to their position in the body, some face the external world, some are surrounded by other sponge cells. This difference in position has allowed cell groups to evolve different functions and forms. Sponges are the most primitive animals to show tissue level of organisation. Some cells, the amoebocytes, are responsible for the formation of the supporting structure of the sponge. This supporting structure can be made of material such as a type of collagen that forms a fibrous "skeleton" or calcium carbonate or silica which forms spicules offering rigidity, support and protection. The spicule shapes are used to help classify sponge species into taxonomic groups.

1.1.3 Molluscs[6]

There are about 100 000 living species of Mollusca and members show a wide range of diversity. Molluscs include such varied forms as chitons,

slugs, clams and octopuses and live in such diverse habitats as terrestrial areas, marine or fresh water systems or a combination of both as found in the littoral zone. Chitons and slugs have a radula, a tongue-like strap covered with horny teeth that scrape off small bits of algae and other marine plants living in the littoral zone. Clams lack the radula and tend to be filter feeders that use cilia to flow water over sieve-like gills. Squid and octopuses are the most advanced molluscs and have modified the radula to contain jaws. Their behaviour is also the most advanced with limited learning capability. The molluscan body has several distinctive regions, a muscular foot used for locomotion, a visceral mass containing internal organs such as the heart, digestive system and excretory system, a head housing the sensory organs, brain and mouth, and the mantle cavity that houses the gills. Molluscs have a true circulatory system with a heart, a few closed blood vessels associated with the gills and an open, blood filled cavity which baths internal tissues.

1.2 The Marine Chemistry Group

The Marine Chemistry Group at the University of Canterbury was formed in 1975 with the main objective being to isolate and identify the structures of biologically active compounds derived from marine sources.

Screening of extracts for a particular biological activity, for example antiviral activity, from plant, animal, microbial or fungal sources with a disease-specific biological assay provides an invaluable guide for the separation and isolation of bioactive natural products. In this way important leads in drug

discovery and development can be revealed for the potential treatment of specific diseases.

A wide range of extracts are screened in the Marine Chemistry Group's in-house *in vitro* antimicrobial, antiviral and antitumour assays (see Appendix I). Those organisms producing extracts with a pertinent biological response are re-extracted on a larger scale in a bioassay-directed chromatographic isolation and the active components identified. The P388 antitumour assay is discussed in detail below and examples of bioassay-directed "hits" (*ie* the isolation of biologically active compounds) are described in Section 1.2.2 which serves to highlight the success of the Marine Chemistry Group's approach.

1.2.1 The P388 Antitumour Assay

The *in vitro* "antitumour" assay uses the P388 cell line (murine leukaemia cells) and it is up to a hundred times more sensitive to cytotoxicity effects than the antiviral BSC-1 cell line (see Appendix I). The P388 assay is therefore a cytotoxicity-based assay against a specific leukaemia cell type. The IC_{50} result obtained from this assay represents the concentration of the test compound at which the number of viable cells is reduced by fifty per cent relative to the control.

A two-fold dilution series of the sample of interest is incubated with P388 cells in 96-well microtitre plates. After seventy-two hours of incubation the concentration of the sample required to reduce the number of viable cells by fifty per cent relative to a control (P388 cells, MTT, a positive control such as

mitomycin C, media and solvent) is calculated. This is achieved by adding MTT, a yellow tetrazolium salt to each well and incubating for a further 4 hours. The mitochondria of viable leukaemia cells can reduce the yellow dye MTT to a purple formazan derivative.[7] By measuring the light absorbance at 540 nm in each well, a direct quantification of formazan formation and therefore the number of viable cells is able to be determined. The absorbance is expressed as a percentage cell viability relative to the control, and is plotted against the logarithm of the sample concentration in the well to generate a sample concentration *vs* cell viability curve. The antilogarithm of the concentration producing a fifty per cent reduction in the number of viable cells gives the IC_{50} result, which is usually expressed in units of ng/mL (Figure 1.2). Those samples not intersecting the fifty percent line are either too dilute (always above, compound "g") or too concentrated (always below, compounds "c" and "e") to return an IC_{50} value.

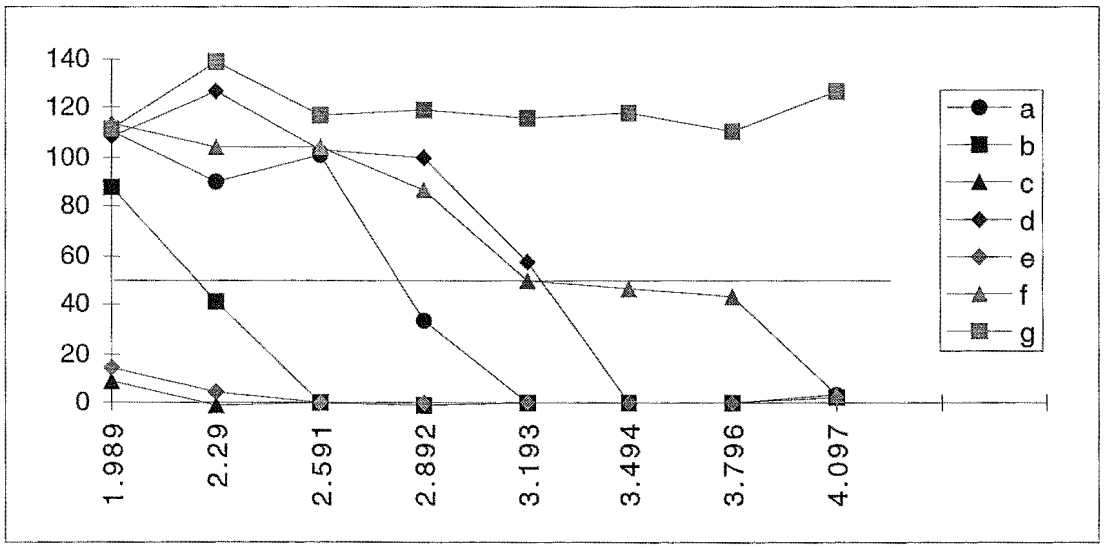

Figure 1.2 A Typical Graph Generated From the P388 Assay

The P388 cell line represents a rapidly dividing cell type, thus its efficacy in finding products with activity in the predominantly occurring slow growing solid tumours of humans such as lung, colon, breast, skin and kidney cancers is strictly limited.[8] However, it is important to note that a P388-active compound may still display a selective activity against these types of tumours.

1.2.2 Bioassay-Directed Isolations

The antiviral and antitumour compounds mycalamide A (**1**) and mycalamide B (**2**) were isolated in a bioassay-directed extraction of a New Zealand species of *Mycale* found in the Otago Harbour.[9, 10]

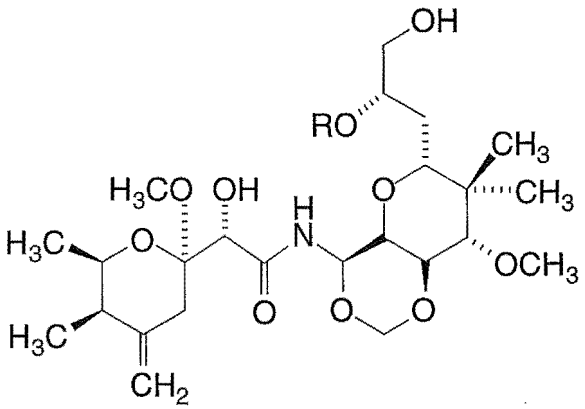

R=H mycalamide A (**1**)
R=CH_3 mycalamide B (**2**)

The mycalamides later proved to be too cytotoxic to be effective as antiviral agents but at present they represent important anticancer leads and synthesis of analogues is currently being undertaken.

Pateamine (**3**) was isolated from a *Mycale* species of marine sponge from Fiordland and is of potential importance as an immunosuppressant agent.[11] The planar structure of pateamine (**3**) was resolved in 1990,[12] but the stereochemistry of the four stereocentres was not elucidated.

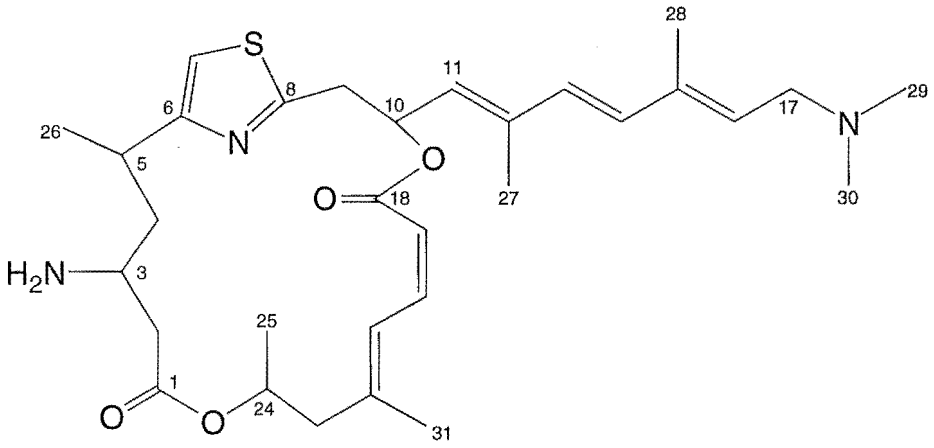

pateamine (**3**)

Attempts to synthesise pateamine (**3**) are currently in progress and the elucidation of the stereochemistry, to enable the synthesis of the correct stereoisomer, is discussed later in this thesis.

A bioassay-directed extraction of the New Zealand sponge *Latrunculia* sp. led to the isolation of the structurally related iminoquinones, discorhabdins A (**4**), B (**5**) and C (**6**) as the major cytotoxic components.[13, 14] These displayed strong antiviral activity *in vitro*; high activity in the *in vitro* P388 assay and selected antimicrobial activity. Discorhabdin C (**6**), like the mycalamides, currently represents an important anticancer lead.

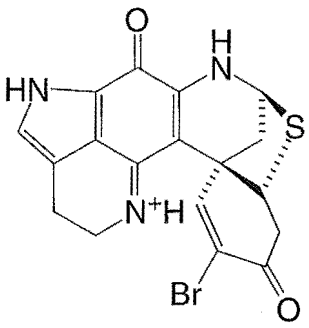

discorhabdin A (**4**)

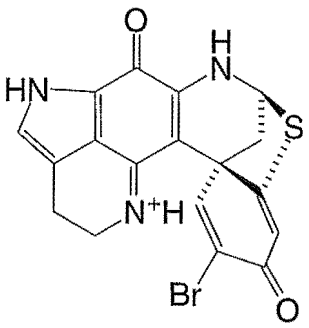

discorhabdin B (**5**)

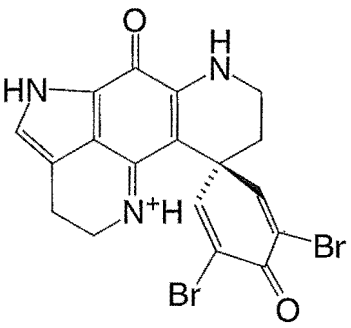

discorhabdin C (**6**)

Bioassay-directed isolation of the active constituents from a sample of the deep-water Kaikoura sponge, *Lissodendoryx* sp., yielded several novel members of the halichondrin series of antitumour compounds and relatively "large" amounts of two known halichondrins. The halichondrins were first reported in 1985 by Uemura *et al.*[15] followed by a related paper in 1986 by Hirata and Uemura.[16] Eight halichondrins were isolated and identified, the most active being halichondrin B (**7**) with an IC_{50} of 0.093 ng/mL. Other members of the halichondrin series, *viz.* norhalichondrins, homohalichondrins or isohomohalichondrins, differ in structure beyond the C49 position. The families A, B and C designate the degree of oxygenation at the C12 and C13 positions.

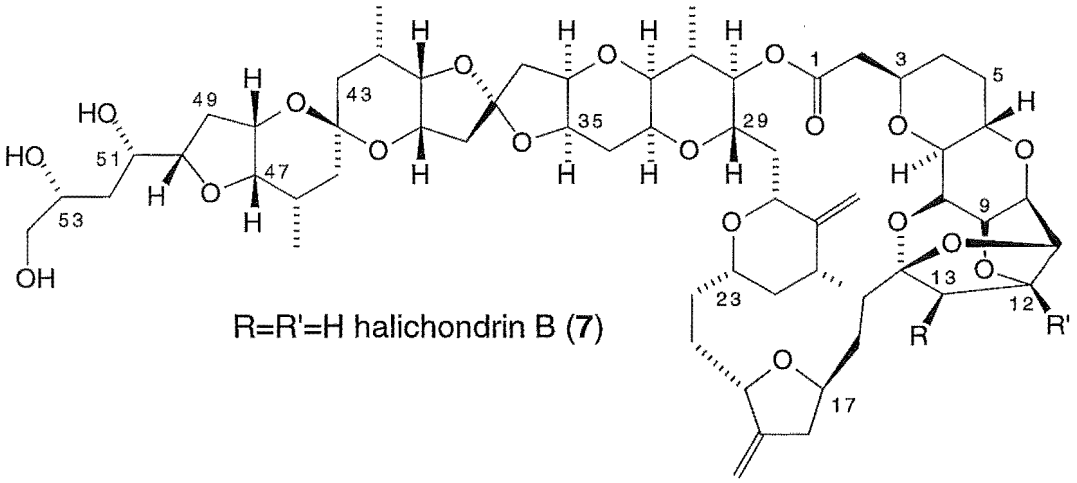

R=R'=H halichondrin B (**7**)

R=R'=H	B series
R=H, R'=OH	C series
R=OH, R'=OH	A series

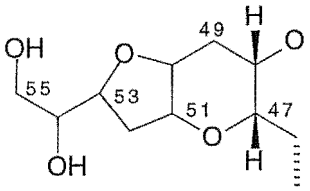

homohalichondrin series

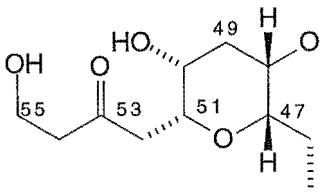

isohomohalichondrin series

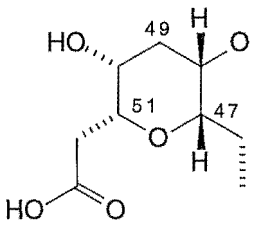

norhalichondrin series

Currently, halichondrin B (**7**) has NCI Decision Network Committee (DNC) "IIA status", awaiting preclinical development and the implementation of an

effective, sensitive method of analysis for halichondrin B (**7**) in body fluids. At the IIA stage in preclinical development, isolation and/or synthesis of the drug is optimised and studies on the feasibility and cost of scale-up are carried out. The DNC allows approximately ten compounds per year past this point. At stage III level, "Investigational New Drug Application" approval is sought, then clinical trials may commence.

1.3 Supply of Marine Natural Products

The bulk supply of a potential anticancer drug is an essential requirement for entry into the clinical trial stage and many of these compounds are isolated in small quantities. There are several options for obtaining large amounts (gram quantities) of a bioactive natural marine product: collection; aquaculture; microbial or tissue culture; genome transfer; or the total synthesis of the compound. Tissue culture and genome transfer are long term options and the viability of a bioactive natural product would have to be well established before these options would be economic. Although the starting points for synthesis typically rely upon inexpensive compounds of known absolute stereochemistry, the synthesis usually includes many reaction steps for any molecule of reasonable size. Multiple reaction steps involving stereospecific reactions lower the yield of the desired enantiomer, making this path a long term option only. Collection, even with its ecological ramifications, or aquaculture remain the options of choice for obtaining significant amounts of bioactive natural marine products.

1.4 The Importance of Absolute Stereochemistry

The pharmaceutical industry has had to address the requirement by regulatory authorities that they must market chiral drugs as pure enantiomers.[17] The majority of marine natural products are isolated as enantiopure compounds due to their specific biosynthesis. However bulk supplies of these potential drugs, which do not rely on biosynthesis, are likely to have different characteristics due to the presence of stereoisomers. Examples of the different pharmacological response of two enantiomers are common: (*S*)-warfarin (**8**) is six times more active as an anticoagulant than the *R* enantiomer, while (*S*)-propranolol (**9**) is an antihypertensive and antiarhythmic used in the treatment of heart disease while the *R* enantiomer acts as a contraceptive.[17]

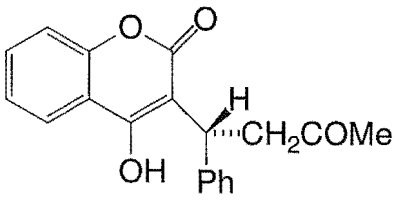

(*S*)-warfarin (**8**)

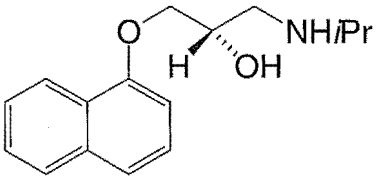

(*S*)-propranolol (**9**)

Only the 2*R*, 3*R* isomer of 2-fluorocitric acid (**10**), a metabolite of the citrate synthase pathway from sodium fluoroacetate (1080) poisoning, is active as a cell poison while the other three stereoisomers (**11**, **12**, **13**) can be successfully metabolised by the cell.[18]

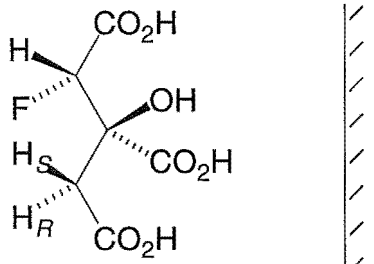

(2*S*, 3*R*)-2-fluorocitric acid (**11**)

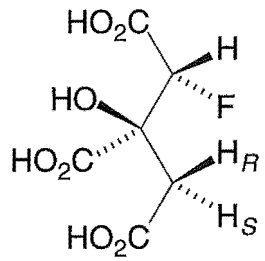

(2*R*, 3*S*)-2-fluorocitric acid (**12**)

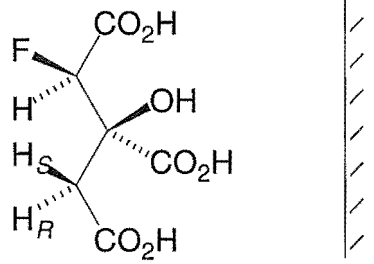

(2*R*, 3*R*)-2-fluorocitric acid (**10**)

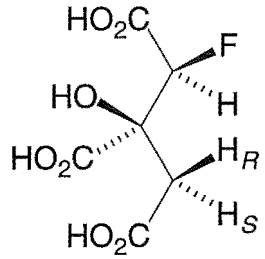

(2*S*, 3*S*)-2-fluorocitric acid (**13**)

Perhaps the most infamous example of an enantiomer causing undesirable side effects is that of thalidomide. (*S*)-thalidomide (**14**) is a powerful tranquilliser while the (*R*) form is a potent teratogen.[19]

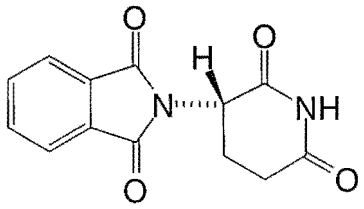

(*S*)-thalidomide (**14**)

It should be realised that, where only one enantiomer is the desired bioactive compound, a racemic mix is in reality two drugs with differing properties.

1.5 Determination of Absolute Stereochemistry

The determination of absolute stereochemistry has become an important aspect of the characterisation of natural products. Elucidating the absolute stereochemistry allows any synthetic effort to target the correct isomer.

The method of choice for the determination of absolute stereochemistry is single crystal X-ray crystallography. This typically provides an unambiguous assignment of the absolute stereochemistry for the molecule. If the R factors for the enantiomers are ambiguous, crystal engineering, where a molecule of known absolute stereochemistry is cocrystallised with the molecule in question, may allow the configuration of the unknown molecule to be assigned. A major drawback for single crystal X-ray crystallography is the requirement for adequate monocrystals. Such monocrystals may be unobtainable.

Gas chromatography (GC),[20] or high performance liquid chromatography (HPLC)[21] methods employing chiral stationary phases, or more rarely chiral solvents, can also be employed with great precision. Compounds of unknown absolute stereochemistry are compared with samples of known absolute stereochemistry or with a series of compounds that are similar in structure with known absolute stereochemistry.

Comparison of optical properties of a compound of unknown stereochemistry with the optical properties of a series of compounds of known absolute stereochemistry is another method for determination of absolute

stereochemistry. The compounds that the unknowns are to be compared with also need to be closely related.

The exciton chirality method is also a reliable method for the determination of absolute stereochemistry. This relies on the chiral interaction between two or more isolated, but spatially close, chromophores which gives rise to Davydov-split Cotton effects.[22]

The GC, HPLC and optical methods that rely on comparison with other compounds are open to interpretation as to the structural similarity of the compounds. The use of optical rotation is also subject to the uncertainty of contamination with an optically active impurity. This is particularly serious when the impurity has a high rotation or a rotation of opposite sign to that of the compound of interest.[17]

1.5.1 NMR Determination of Absolute Stereochemistry

As enantiomers cannot be distinguished in an achiral medium, a chiral auxiliary must be employed to convert the enantiomers into a diastereoisomeric mixture. This leads to NMR chemical shift nonequilvalance ($\Delta\delta$) of groups adjacent to the chiral centre which can then be correlated to give the absolute stereochemistry of the chiral alcohol or amine.[23] There are three types of chiral auxiliary in use. Chiral lanthanide shift reagents and chiral solvating agents form diastereotopic complexes *in situ* with the enantiomers and may be used directly in the NMR tube. Derivatisation of enantiomers with an enatiomerically pure compound is the most widely used technique and there are a number of such agents available

(Table 1.1). This requires the separate formation of discrete diastereoisomers prior to NMR spectroscopic analysis without racemisation or kinetic resolution. The advantage of chiral derivatising agents is that the observed chemical shift nonequilvalance $\Delta\delta$ is typically five times greater than for related complexes with a chiral solvating agent.[17]

Table 1.1 A Selection of the Most Useful Chiral Derivatising Agents for ^{1}H NMR Spectroscopic Analysis

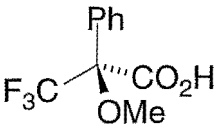

(*S*)-MTPA (**15**)

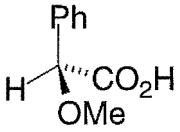

(*S*)-α-methoxy-α-phenylacetic acid (**16**)

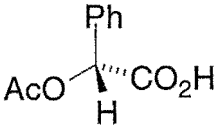

(*R*)-O-acetyl mandelic acid (**17**)

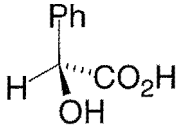

(*S*)-methyl mandelate (**18**)

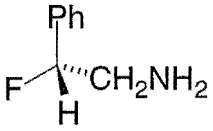

(*R*)-2-fluoro-2-phenylethylamine (**19**)

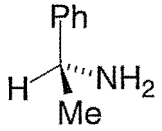

(*S*)-α-phenyl ethylamine (**20**)

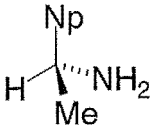

(*S*)-α-naphthyl ethylamine (**21**)

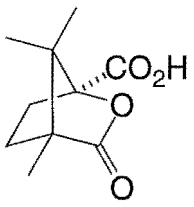

camphanic acid (**22**)

The most widely used chiral derivatising agent is α-methoxy-α-(trifluoromethyl)phenylacetic acid (MTPA) in what is known as the Mosher method.[24] For MTPA esters, the preferred conformation adopted is where

the carbinyl hydrogen, carbonyl oxygen and α-trifluoromethyl group are all eclipsed (Figure 1.3 and Figure 1.4).[17, 24]

Figure 1.3 Conformational Models for (*R*) and (*S*)-MTPA Esters[23]

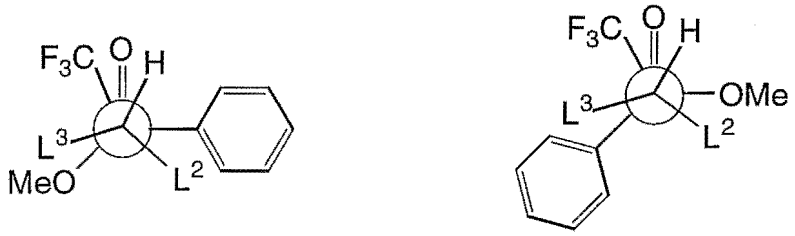

Figure 1.4 Extended Newman Projections of the Conformational Models for (*R*) and (*S*)-MTPA Esters

For (*R*)-MTPA esters and amides, this places one group (L^2 in Figure 1.4) consistently close to the shielding influence of the phenyl ring. This group, (L^2), consequently resonates upfield of the L^2 resonance in the (*S*)-MTPA ester or amide (where the OMe and phenyl ring have exchanged sites) as this shielding is not present in the latter case. The reverse is true for L^3. Careful analysis of the chemical shifts for the same groups β to the chiral centre for the two diastereoisomers, allows assignment of L^2 as having $\Delta\delta_{(R)-(S)}<0$ and L^3 as having $\Delta\delta_{(R)-(S)}>0$. ^{19}F NMR chemical shifts of the MTPA trifluoromethyl group can also be used for the determination of absolute stereochemistry.[25]

The Mosher method relies on few data points, just those of the β position. Ohtani *et al.*[26, 27] have pointed out that the γ, δ, and ε positions may cause a greater steric interaction with the MTPA group and hence display a greater difference in the Δδ chemical shifts. These workers use this observation in a modified Mosher's method that enables the examination of as many protons as can be assigned and, due to the number of data points, may be more reliable.

α-Methoxy-α-phenylacetic acid (MPA) is another chiral derivatising agent assessed by Dale and Mosher[23]. Riguera[28] has suggested that MPA has advantages over MTPA due to the lower number of possible conformers, therefore giving rise to greater time-averaged chemical shift differences.

The conformation proposed by Dale and Mosher[23] for the MPA moiety is one in which the torsional angle between the C_α-OMe and the C=O bonds is *syn*-periplanar but this is only one of the two stable conformers, the other (*anti*-periplanar) being one in which the methoxy group comes close to the ester carbonyl (Figure 1.5).[29]

Figure 1.5 *Syn*-periplanar and *Anti*-periplanar Rotamers for Methoxyphenylacetates

If the *anti*-periplanar conformation has a significant population, the time-averaged $\Delta\delta$ will be reduced, possibly to a point where distinction is no longer observed. Because the energies of the *anti*-periplanar and the *syn*-periplanar rotamers are very close, the equilibrium between them can be significantly altered by temperature effects if required.[30]

The direction of the chemical shift differences between diastereotopic MTPA amides and esters are the same. However the direction of the chemical shift differences between diastereotopic MPA amides are opposite to that observed for esters of similar absolute configuration.[23,31] The conformational preferences of amide and ester functional groups do show clear differences. The COC=O skeletal fragment shows a preference for the *Z* conformation, while the conformational distribution of CNHC=O is more complex, with *Z/E* ratios ranging from 90/10 to 50/50 known (Figure 1.6).[32] The *anti*-periplanar-*Z* conformer is the most populated followed by the *syn*-periplanar-*Z* conformer.

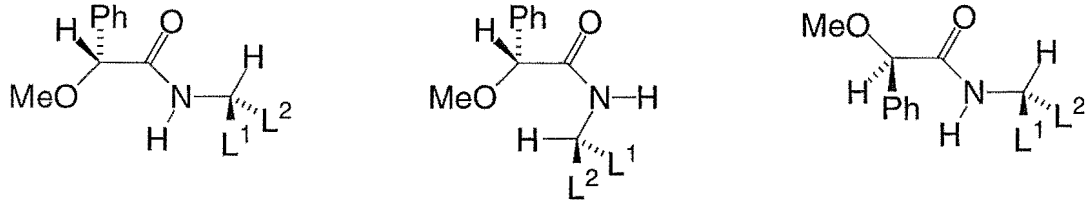

Figure 1.6 Some of the Conformational Models for *Anti*-periplanar-*Z*, *Anti*-periplanar-*E* and *Syn*-periplanar-*Z* (*R*)-MPA Amides[32]

For the (*R*)-MPA amide this places one group (L^2 in Figure 1.7) close to the shielding influence of the phenyl ring which consequently resonates upfield of

L^2 in the corresponding (*S*)-MPA amide due to the shielding influence not being present in the latter case. The reverse is true for L^1.

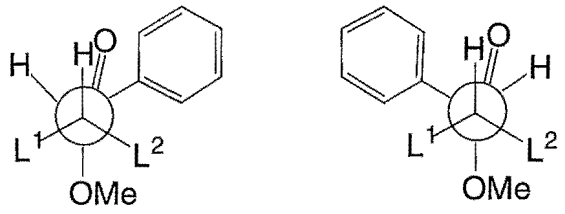

Figure 1.7 Extended Newman Projections of the Conformational Models for (*R*) and (*S*)-MPA Amides[31]

The esters adopt a *syn*-periplanar conformation where the carbinyl hydrogen, carbonyl oxygen and α-methoxy group are all eclipsed (Figure 1.8).[29]

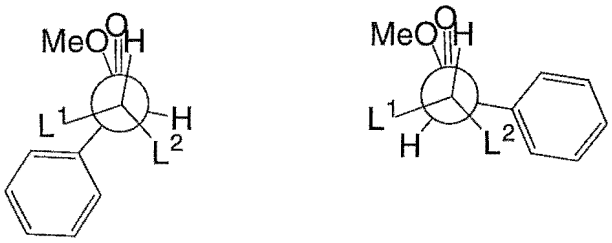

Figure 1.8 Extended Newman Projections of the Conformational Models for (*R*) and (*S*)-MPA Esters[30]

Due to the differing dipole moment of the *syn*-periplanar and *anti*-periplanar rotamers,[31] solvent polarity has a marked effect on the ratio of the two rotamers. The more polar, unwanted conformers are less stabilised in nonpolar solvents, such as $CDCl_3$ and CCl_4, allowing some optimisation of the chemical shift differences for MPA amides.[32]

The change in the conformation between MPA esters and amides may result from an intramolecular hydrogen bond between the amide hydrogen and the methoxy substituent.[31] MTPA is not subject to this directional chemical shift difference due to the electronegative CF_3 group aligning with the carbonyl rather than the methoxy group for MPA.

The validity of the Mosher method has been well established[17] with numerous examples of the use of MTPA esters to demonstrate the stereochemistry of compounds with previously known absolute stereochemistry.[29] The Mosher method however, is not infallible. Sipholenol-A (**23**) is one such case. The MTPA esters of position 4 were prepared but it was found that the positive and negative $\Delta\delta$ values were irregularly placed on the left and right sides of the MTPA plane.[33]

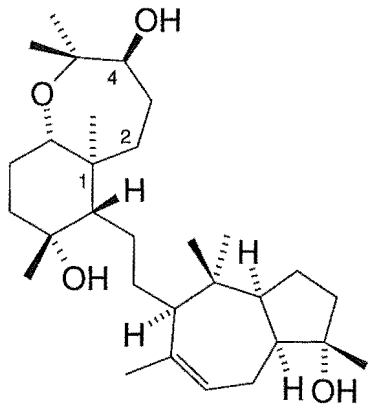

sipholenol-A (**23**)

Steric hindrance around the MTPA moiety, which in this case is in the axial position, forced the conformation of the MTPA group from an ideal orientation. As a result, alternative competing conformations were possible

which reduced the chemical shift differences between the diastereoisomers to a level where a decision was not possible. Steric hindrance, such as cited here, has been claimed to be the cause of such failures.[34]

1.6 Project Aims

The objectives of this project were as follows:

1) The isolation of biologically active natural products from the marine sponge *Halisarca* sp. This sponge displayed activity in the P388 assay at 2322 ng/mL in the chemical screening process of a small (2 g) sample.

2) The determination of the stereochemistry of pateamine.

3) To ascertain if the sea-hare *Aplysia parvula*, a herbivorous shell-less mollusc, sequesters selected metabolites from the red alga *Laurencia thyrsifera*. *A. parvula* is thought to use such compounds, or derivatives, for its own defence against predators higher up in the food chain and also to protect its egg masses.

Chapter 2

Halisarca sp.

2.1 Introduction

Halisarca sp. is a member of the family Halisarcidae. This family is placed in the order Dendroceratida which Bergquist[35] describes as "lack[ing] siliceous spicules and which have a skeleton composed entirely of spongin fibres arranged in a dendritic pattern... In one family the spongin skeleton is lost completely." Halisarcidae is the family characterised by a complete lack of both spongin and mineral skeleton. This lack of a skeleton hinders greatly the classification of members of this family as sponge taxonomic descriptions typically rely on skeletal characteristics. The classification of specimens of *Halisarca* species must rely on ecological, histological and reproductive information.[35]

A search in the marine chemistry literature database, MarinLit,[36] revealed that no compounds had previously been isolated from the *Halisarca* genus. The specimens used in this study were collected from three deep water (80 m) dredging operations in Otago harbour from which 2.54 kg of *Halisarca* sp. was collected. Guided by the strong activity displayed in the initial in-house antiviral and P388 murine leukaemia assays of an extract of a small (2 g) sample (HSV, ?; Hcyt 3+ (10, 4); PV1, ?; Pcyt, 4+, (4); P388, 4230 10^{-6} dil, see Appendix I for an explanation of the assays), an investigation of this sponge was initiated.

2.2 Attempted Isolation of Active Material

2.2.1 1st Extraction

Solvent partitioning of the crude organic extracts from *Halisarca* sp. (1 kg) was undertaken. This concentrated the activity into the non-polar fraction and a small amount of this was used for chemical screening.

2.2.2 Chemical Screening

Chemical screening is the term given to taking a small amount of crude extract and eluting aliquots' of this material off a variety of cartridges to assess the physical, chromatographic and stability properties of an extract on various sorbents.[37] This process enables dereplication of extracts so as to avoid the considerable effort expended in purifying the active component(s) to a stage where spectroscopic properties allow comparison with known compounds. Chemical screening also allows rapid identification of chromatographic methods suitable for the purification of the active component(s) present in the extract. This investigation of the *Halisarca* sp. extract was part of the chemical screening development effort.

An aliquot of the active fraction was dissolved in methanol/water and loaded onto a 500 mg reverse-phase octadecyl (C18) cartridge. Four fractions were collected with the activity eluting in the last two fractions (methanol and 10 % dichloromethane/methanol). Another aliquot of the same active fraction was dissolved in benzene and loaded onto a DIOL cartridge. Not all of the material was soluble but the insoluble material was transferred onto the frit,

enabling subsequent solvents to dissolve material. Five fractions were collected with the activity solely in the final, methanol fraction. Finally another aliquot of the same active fraction was dissolved in methanol and loaded onto a CBA cartridge. Three fractions were collected from a "pH" gradient with the active material eluting in the initial methanol wash.

The chemical screening carried out suggested that the P388 active material was a moderately non-polar, acidic compound and that C18 and DIOL sorbents would be ideal initial chromatographic methods.

The investigation of *Halisarca* sp. made a significant contribution to the initial development of the chemical screening process. This development has continued through the work of others in the Marine Chemistry Group, and a full description of the current chemical screening protocol is included as Appendix II.

2.2.3 Further Chromatography

Solvent partitioning of the crude organic extracts concentrated the activity into the non-polar fraction which analysis by thin layer chromatography revealed contained much sterol material. In an effort to separate the active material from the very non-polar material, C18 reverse-phase column chromatography was employed. This resulted in the shedding of a significant amount of the mass while concentrating the active material into seven fractions (fractions 6 to 12, Figure 2.1).

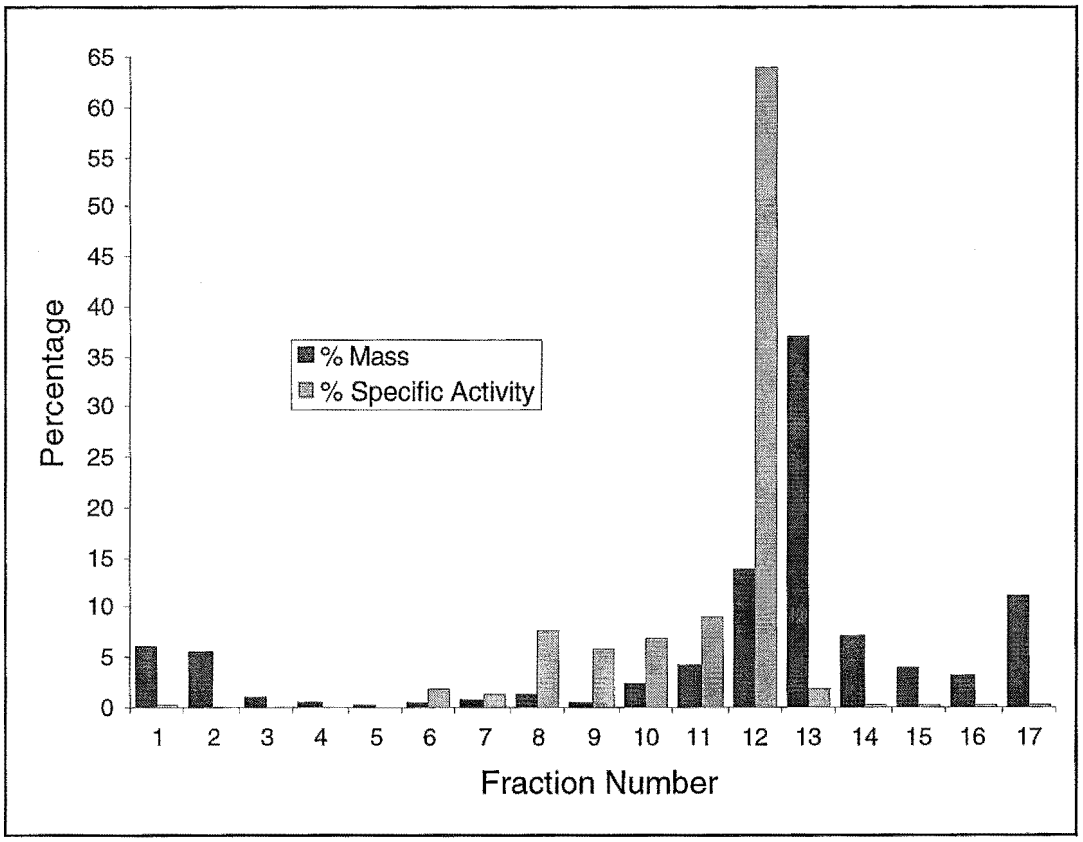

Figure 2.1 % Mass versus % Specific Activity for the C18 Reverse-phase Column of *Halisarca* sp. Active Material (Specific Activity = mass/IC_{50})

Thin layer chromatography using DIOL sorbent showed good separation of some of the components of the active fractions but some streaking was present. Subsequent chromatography on a normal-phase DIOL column further concentrated the active material while most of the mass eluted later off the column (Figure 2.2).

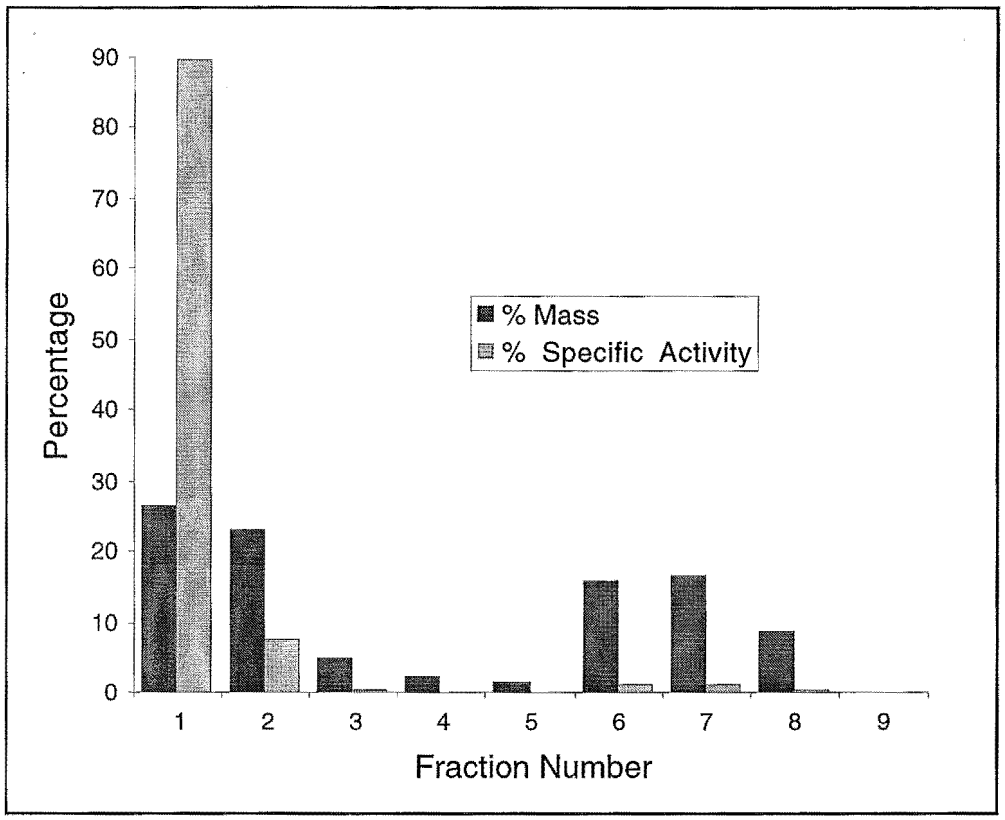

Figure 2.2 % Mass versus % Specific Activity for the DIOL Normal-phase Column of the *Halisarca* sp. Active Material

Thin layer chromatography of the active fractions employing cyano, amino, DIOL and C18 sorbents gave little information as to the identity of the active spot due to streaking on all sorbents tested. The amino plate withheld a yellow spot on the baseline and so a trial column of this sorbent was carried out. The chemical screening on an extract of this sponge had indicated that the active material was acidic in nature so it was assumed that the active material was one of the components sticking to the baseline of the amino plate. Further chemical screening was carried out on the active material with amino cartridges.

2.2.4 Further Chemical Screening

Amino cartridges with different preparation schemes *viz.* cartridge 1, MeOH followed by 0.01 % TFA in MeOH; cartridge 2, MeOH, 2 % NH_4OH/MeOH; cartridge 3, MeOH; cartridge 4, a used column prepared by MeOH followed by 0.01 % TFA in MeOH. These different cartridges were trialed with equal aliquots of the active material loaded and the columns eluted with neutral, basic and acidic solvents in varying order. None of these amino cartridges returned any activity. In most cases a yellow band refused to elute regardless of what solvent was used. Strong anion exchanger (SAX) sorbent was trialed with some success but this sorbent was unable to be scaled up as only 100 mg cartridges were available. Further chemical screening was carried out later with an amino and a CBA cartridge. The amino cartridge was prepared by MeOH followed by 0.1 % TFA in MeOH, then eluted with MeOH, followed by 2 % NH_4OH/MeOH, and 2 % TFA/MeOH. The CBA cartridge was prepared by MeOH followed by 0.1 % TFA in MeOH, then eluted with MeOH, 2 % NH_4OH/MeOH. The amino cartridge returned activity early (F1, MeOH, 1.5 mg, 97.5 ng/mL) and the CBA cartridge returned activity late (F2, 2 % NH_4OH/MeOH, 3.9 mg, 200 ng/mL).

This result was at odds with the previous amino cartridge chemical screening but the higher concentration of TFA in the preparation was thought to have deactivated the amino cartridge sufficiently to allow the active material to pass through. The late elution of the active material off the CBA cartridge was also at odds with the initial chemical screening as this latest result suggested that the active material was basic.

2.2.5 Further Chromatography

Sephadex LH-20 gel permeation is a method of chromatography that can be based on size separation or polarity, depending on the eluent selected. The ability of gel permeation to differentiate the size of molecules is advantageous when active compounds consistently coelute with other compounds with similar polarity by adsorption chromatography.[38] Gel permeation is of particular importance in the isolation of large bioactive compounds as those with a molecular weight of greater than around 500 a.m.u. are typically not retained by the gel and rapidly elute with the solvent front. Compounds that degrade on silica or other sorbents are also candidates for gel permeation and this method typically returns good recovery of mass. Sephadex LH-20 was selected for further chromatography of the active material from *Halisarca* sp. A column of this material was prepared (20 g) with methanol, so as to utilise the size separation properties of LH-20 with a minimum adsorption chromatography, and loaded with the active material (40 mg). Eighty three fractions were collected and the P388 assay results showed that the activity was concentrated in the first 29 fractions. Combination of the 29 active fractions gave 43.4 mg of material. However, the resultant ^{1}H NMR spectrum indicated that the combined fractions contained much plasticiser. Subsequent chromatography of this material on a DIOL column saw a significant loss of activity. Just one fraction (1.5 mg) was active. A second extraction was initiated.

2.2.6 2nd Extraction

One of the problems with the previous extraction was the persistent streaking of some spots on the TLC that obscured other, more resolved spots.

Halisarca sp. is a very slimy sponge and the streaking was thought to be due to this mucus. In an attempt to overcome this, the sponge (740 g) was twice sonicated in water and the resulting solutions drained and freeze dried. The sponge was then extracted with methanol and dichloromethane. All the activity was found in the methanol extract (14 g) with no activity in the water wash or in the dichloromethane extract. Chromatography of the methanol extract on a C18 reverse-phase column yielded five fractions with minimal activity and one fraction (667 mg) with substantial specific activity. Another attempt at size separation using LH-20 gel permeation was undertaken utilising the four fractions containing minor activity without success, none of the 41 fractions returning detectable activity. The fraction with the greatest specific activity from the C18 reverse-phase column was loaded onto a DIOL column and eluted with a stepped gradient from hexane to methanol. Only 8 % of the activity was recovered, all in one fraction which eluted with dichloromethane. The activity recovered off this column eluted much later than on the DIOL column of the previous extract. The active fraction (14 mg) was consumed in attempting to develop an analytical HPLC method using various sorbents for the separation and isolation of individual peaks. At this point the third and final extraction of *Halisarca* sp. was initiated.

2.2.7 3rd Extraction

The sponge (800 g) was sonicated as in the previous extraction. The methanol extract (8.6 g) was partitioned between dichloromethane and water with the activity found in the organic phase. Partitioning between hexane and methanol/water equally divided the activity and mass so the partitions were recombined. Chromatography by C18 was again employed as the

previous extractions had shown this to be an ideal and rapid method to concentrate the activity. DIOL chromatography was used again to shed a large proportion of the mass from the active fractions. At this point in the isolation cyano TLC indicated that this sorbent could be a possible route for further purification of the active component. However, a cyano cartridge was trialed with a large loss of mass and activity.

The use of a preparative HPLC C18 reverse-phase column was employed in an attempt at further purification due to the fact the active material had already come into contact with C18 packing material on numerous occasions with good results and the much larger number of theoretical plates of the HPLC column would give rise to greater resolution of components in the mixture. The column was eluted with acetonitrile/water (55:45, isocratic) with detection at 200 nm. Upon solvent removal the mass of the six fractions collected did not sum to the mass loaded onto the column. Subsequently the column was stripped with stronger solvents but this additional mass still did not explain the missing material. The ^{1}H NMR spectra of the fractions and the strip did not show any of the character of the material that was injected onto the column and it can only be assumed that the octadecyl moiety of the C18 packing material had in some way been damaged or leached so as to expose fresh Si-OH groups to which the active material irreversibly bound or degraded. No further sponge was available for extraction.

The ^{1}H NMR spectrum of the material combined and loaded onto the reverse-phase C18 HPLC column (Figure 2.3) displayed some character however. One of the notable characteristics of this spectrum is the similarity

to the ^{1}H NMR spectrum of polyether type compounds such as okadaic acid (**24**) (Figure 2.4) and halichondrin B (**7**) (Figure 2.5).

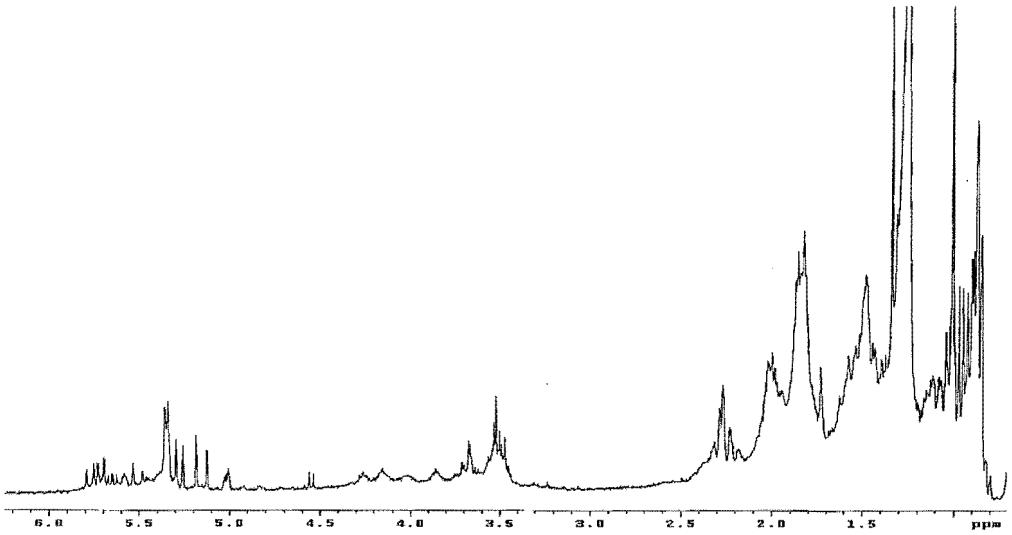

Figure 2.3 ^{1}H NMR Spectrum of Pre-HPLC Fraction

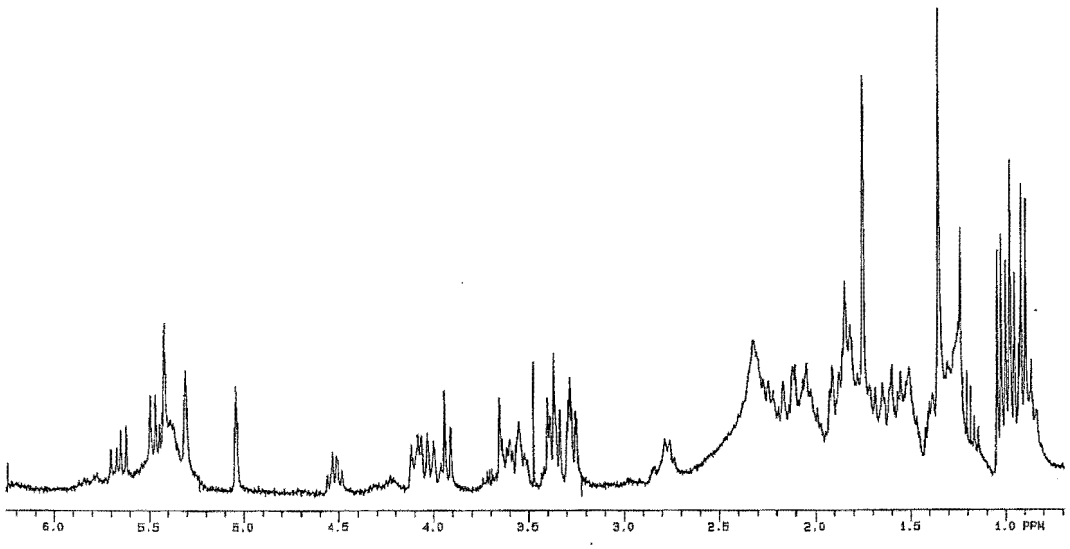

Figure 2.4 ^{1}H NMR Spectrum of Okadaic acid (**24**)

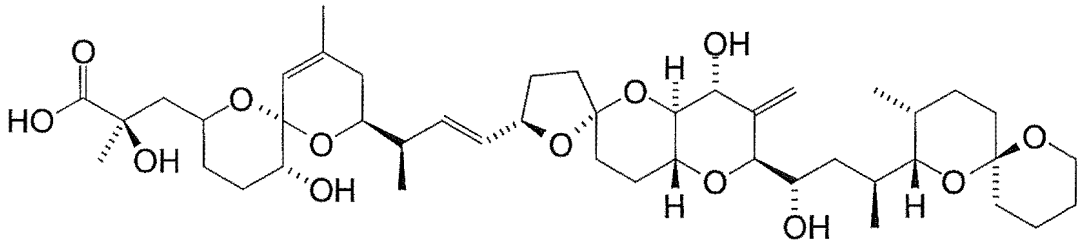

okadaic acid (**24**)

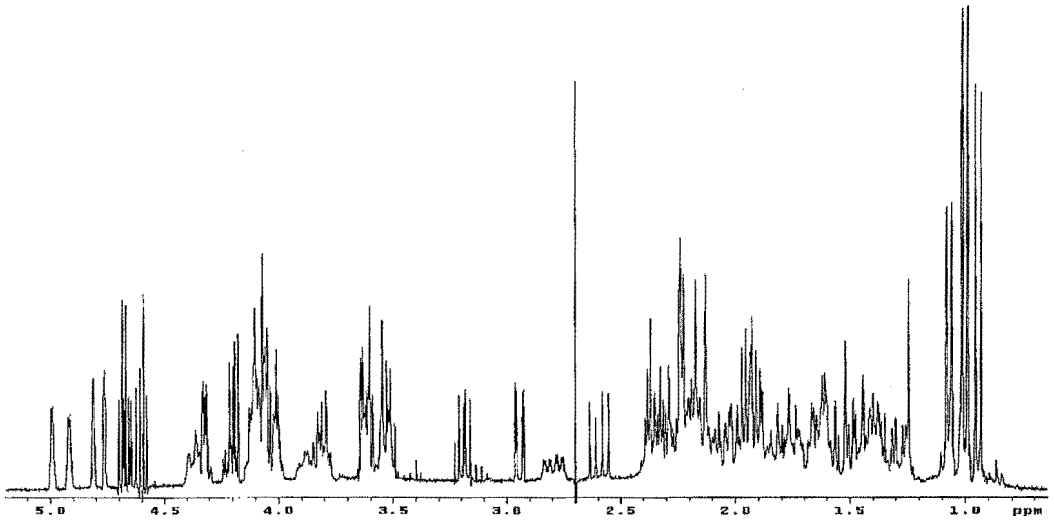

Figure 2.5 ^{1}H NMR Spectrum of Halichondrin B (**7**)

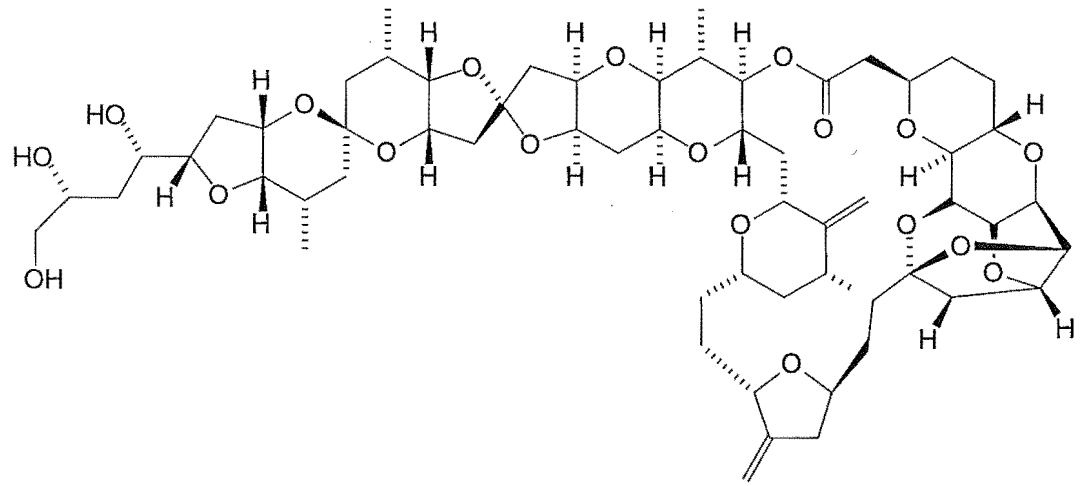

halichondrin B (**7**)

2.3 Conclusion

The ^{1}H NMR spectra of various active fractions from the three extractions did not yield any conclusive evidence on the structure of the compound that was causing the cytotoxicity. The most active fraction, one of those combined for injection onto the C18 preparative HPLC column, was assayed at 17 ng/mL, which when compared to the value pure okadaic acid (**24**) returned in our assay (11 ng/mL[39]), gives an idea of the extreme cytotoxicity of the compound(s) that was present in the samples of *Halisarca* sp. used in this study. The activity of the extract is indeed reminiscent of that recorded for tedanolide (**25**), another polyether cytotoxin.

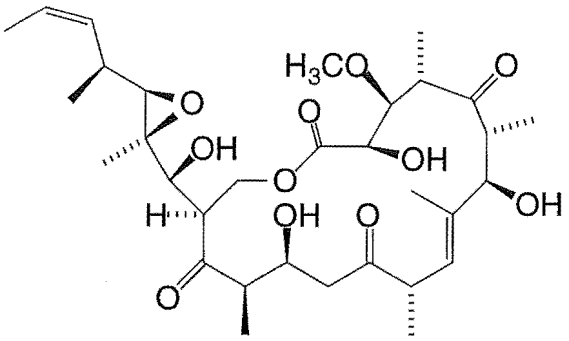

tedanolide (**25**)

Tedanolide (**25**) was first isolated by Schmitz *et al*[40] from *Tedania ignis* and was recorded to have an ED_{50} against lymphocytic leukaemia (P388 assay) of 16 pg/mL. In earlier, unpublished work from this laboratory,[41] Dr. John McCombs expended considerable effort in following the activity of an extract from *Tedania* n. sp. B also from Otago Harbour. In the final analysis some 100 μg of material was obtained from 25 kg of sponge. Virtually all the

activity was concentrated into that fraction, which was still grossly impure. From mass spectral arguments it was concluded that *Tedania* n. sp. B. contained tedanolide (**25**) and a new monochlorinated analogue. More recently Dr. Laurent Ettouati encountered a similar problem working on extracts from a Fiordland sample of *Chondropsis kirkii.* In this case the polyether cytotoxin was most likely okadaic acid (**24**).[42] In each of these cases a large quantity of sponge had to be processed to even start to detect the cytotoxin, let alone isolate the compound pure and determine the structure. The current work on the *Halisarca* sp was limited by the small amount of this deep water sponge that was available. Perhaps if a larger amount of the sponge had been available there may have been a more conclusive result. These three cases serve to emphasis and highlight the problems associated with this aspect of marine natural products chemistry. When the emphasis is on finding potent cytotoxins from a natural source, sometimes the compounds discovered are so toxic that the concentration in the marine species is so minute that vast quantities of source material are needed, accompanied by a prodigious effort to reduce the mass of the extracts to a point that conventional laboratory based approaches can be used to isolate and purify the target compound. The recent isolation of spongistatins 8 (**26**) and 9 (**27**) by the Arizona group of Professor G R Pettit is an excellent example.[43] In this work 2409 kg of *Spirastrella spinispirulifera* was extracted to yield 1.8 mg and 5.4 mg of spongistatin 8 (**26**) and spongistatin 9 (**27**) respectively.

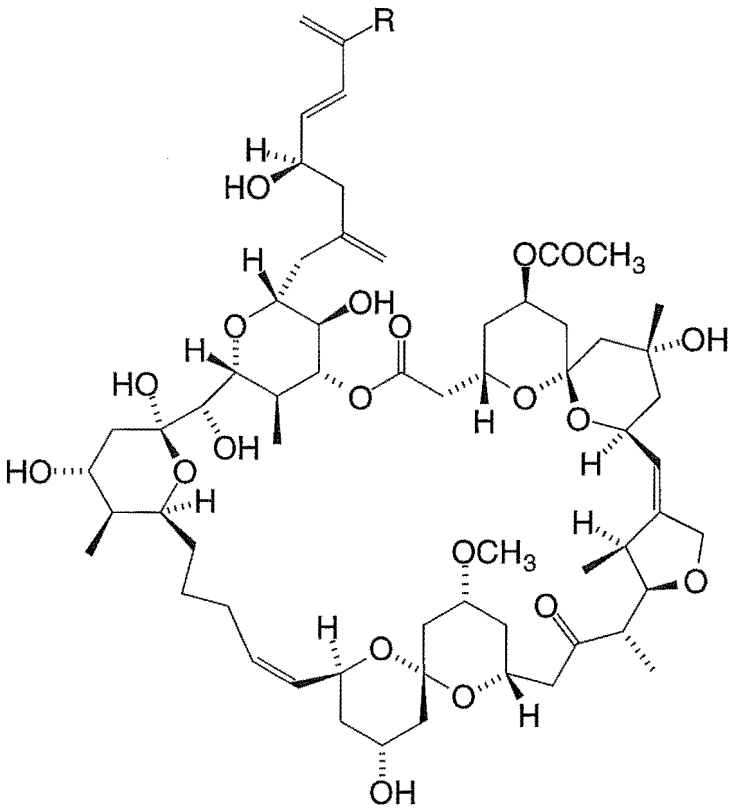

R=H spongistatin 8 (**26**)
R=Cl spongistatin 9 (**27**)

Other examples of large extractions with small amounts of active material isolated can be found in the literature, such as the isolations of the bryostatins,[44] ciguatoxin,[45] the goediastatins,[46] okadaic acid (**24**)[47] and the halichondrins.[48] Many of these examples originate from laboratories equipped to deal with routine extraction of material in excess of 1 tonne, with the expertise to carry out preliminary extraction and isolation work involving large quantities. The maximum batch quantity that our laboratory here at the University of Canterbury can cope with is about 20 kg.

Collection of vast quantities of marine organisms from a localised habitat is fraught with risk. If insufficient data as to the extent of the habitat,

recruitment from other areas, and growth rates is collected, or available, the organism may become extinct, not only locally, but completely, if the entire population inhabits only the one area. This extinction may, in turn, affect specialist organisms that are dependent upon the collected species for food, or as a source of defensive chemicals. In addition to environmental impact considerations, biodiversity issues also need to be considered. This, however, is a moral issue and as such lies beyond the direct scope of this thesis. None-the-less, biodiversity issues increasingly have an impact on marine natural products chemists be it at the national level as governments become involved (eg Manila Convention, Melaka Accord, and the Rio Treaty), or as Editors of journals seek comment on such issues.[18] The accusation of bio-piracy is now a distinct possibility for anyone making large-scale (>1 tonne) collections anywhere in the world without having first examined the environmental issues and obtained the appropriate collection permits from the country concerned.

The work outlined above has provided the basis for further work on the *Halisarca* sp. The method of purification of the active material evolved over the course of the three extractions of *Halisarca* sp. has concentrated the activity from the initial activity of 8103 10^{-6}dil to the low ng/mL level. Once it is possible to obtain significantly more material to work on, with the insights provided by these exploratory approaches, it should be possible to move quite rapidly to obtaining the pure cytotoxic polyether compound present in this sponge. The initial bioactivity results, and what was found subsequently, suggest that this is a potent compound and should be pursued actively by the Marine Chemistry group as the opportunity arises.

Chapter 3

Pateamine

3.1 Introduction

Pateamine (**3**) is an extremely potent cytotoxin isolated from a *Mycale* species of marine sponge from Fiordland. This 19-membered macrocyclic diamino dilactone is of potential importance as an anticancer agent and some biological assay data suggest it might have applications as an immunosuppressant agent.[11] The planar structure of pateamine (**3**) was resolved in 1990,[12] but the stereochemistry of the four stereocentres was not elucidated.

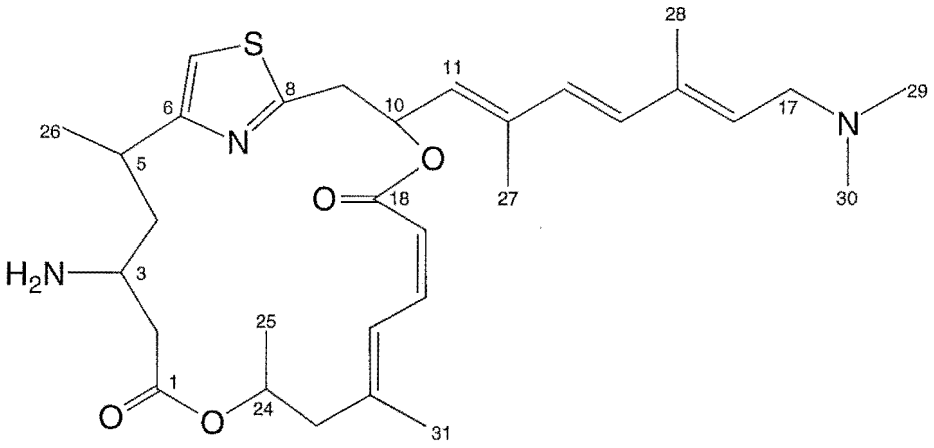

pateamine (**3**)

Although pure samples of pateamine (**3**) have been available and despite numerous attempts to date,[42, 49] crystals or crystalline derivatives have so far been unobtainable. Molecular modelling carried out by Shane Blincoe as part of his M.Sc. thesis[50] showed that the most likely diastereoisomer was 3*S*, 5*R*, 10*S*, 24*R* or its enantiomer. The molecular modelling was carried out with the side chain of pateamine (**3**) substituted by a methyl group. This

reduced the amount of computer time taken to minimise the large number of conformers generated while still retaining chirality at C10.

In this section of work the aim was to elucidate, in a systematic fashion, the chirality at each of the four stereocentres in pateamine (**3**). The approach taken was to create optically active analogues of products by the selective degradation of pateamine (**3**) followed by derivatisation of the fragments with chiral derivatisation agents.

3.2 Strategy

The philosophy was to use chemical methods of sufficient mildness that the chirality at the critical centres was not destroyed or racemised. The approaches considered were primarily targeted at opening the dilactone ring that would release one stereocentre, that at C24, and if the major fragment (C1-C17) survived without elimination this would allow a direct examination of C10. The only stereocentre that was directly accessible in pateamine (**3**) itself was that at C3. It was never envisaged that it would be possible to directly probe the chirality of the C5 stereocentre. The chirality at this centre would have to be ascertained by modelling. In principle, elements of the chirality of pateamine (**3**) could have been obtained from exciton methods. However the lack of information on the relative stereochemistry around the ring would still have required application of Mosher's methodology.

3.3 Stereochemistry at C24

3.3.1 Initial Approaches: 4-Hydroxy-pentan-2-one

Position 24 was the first to be examined. In this first attempt the target was to extract 4-hydroxy-pentan-2-one (**28**) from pateamine (**3**) and compare this directly, by chiral GC methods, with synthetic samples of the chiral and racemic hydroxy ketone. Selective degradation of pateamine (**3**) by a combination of hydrolysis and osmylation would give rise to 4-hydroxy-pentan-2-one (**28**), retaining the original chirality of position 24 (Figure 3.1).

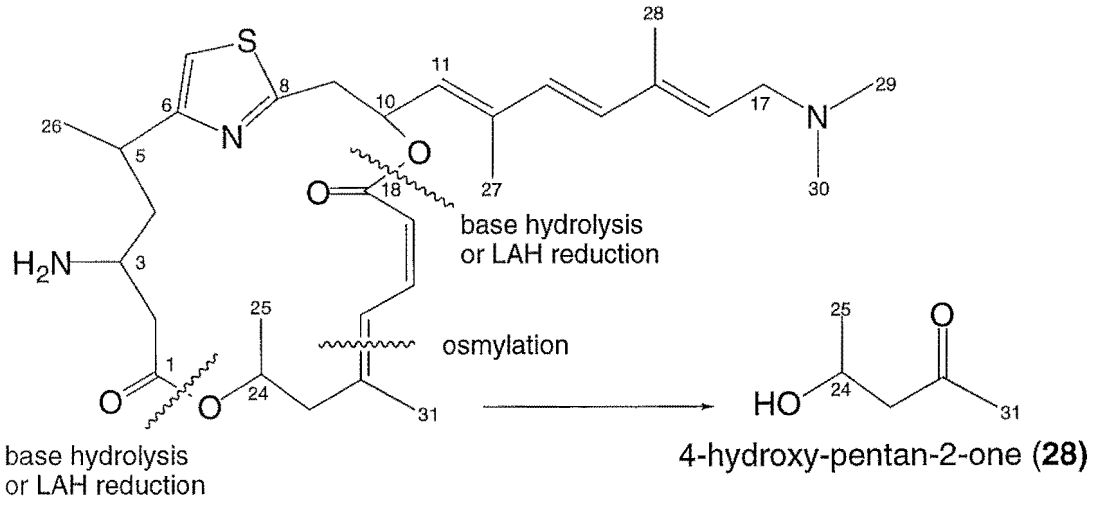

Figure 3.1 Proposed Method for Isolation of 4-Hydroxy-pentan-2-one (**28**)

This fragment was then to be compared with synthetic 4-hydroxy-pentan-2-one (**29**) of known chirality.

3.3.2 Synthesis of 4*S*-Hydroxy-pentan-2-one (**29**)

4*S*-Hydroxy-pentan-2-one (**29**) was prepared by the selective yeast reduction of 2,4-pentandione.[51, 52] As there is no corresponding microbiological method for the production of the (*R*) isomer, racemic 4-hydroxy-pentan-2-one (**30**) was obtained by a crossed aldol condensation (Figure 3.2).[53]

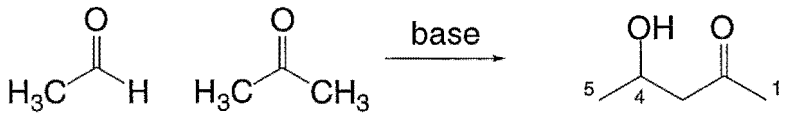

Figure 3.2 Synthesis of Racemic 4-Hydroxy-pentan-2-one (**30**)

3.3.3 ^{1}H NMR Spectroscopic Assignment of 4*S*-Hydroxy-pentan-2-one (**29**)

The assignment of the ^{1}H NMR spectrum (Figure 3.3) of 4*S*-hydroxy-pentan-2-one (**29**) started with the unambiguous assignment for a proton α to an hydroxy group at δ_H 4.22 ppm as H4. Irradiation of H4 collapsed the pair of doublet of doublets at δ_H 2.62 ppm and δ_H 2.52 ppm to a pair of doublets and also collapsed a doublet at δ_H 1.16 ppm. The δ_H 2.62 ppm and δ_H 2.52 ppm resonances were assigned as the diastereotopic H3 protons. Coupling constants allowed these to be assigned as $H3_S$ ($J_{3,4}$=3.4 Hz) and $H3_R$ ($J_{3,4}$=8.5 Hz) respectively. The remaining doublet at δ_H 1.16 ppm was assigned as CH_3-5. This left the singlet at δ_H 2.15 ppm to be assigned as CH_3-1.

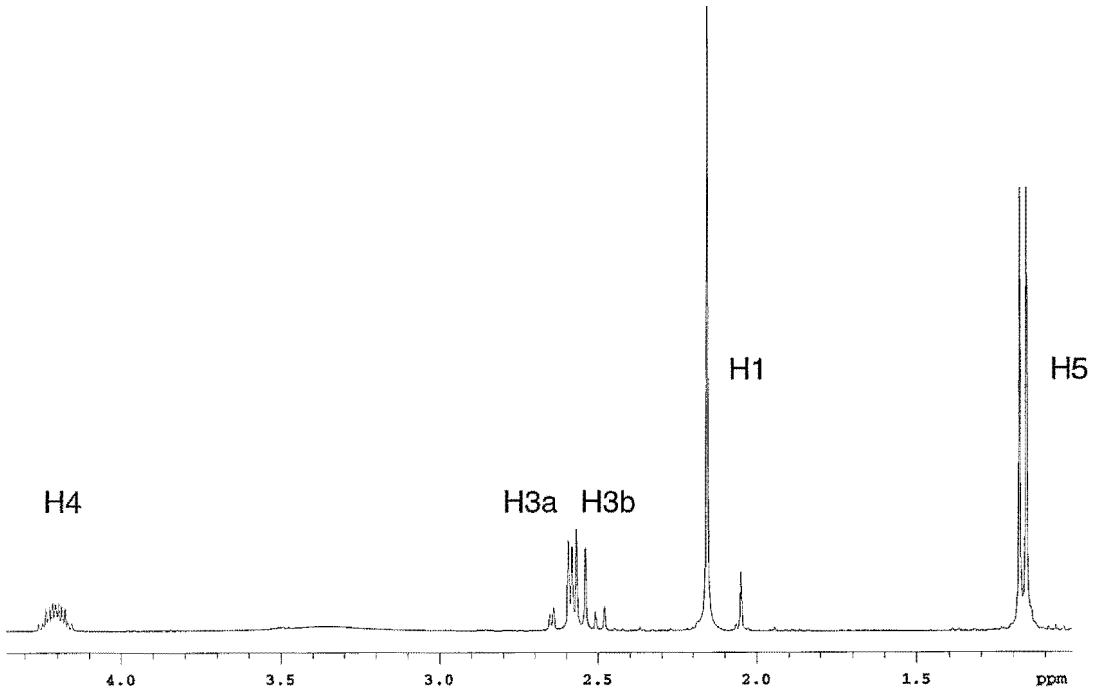

Figure 3.3 ^{1}H NMR Spectrum of 4*S*-Hydroxy-pentan-2-one (**29**)

The stereochemistry of the stereocentre was confirmed by the use of (*R*) and (*S*)-α-methoxy-α-(trifluoromethyl)phenylacetic acid (MTPA) (**31**, **15**).

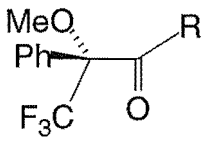

R=OH (*R*)-MTPA (**31**)
R=Cl (*S*)-MTPACl (**32**)

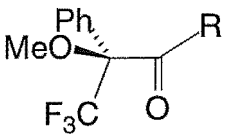

R=OH (*S*)-MTPA (**15**)
R=Cl (*R*)-MTPACl (**33**)

4*S*-Hydroxy-pentan-2-one (**29**) was derivatised with (*S*)-MTPA (**15**) *via* the acid chloride (**33**) to give 4*S*((*S*)-MTPA)-pentan-2-one (**34**).

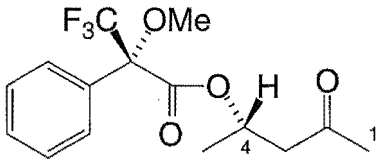

4*S*((*S*)-MTPA)-pentan-2-one (**34**)

The racemic mixture was derivatised with (*R*)-MTPACl (**33**) to give 4*S*((*S*)-MTPA)-pentanonate (**34**) and 4*R*((*S*)-MTPA)-pentan-2-one (**35**).

3.3.4 ^{1}H NMR Spectroscopic Assignment of 4*S*((*S*)-MTPA)-pentan-2-one (**34**)

The ^{1}H NMR spectroscopic assignment of 4*S*((*S*)-MTPA)-pentan-2-one (**34**) began with the unambiguous assignment of the multiplet resonance for a proton α to an ester group at δ_H 5.56 ppm as H4. The singlet at δ_H 3.53 ppm was assigned as the MTPA methyl ester due to the chemical shift value. The complex multiplet signals at δ_H 7.49 and 7.40 ppm were assigned as the phenyl protons of the MTPA moiety. The remainder of the molecule was assigned by comparison to 4*S*-hydroxy-pentan-2-one (**29**).

Comparison of the ^{1}H NMR spectrum of 4*S*((*S*)-MTPA)-pentan-2-one (**34**) (Figure 3.4) with that of the products from the racemic (Figure 3.5) reaction, allowed the ^{1}H NMR spectroscopic assignment of 4*R*((*S*)-MTPA)-pentan-2-one (**35**).

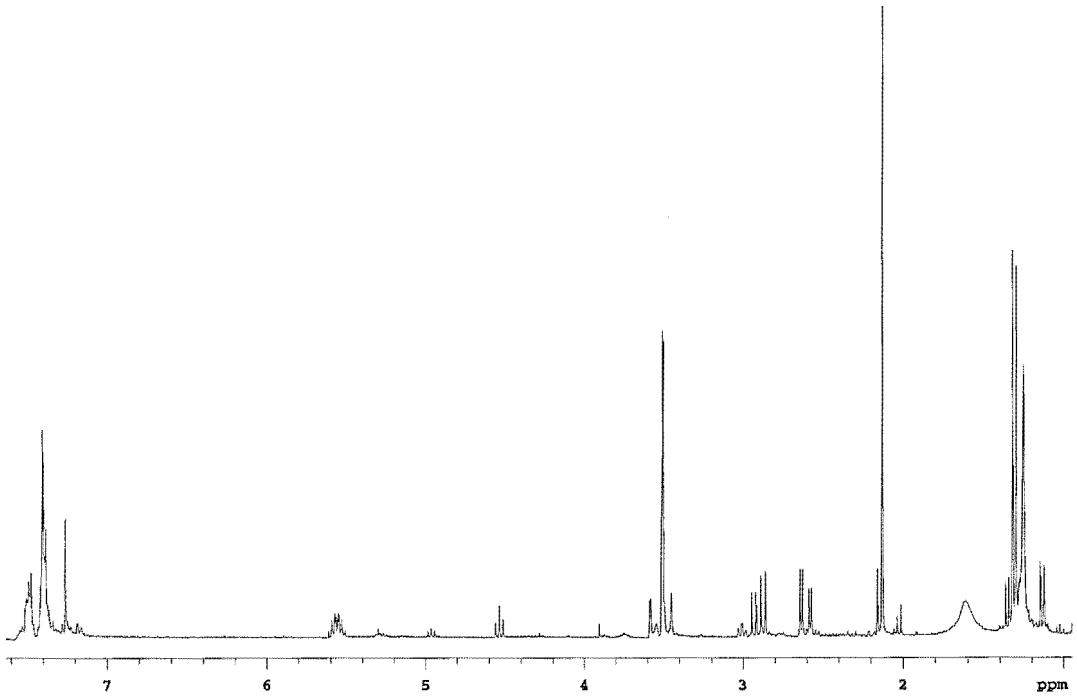

Figure 3.4 ^{1}H NMR Spectrum of
4*S*((*S*)-MTPA)-pentan-2-one (**34**)

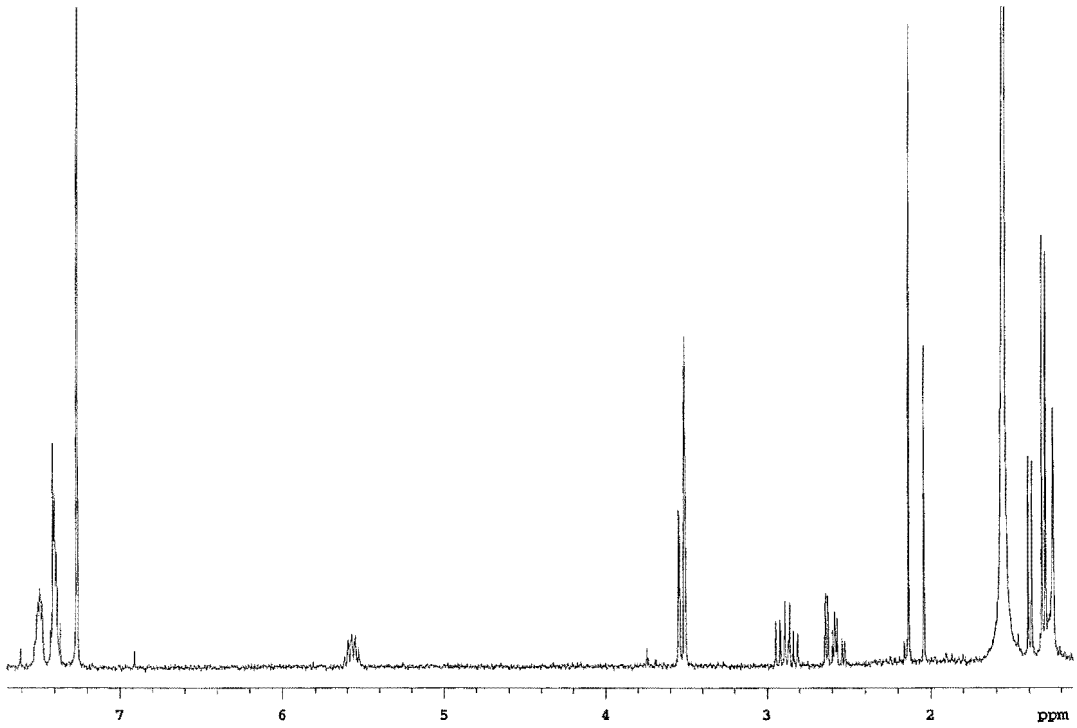

Figure 3.5 ^{1}H NMR Spectrum of
Diastereotopic 4((*S*)-MTPA)-pentan-2-ones (**34**, **36**)

Table 3.1 ^{1}H NMR Spectroscopic Data for (*S*)-MTPA Esters of (*R*) and (*S*) 4-Hydroxy-pentan-2-one (**34**, **36**)

Proton	(*S*,*R*)=(*R*,*S*) δ ppm (*J* in Hz)	(*S*,*S*) δ ppm (*J* in Hz)	(*S*,*R*)-(*S*,*S*) Δδ ppm
CH_3-1	2.04	2.13	-0.09
H3a	2.85 (7.8, 17.1)	2.91 (8.3, 17.1)	-0.06
H3b	2.56 (5.1, 17.1)	2.60 (4.3, 17.1)	-0.04
H4	5.56	5.56	
CH_3-5	1.39(5.9)	1.31 (5.9)	0.08
MTPA OMe	3.55	3.51	
Phenyl	7.40	7.40	
Phenyl	7.49	7.49	

As enantiomers are isochronous in the NMR spectrometer, 4*R*((*S*)-MTPA)-pentan-2-one (**35**) has a ^{1}H NMR spectrum equivalent to that of 4*S*((*R*)-MTPA)-pentan-2-one (**36**) and so the ^{1}H NMR spectrum of the product from the racemic reaction can be treated as having present 4*S*((*S*)-MTPA)-pentan-2-one (**34**) and 4*S*((*R*)-MTPA)-pentan-2-one (**36**) allowing the use of the Mosher method.

From Table 3.1 the (*R*)-(*S*) values show a distinct pattern. All Δδ values listed of (*R*)-(*S*) are negative except for the protons of CH_3-5 which are positive. From Mosher's chemical shift tables[23] for MTPA esters, all positive Δδ values are assigned the designation L^3 and all negative Δδ are assigned L^2 (Figure 3.6).

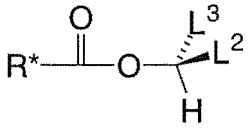

Figure 3.6 Mosher Assignment Model

Substituting CH_3-5 for L^3 and CH_2-3 for L^2, the stereochemistry of the MTPA esters of 4-hydroxy-pentan-2-one and therefore the yeast reduction derived 4-hydroxy-pentan-2-one (**29**) itself can be confirmed as (*S*).

3.3.5 Chiral GC Analysis of Yeast Reduction Product

Analysis by chiral GCMS of the yeast reduction product gave the retention time for 4*S*-hydroxy-pentan-2-one (**29**) while the racemic aldol product showed the retention times of both the (*S*) and the (*R*) isomers (Figure 3.7). A co-injection of (*S*) and racemic 4*S*-hydroxy-pentan-2-one confirmed the order of elution.

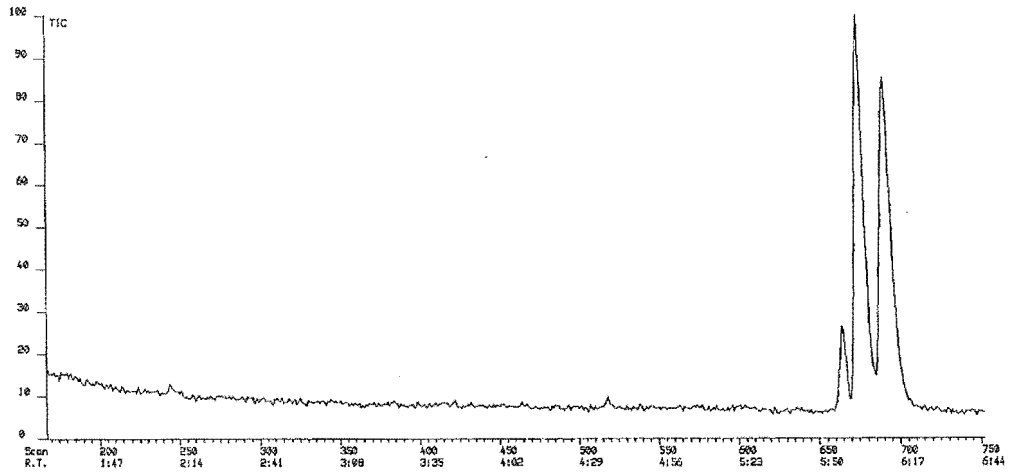

Figure 3.7 Chiral GCMS of Racemic 4-Hydroxy-pentan-2-one (**30**)

On comparison of these retention times with the pateamine-derived fragment the absolute chirality of C24 could have been assigned.

3.3.6 Base-Catalysed Hydrolysis of Pateamine (3)

Small scale partial degradation of pateamine (**3**) by potassium hydroxide hydrolysis or lithium aluminium hydride reduction to give the hydroxydiene moiety failed to open the dilactone ring in a clean manner and led to the degradation of the entire molecule. The subsequent approach explored (see below) was to open the dilactone ring by methanolysis and to recover the hydroxydiene moiety as the hydroxydienoate ester (**37**).[54]

3.3.7 Methanolysis of Pateamine (3)

This approach was again based on the anticipated use of the hydroxyketone (**37**) to ascertain the chirality at the C24 stereocentre of pateamine (**3**). Methanolysis of pateamine (**3**) by sodium methoxide successfully cleaved the dilactone with the hydroxydienoate (**37**) easily extracted from the reaction mix by having the characteristic of being soluble in CH_2Cl_2, while the remainder of the reaction mix was only MeOH soluble. The hydroxydienoate (**37**) was further purified by small scale chromatography.

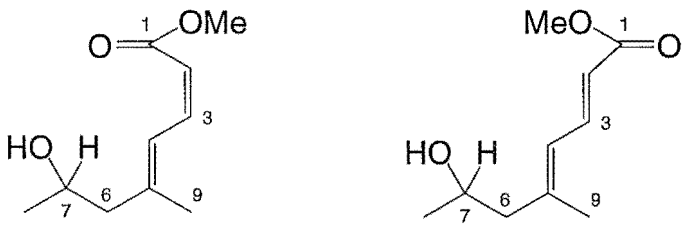

Z,E-hydroxydienoate (**37**) and *E,E* isomer (**38**)

3.3.8 ^{1}H NMR Spectroscopic Assignment of the Hydroxydienoate (**37**)

The assignment of the ^{1}H NMR spectrum (Figure 3.8) of the natural *Z,E*-hydroxydienoate (**37**) started with the unambiguous assignment for a proton α to an hydroxy group at δ_H 4.02 ppm as H7. Irradiation of H7 collapsed the doublets at δ_H 1.23 ppm and δ_H 2.32 ppm. These were assigned as CH_3-8 and H6 respectively. Irradiation of the doublet at δ_H 7.23 ppm collapsed the triplet at δ_H 6.88 ppm to a doublet and also collapsed the fine doublet at δ_H 1.89 ppm. The doublet at δ_H 7.23 ppm was assigned as H4, the triplet at δ_H 6.88 ppm as H3 and the fine doublet at δ_H 1.89 ppm as H9. Irradiation of H3 collapsed both H4 and the doublet at δ_H 5.63 ppm which was assigned as H2. The resonance at δ_H 3.72 ppm was assigned as the methyl ester. The coupling constant between H2 and H3 ($J_{2,3}$=11.7 Hz) arises from a *Z* arrangement across the double bond. An NOE difference experiment irradiating CH_3-9 led to an enhancement of H3 which assigned this double bond as *E*. Present in this sample of hydroxydienoate (**37**) was a small amount of the *E,E* isomer (**38**) (minor peaks in Figure 3.8) which could be distinguished from the *Z,E* isomer by the coupling constant between H2 and H3 ($J_{2,3}$=15.6 Hz).

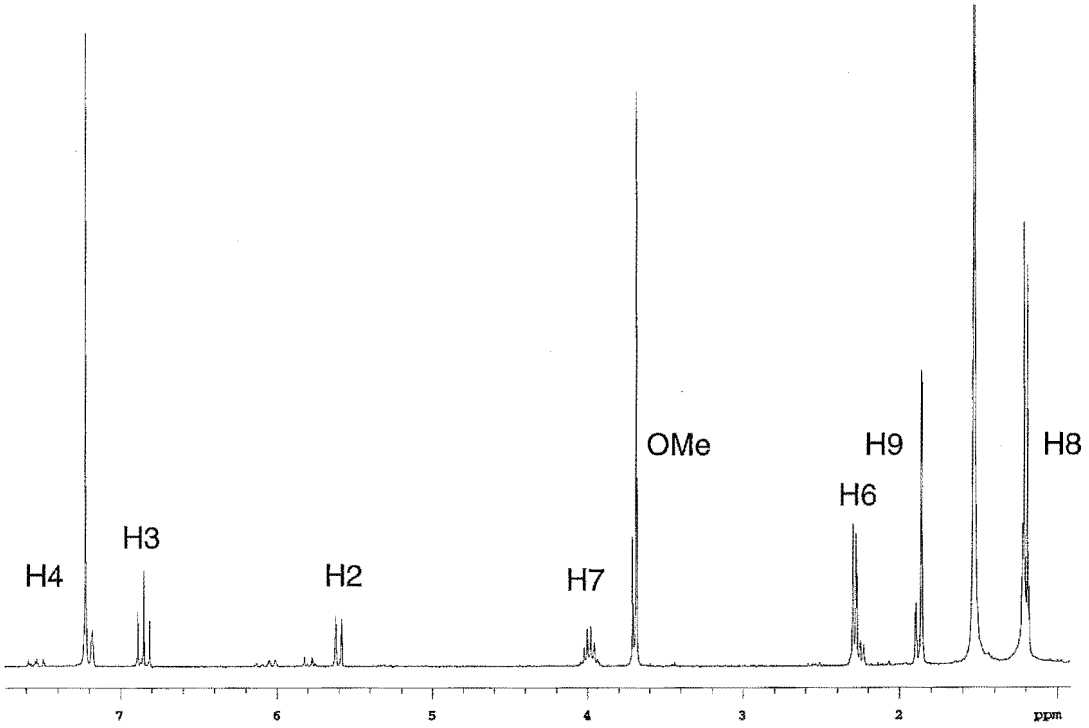

Figure 3.8 ^{1}H NMR Spectrum of the Hydroxydienoate (**37**)

3.3.9 Osmylation of the Hydroxydienoate

Attempts to cleave the double bonds of this fragment by osmylation to yield 4-hydroxy-pentan-2-one failed and led to degradation of the hydroxydienoate (**37**).

3.3.10 Final Method

An alternative route to the determination of the stereochemistry at C24 was the preparation of diastereoisomeric Mosher's esters utilising both enantiomers of MTPA (**31**, **15**). The hydroxydienoate (**37**) was derivatised with (*R*)-MTPA (**31**) *via* the acid chloride[55] to give one of the Mosher esters.[24]

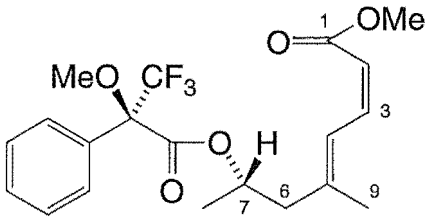

24*S*((*R*)-MTPA)-dienoate (**39**)

A sample of synthetically-derived (*S*)-hydroxydienoate was obtained from Professor Daniel Romo, Texas A & M University, whose group has been undertaking the total synthesis of pateamine (**3**). This synthetic hydroxydienoate was derivatised with both enantiomers of MTPA and all proton resonances in the ^{1}H NMR spectra of the resultant diastereoisomers were assigned (Figure 3.9, 3.10).

3.3.11 ^{1}H NMR Spectroscopic Assignment of 24((*R*)-MTPA)-dienoate (**39**)

The ^{1}H NMR spectroscopic assignment of the natural 24((*R*)-MTPA)-dienoate (**39**) began with the unambiguous assignment of the multiplet resonance for a proton α to an ester group at δ_H 5.37 ppm as H7. The fine doublet (J=1.0 Hz) at δ_H 3.53 ppm was assigned as the MTPA methyl ester. The pair of doublets of doublets at δ_H 2.52 ppm and δ_H 2.36 ppm were assigned as the diastereotopic protons at C6. These protons resonated as a doublet in the hydroxydienoate (**37**). The derivatisation with MTPA appears to have restricted rotation around the C6-C7 bond making the resonances for the H6 protons anisochronous. The remainder of the molecule was assigned by comparison to the hydroxydienoate (**37**). 24((*S*)-MTPA)-dienoate (**40**) was assigned in an identical manner.

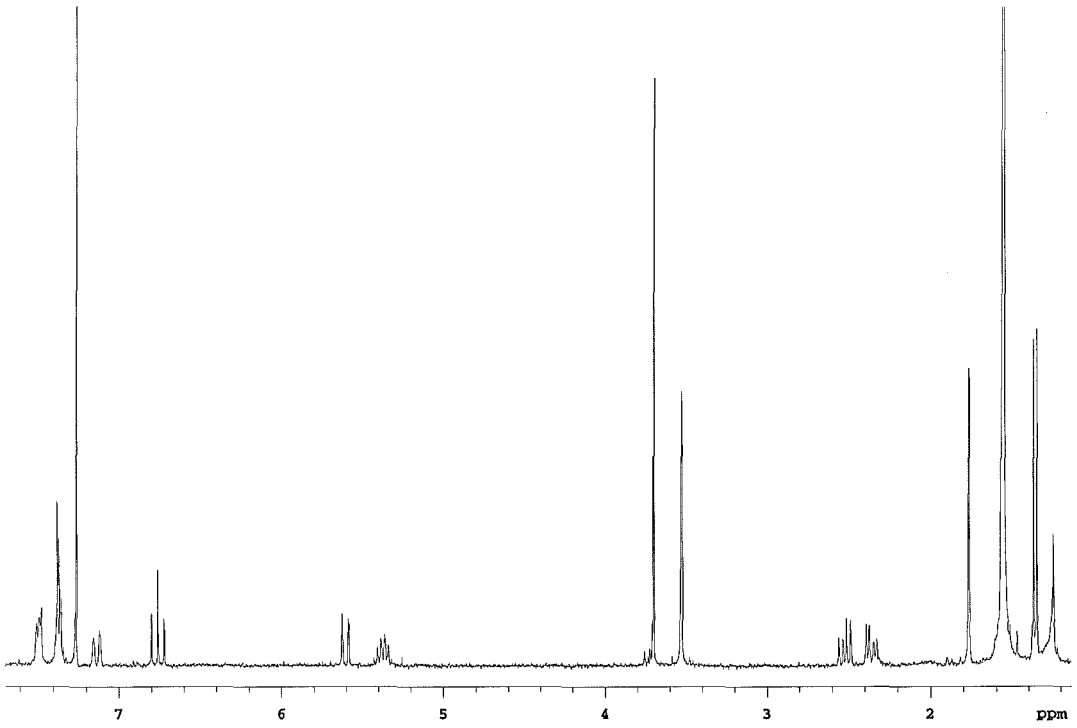

Figure 3.9 ^{1}H NMR Spectrum of 24((*R*)-MTPA)-dienoate (**39**)

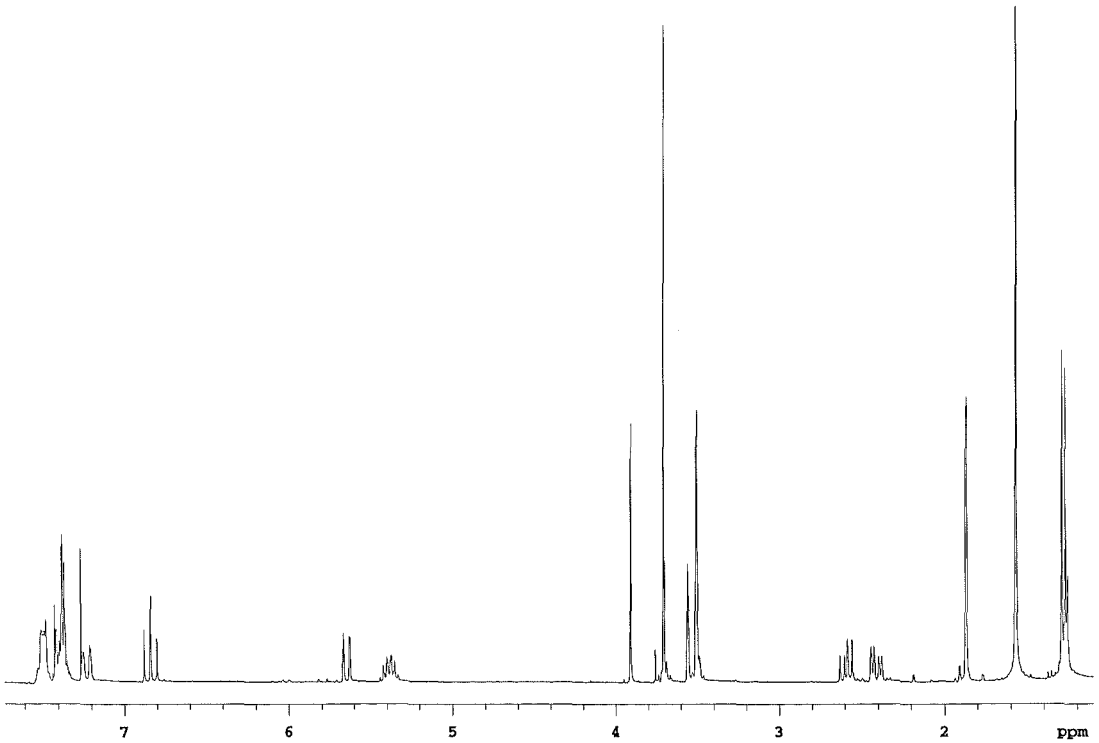

Figure 3.10 ^{1}H NMR Spectrum of 24((*S*)-MTPA)-dienoate (**40**)

Table 3.2 ^{1}H NMR Spectroscopic Data for (*R*) and (*S*)-MTPA Esters of Natural and Synthetic Hydroxydienoates (**39**, **40**)

Proton	(*R*)-MTPA Nat δ ppm (*J* in Hz)	(*R*)-MTPA Syn δ ppm (*J* in Hz)	(*S*)-MTPA Syn δ ppm (*J* in Hz)	(*R*)-(*S*) Δδ ppm
H2	5.60 (11.7)	5.60 (11.7)	5.64 (11.2)	-0.04
H3	6.76 (11.5)	6.76 (11.7)	6.84 (11.5)	-0.08
H4	7.14 (12.2)	7.14 (11.7)	7.23 (11.7)	-0.09
$H6_S$	2.52 (8.0, 14.0)	2.52 (7.8, 13.7)	2.59 (8.0, 14.0)	-0.07
$H6_R$	2.36 (5.1, 14.0)	2.36 (5.6, 13.9)	2.40 (5.4, 14.0)	-0.04
H7	5.37	5.37	5.38	-0.01
CH_3-8	1.36 (6.3)	1.36 (6.4)	1.28 (6.4)	0.08
OMe	3.70	3.70	3.71	-0.01
CH_3-9	1.77 (1.0)	1.77 (1.5)	1.87 (1.5)	-0.10
MTPA OMe	3.53 (1.0)	3.53 (1.0)	3.53 (1.5)	
Phenyl	7.46	7.49	7.50	
Phenyl	7.36	7.36	7.36	

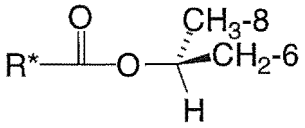

Figure 3.11 Mosher Assignment Model with L^2 and L^3 Replaced with CH_2-6 and CH_3-8 Respectively

All Δδ values listed of (*R*)-(*S*) are negative except for the protons of CH_3-8 which are positive (Table 3.2). From Mosher's chemical shift tables[23] for MTPA esters, all positive Δδ values are assigned the designation L^3 and all negative Δδ are assigned L^2. Substituting CH_3-8 for L^3 and CH_2-6 for L^2 (Figure 3.11), the chirality of position 24 can be designated as (*S*). This also confirmed that the synthetic material was indeed (*S*).

Comparison of the ^{1}H NMR spectroscopic data for the (*R*)-MTPA ester of the natural hydroxydienoate with the data obtained from the 24*S*((*R*)-MTPA)-

dienoate ester (**39**) of synthetic origin showed identical chemical shifts and coupling constants.

The retention times of both MTPA esters of the synthetic hydroxydienoate (**39**, **40**) were determined on a Supelcosil-LC-(*R*)-UREA phase HPLC column. These were compared with the retention time for the (*R*)-MTPA ester of the pateamine-derived hydroxydienoate. The retention times for both (*R*) diastereoisomers were virtually identical. As a further check a co-injection of the synthetically derived (*R*)-MTPA ester and the pateamine-derived (*R*)-MTPA ester was performed (Figure 3.12). This gave widths at half peak height and retention times identical to those for the individually injected chromatograms. This result from the chiral HPLC of the diastereoisomers produced agreed with the conclusion that the chirality at C24 of pateamine (**3**) was (*S*).[56]

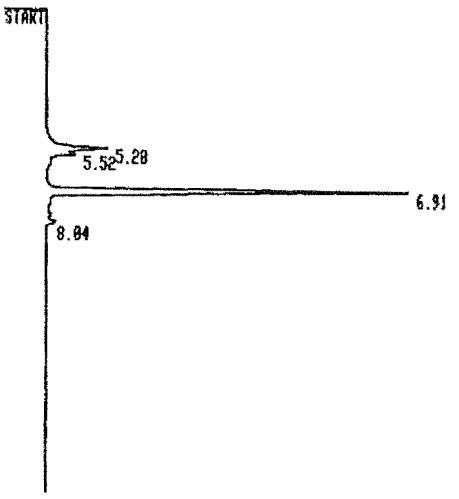

RUN # 94 MAR/16/95 15:43:53
ID 18-1122187

AREA%

RT	AREA	TYPE	AR/HT	AREA%
5.28	13205	BV	0.184	15.654
5.52	4340	VB	0.137	5.145
6.91	65544	PB	0.140	77.697
8.04	1269	BB	0.133	1.504

TOTAL AREA= 84358
MUL FACTOR= 1.0000E+00

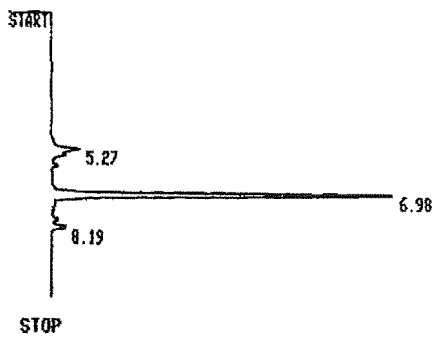

RUN # 101 MAR/16/95 18:32:02
ID 18-1122187

AREA%

RT	AREA	TYPE	AR/HT	AREA%
5.27	5196	BV	0.163	7.428
6.98	62398	PB	0.147	89.194
8.19	2363	BB	0.145	3.378

TOTAL AREA= 69949
MUL FACTOR= 1.0000E+00

Figure 3.12 HPLC traces of 1) the pateamine-derived (*R*)-MTPA ester and 2) co-injection with synthetically derived (*R*)-MTPA ester

3.4 Stereochemistry at C3

3.4.1 Preparation of MTPA Amides

The first attempt at solving the stereochemistry of this centre was made by N,N'-dicyclohexylcarbodiimide (DCC) mediated coupling of the primary amine at C3 with (*R*) and (*S*)-MTPA. This should have given rise to resonances in the ^{1}H NMR spectrum which were distinct for each diastereoisomer. Mosher's method could then have been used to elucidate the chirality of C3. With considerable difficulty (*R*) and (*S*)-MTPA amides of pateamine (**41**, **42**) were prepared. High resolution fast atom bombardment mass spectrometry (Lewis Pannell, NIDDK, NIH, U.S.A.) of 3((*R*)-MTPA)-pateamine (**41**) gave a parent ion (MH^+) at 772.3622 a.m.u. which was within experimental error of the calculated mass ($C_{41}H_{53}F_3N_3O_6S$ calc. 772.3607).

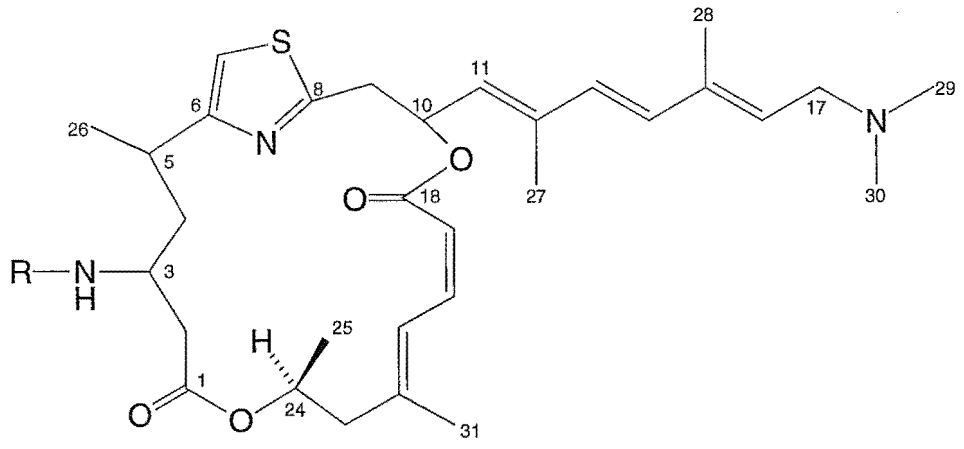

R= (*R*)-MTPA (**41**)
(*S*)-MTPA (**42**)
(*R*)-MPA (**43**)
(*S*)-MPA (**44**)

3.4.2 ^{1}H NMR Spectroscopic Assignment of 3((*R*)-MTPA)-pateamine (**41**)

The ^{1}H NMR spectroscopic assignment of 3((*R*)-MTPA)-pateamine (**41**) started with the multiplet at δ_H 3.67 ppm. This resonance had a correlation in an HMQC experiment to δ_C 46.9 ppm. Comparison of this correlation to that of the totally assigned HMQC experiment on pateamine (**3**) led to this resonance being assigned as H3. While H3 resonates at δ_H 2.58 ppm for pateamine (**3**) compared with δ_H 3.69 ppm for 3((*R*)-MTPA)-pateamine (**41**), the carbon chemical shift for C3 in both molecules is similar (δ_C 45.5 and 46.9 ppm respectively). A 1D-TOCSY experiment (20 ms mixing time) selectively exciting H3 revealed correlations to δ_H 6.85, 2.65, 2.36, 1.97, and 1.26 ppm. Comparison of these correlations to those of the HMQC experiment on pateamine (**3**) led to these resonances being assigned as NH, H2a, H2b, H4 and H26 respectively. This combination of data confirmed the identity of the resonance at δ_H 3.67 ppm as being H3. A 1D-TOCSY (100 ms mixing time) selectively exciting H3 revealed a further correlation to a multiplet at δ_H 2.89 ppm which was assigned as H5. The multiplet resonances at δ_H 7.38 and 7.51 ppm correlated to δ_C 127.5 and 128.3 ppm in the HMQC experiment and were assigned as the MTPA aromatic protons. The fine multiplet resonance at δ_H 3.40 ppm correlated to δ_C 54.6 ppm in the HMQC experiment and was assigned as the OMe of the MTPA moiety. All other resonances were assigned by comparison to the HMQC experiments of pateamine (**3**) and 3((*R*)-MTPA)-pateamine (**41**).

Table 3.3 Selected ^{1}H NMR Spectroscopic Data for (*R*) and (*S*)-MTPA Amides of Pateamine (**41**, **42**)

Proton	(*R*)-MTPA pateamine δ ppm (*J* in Hz)	(*S*)-MTPA pateamine δ ppm (*J* in Hz)	(*R*)-(*S*) Δδ ppm
2a	2.64 (11.3, 16.6)	2.58 (11.2, 16.6)	0.06
2b	2.36 (3.8, 16.6)	2.40 (3.8, 16.6)	-0.04
3	3.67	3.70	n/a
4	1.97	1.98	-0.01
5	2.89	2.80	0.09
7	6.80	6.72	0.08

Upon comparison of the Δδ data for the H2 and H4 protons a clear-cut result was not obtained (Table 3.3). This inconclusive result was thought to be due to either the constraining nature of the macrolide ring system or due to the number of conformations possible for MTPA amides[28] which may have been preventing the MTPA moiety from adopting the conformation required to observe the necessary time-averaged chemical shift differences. Examples of the failure of the Mosher method can be found in the literature (see Introduction Section 1.5).[33]

As a method had already been established for the cleavage of the hydroxydienoate from the major fragment of pateamine (**3**), this was seen as a way of removing any possibly unfavourable constraints put upon this part of the molecule, if this indeed was the cause of the lack of discrimination between these derivatives. The methanolysis was carried out on these two MTPA amide derivatives but due to the low yield from the reaction and the small amount of starting material, ^{1}H NMR spectroscopy revealed neither reaction mixture contained the cleaved MTPA major fragments.

3.4.3 Formation of MPA Amides

In an attempt to circumvent the problems mentioned above, an alternative form of chiral auxiliary, α-methoxyphenylacetic acid (MPA), was employed for the second attempt at obtaining the stereochemistry at C3. MPA amides adopt different conformations to those of both MTPA esters and amides. It was thought that an alternative conformation may yield an answer (see Introduction Section 1.5).

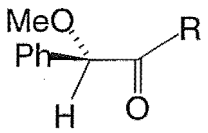

R=OH (*R*)-MPA (**45**)
R=Cl (*R*)-MPACl (**46**)

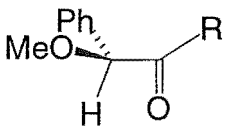

R=OH (*S*)-MPA (**16**)
R=Cl (*S*)-MPACl (**47**)

The (*R*) and (*S*)-MPA amides of pateamine (**43**, **44**) were prepared *via* the acid chlorides (**46**, **47**). The ^{1}H NMR spectra of (*R*) and (*S*)-MPA amides of pateamine (**43**, **44**) were assigned through the use of HMQC, 1D- and 2D-TOCSY experiments.

High resolution fast atom bombardment mass spectrometry of 3((*R*)-MPA)-pateamine (**43**) gave a parent ion (MH^+) at 704.3748 a.m.u. which was within experimental error of the calculated mass ($C_{40}H_{54}N_3O_6S$ calc. 704.3733).

3.4.4 ^{1}H NMR Spectroscopic Assignment of 3((*S*)-MPA)-pateamine (**44**)

The ^{1}H NMR spectroscopic assignment of 3((*S*)-MPA)-pateamine (**44**) started with the multiplet at δ_H 3.65 ppm. This resonance had a correlation in

an HMQC experiment to δ_C 46.2 ppm. Comparison of this correlation to that of the HMQC experiment on pateamine (**3**) led to this resonance being assigned as H3. A 2D-TOCSY experiment (80 ms mixing time) revealed correlations from δ_H 3.65 ppm to δ_H 6.81, 2.83, 2.61, 2.34, 1.96, and 1.21 ppm. Due to the similarity of carbon resonances for 3((*S*)-MPA)-pateamine (**44**) and 3((*R*)-MTPA)-pateamine (**41**), comparison of the HMQC experiments led to these resonances being assigned as NH, H5, H2a, H2b, H4 and H26 respectively. These combinations of data confirmed the identity of the resonance at δ_H 3.65 ppm as being H3. The multiplet resonance at δ_H 7.35 ppm correlated to δ_C 126.9 ppm in the HMQC experiment and was assigned as the MPA aromatic protons. The resonance at δ_H 3.34 ppm correlated to δ_C 56.9 ppm in the HMQC experiment and was assigned as the OMe of the MPA moiety. The singlet resonance at δ_H 4.56 ppm correlated to δ_C 83.6 ppm in the HMQC experiment and was assigned as MPA-C<u>H</u>. All other resonances were assigned by comparison of the HMQC experiments of pateamine (**3**), 3((*R*)-MTPA)-pateamine (**41**) and 3((*S*)-MPA)-pateamine (**44**).

Table 3.4 Selected ^{1}H NMR Spectroscopic Data for (*R*) and (*S*)-MPA Amides of Pateamine (**43**, **44**)

Proton	(*R*)-MPA pateamine δ ppm (*J* in Hz)	(*S*)-MPA pateamine δ ppm (*J* in Hz)	(*R*)-(*S*) Δδ ppm
H2a	2.49 (12, 16)	2.61 (10, 16)	-0.12
H2b	2.29 (12)	2.34 (3, 16)	-0.05
H3	3.69	3.65	n/a
H4	1.94	1.96 (5.7)	-0.02
H5	2.81	2.83	-0.22
H7	6.72	6.81	-0.59

This chiral auxiliary also failed to give a clear-cut result due to all of the proton $\Delta\delta$ values being negative (Table 3.4).

3.4.5 Methanolysis of the MPA Amides

Consequently, methanolysis was carried out on both MPA amides to remove any possible conformational restrictions imposed by the macrolide ring.

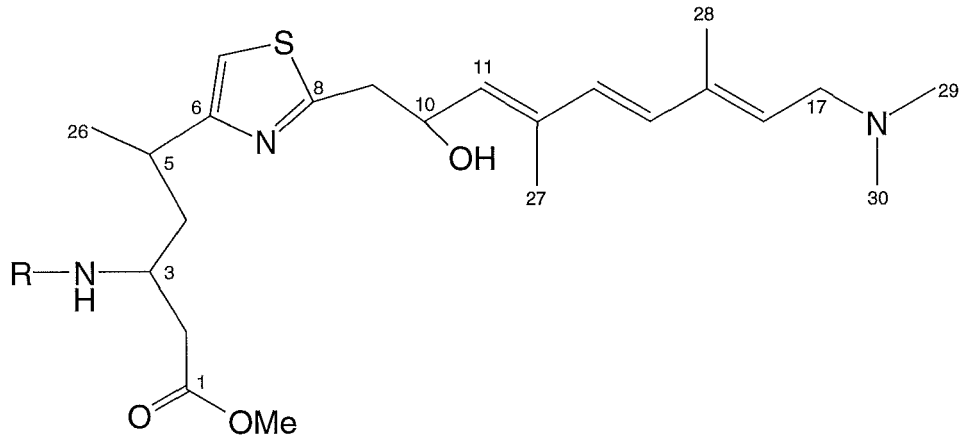

R= (*R*)-MPA (**48**)
(*S*)-MPA (**49**)

High resolution fast atom bombardment mass spectrometry of (*R*)-MPA-pateamine Major Fragment (**48**) gave a MH^+ parent ion at 584.3145 a.m.u. which was within experimental error of the calculated mass ($C_{32}H_{46}N_3O_5S$ calc. 584.3158).

The ^1H NMR spectra (Figure 3.13) of each of the methanolysis products (**48**, **49**) were complex with the resonances of H4 being buried by those for H27 and H28. This required the use of selective 1D- and 2D- NMR experiments to remove any overlap from other resonances and extract relevant chemical

shifts and coupling constants. A 2D-TOCSY experiment on 3((*S*)-MPA)-pateamine major fragment (**49**) showed correlations from H3 to the amide NH, H5, the coincident H2 resonances, the multiplet of the H4 resonances and H26. A 1D-TOCSY (10 ms mixing time) selectively exciting H3 (δ_H 3.65 ppm) confirmed that the resonances for both the H2 protons were coincident. An HMQC experiment also showed a single correlation from the H2 signal to a carbon resonating at δ_C 43.8 ppm. The 1D-TOCSY experiment gave a splitting pattern for the H4 proton resonances that was not first order (Figure 3.14). To obtain these crucial chemical shifts some simulations of the spin system from C2 to C5 were undertaken.

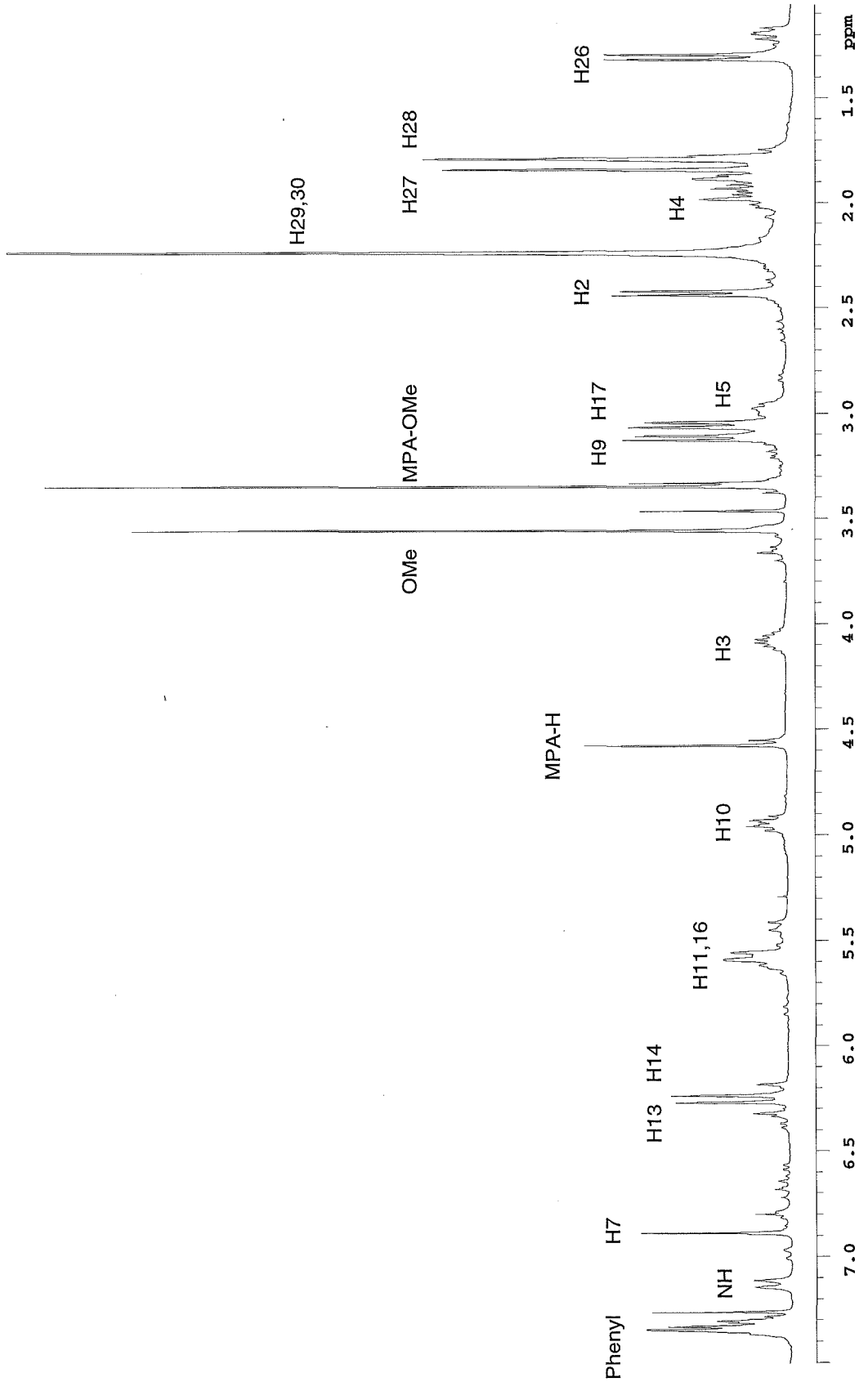

Figure 3.13 ^{1}H NMR Spectrum of 3-((*S*)-MPA)-pateamine Major Fragment (**49**)

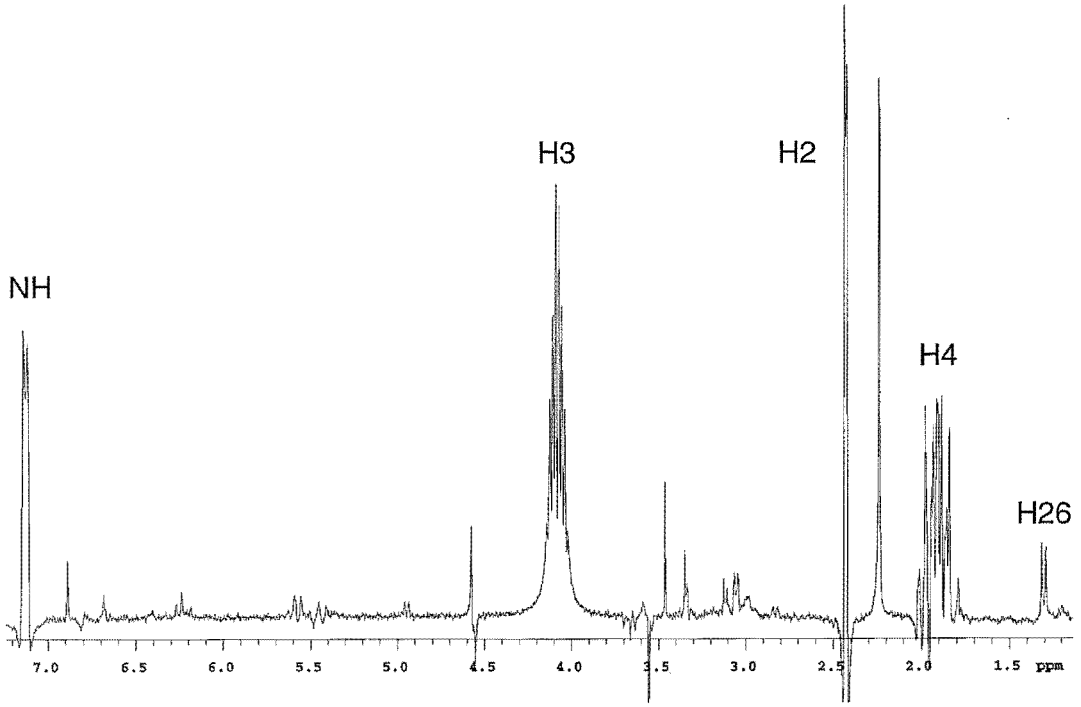

Figure 3.14 1D-TOCSY NMR Spectrum of 3((*S*)-MPA)-pateamine Major Fragment (**49**) Selectively Excited at H3

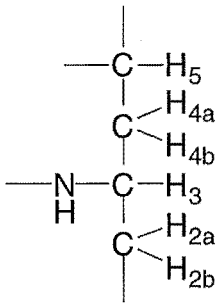

Figure 3.15 Spin System of C2 to C5 Simulated to Obtain NMR Data

3.4.6 Spectral Simulation

Coupling constants for the C2 to C5 spin system (Figure 3.15) were initially extracted from the 1D-TOCSY experiment as far as possible and were further refined as the simulation progressed. The spectrum eventually generated from the simulation was identical to the spectrum obtained from the 1D-TOCSY experiment (Figure 3.16).

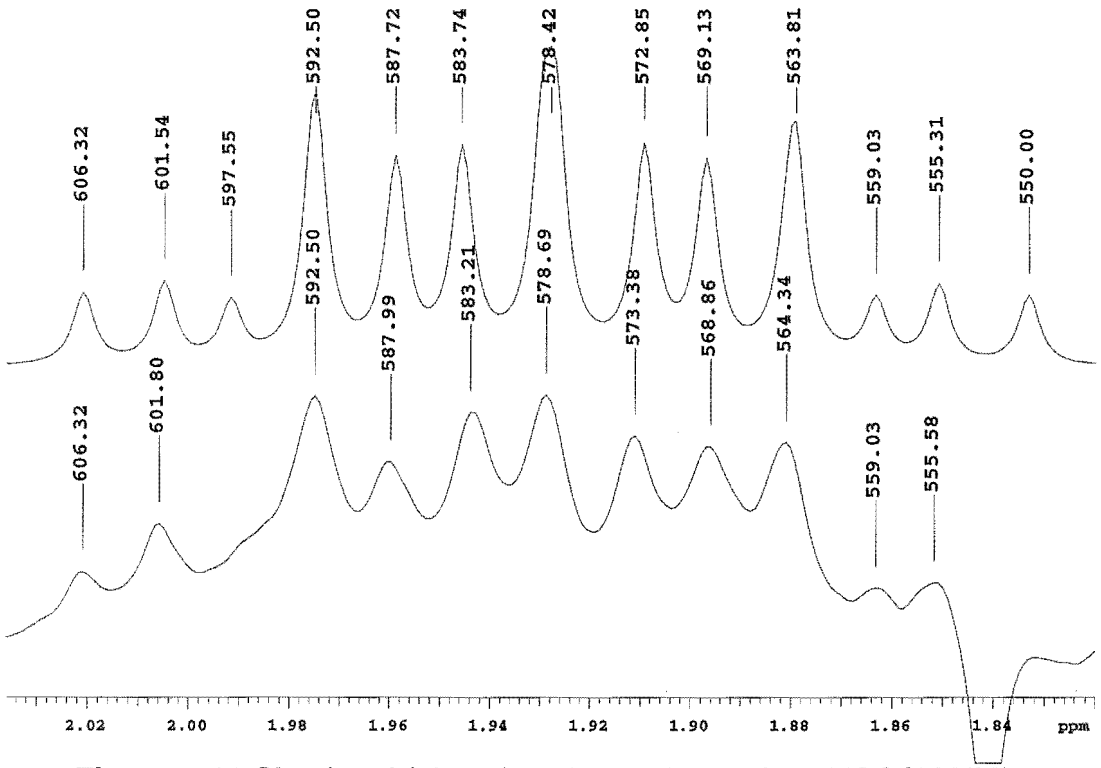

Figure 3.16 Simulated (above) and Experimental 1D-TOCSY NMR Spectra of the H4's of 3((*S*)-MPA)-pateamine Major Fragment (**49**) Selectively Excited at H3

The correctness of the simulation was tested by a 1D-TOCSY (10 ms mixing time) experiment selectively exciting H3 with the concurrent decoupling of H5. The resultant spectrum was compared to a simulation with the coupling constants $J_{5,4a}$ and $J_{5,4b}$ set to 0.0 Hz (Figure 3.17). This absence of coupling constants for coupling of H5 to the H4 protons in the simulation is the equivalent of the decoupling of H5 in the 1D-TOCSY experiment. Further testing of the simulation was carried out with the selective excitation of H5 and the concurrent decoupling of H3 in a subsequent 1D-TOCSY (10 ms mixing time) experiment and comparison of this experimental spectrum with the simulated spectrum, having coupling constants $J_{3,4a}$ and $J_{3,4b}$ set to 0.0 Hz (Figure 3.18). This set of simulated and experimental spectra also matched.

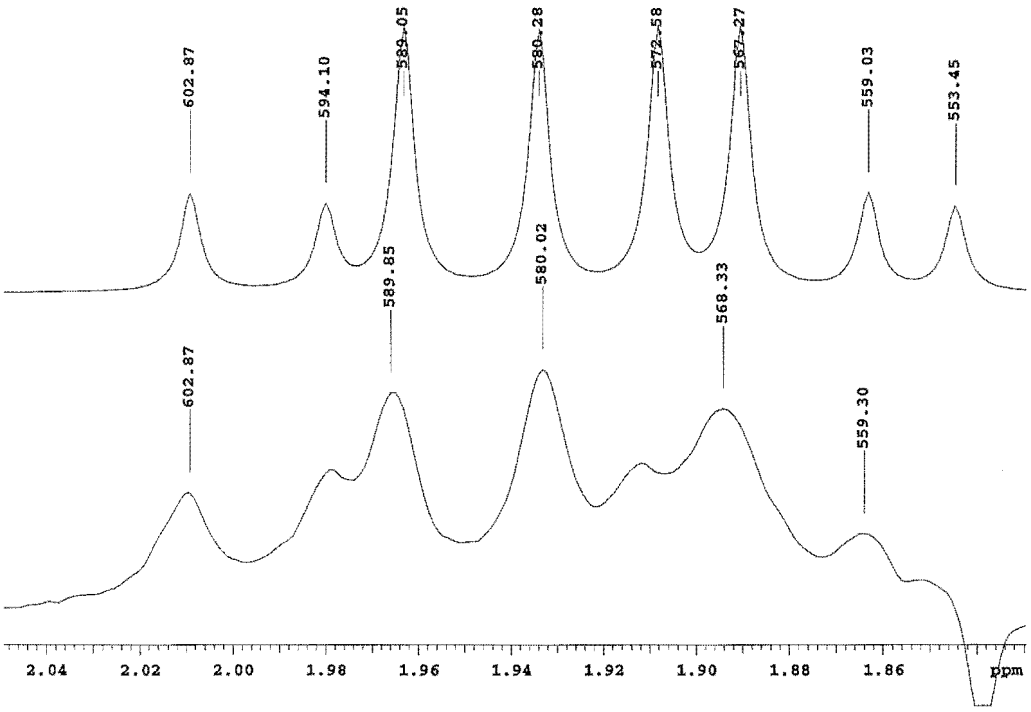

Figure 3.17 Simulated (above) and Experimental 1D-TOCSY NMR Spectra of 3((*S*)-MPA)-pateamine Major Fragment (**49**) Selectively Excited at H5 and Decoupled at H3

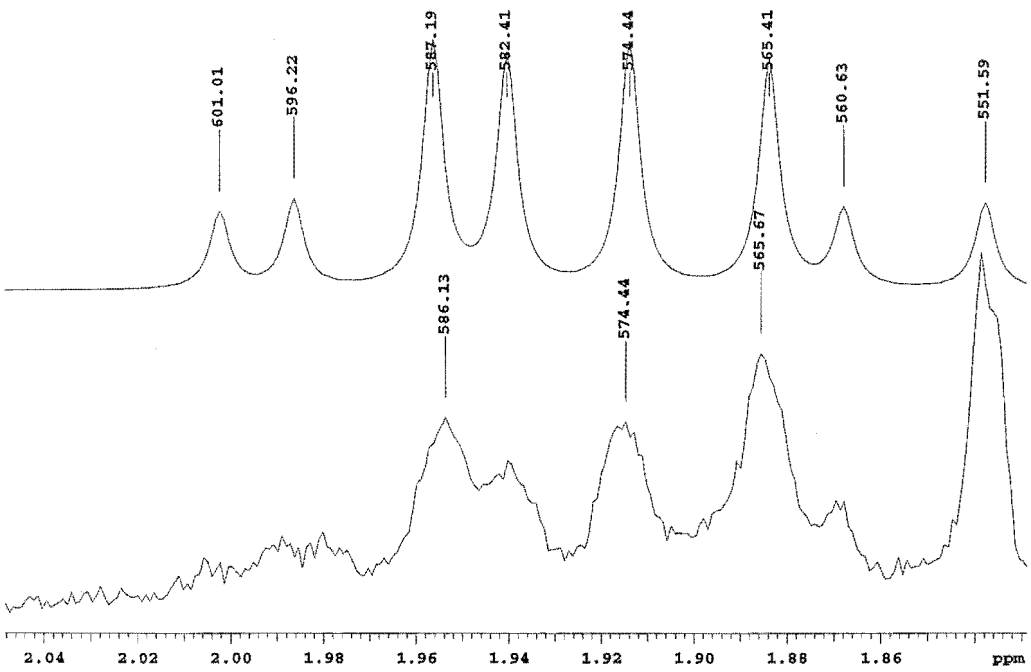

Figure 3.18 Simulated (above) and Experimental 1D-TOCSY NMR Spectra of 3((*S*)-MPA)-pateamine Major Fragment (**49**) Selectively Excited at H3 and Decoupled at H5

3((*R*)-MPA)-pateamine major fragment (**48**) also gave a very complex ^{1}H NMR spectrum and was simulated following the same procedure.

Table 3.5 Data Extracted from Simulation of C2 to C5 Spin System of 3-((*S*)-MPA)-pateamine Major Fragment (**49**)

Proton	δ (ppm)	δ (Hz)	Couplings	*J* (in Hz)
5	2.99	897.12	$J_{5,4a}$	9.1
4a	1.97	591.00	$J_{5,4b}$	5.2
4b	1.89	566.00	$J_{4a,4b}$	13.8
3	4.08	1224.16	$J_{4a,3}$	4.5
NH	7.13	2139.28	$J_{4b,3}$	9.3
2a	2.43	729.10	$J_{3,NH}$	9.45
2b	2.43	729.10	$J_{3,2a}$	5.5
			$J_{3,2b}$	5.5
			$J_{2a,2b}$	15.0

Table 3.6 Data Extracted from Simulating of C2 to C5 Spin System of 3-((*R*)-MPA)-pateamine Major Fragment (**48**)

Proton	δ (ppm)	δ (Hz)	Couplings	*J* (in Hz)
5	2.76	828.11	$J_{5,4a}$	9.8
4a	1.94	582.38	$J_{5,4b}$	4.5
4b	1.84	550.67	$J_{4a,4b}$	13.6
3	3.98	1194.16	$J_{4a,3}$	4.5
NH	7.14	2142.28	$J_{4b,3}$	10.0
2a	2.54	761.10	$J_{3,NH}$	9.5
2b	2.47	739.60	$J_{3,2a}$	5.2
			$J_{3,2b}$	5.2
			$J_{2a,2b}$	16.0

Once the model was optimised, chemical shift data were extracted (Tables 3.5 and 3.6) and the values fitted to the MPA-amide assignment model (Figure 3.19).[31]

Table 3.7 Selected ^{1}H NMR Spectroscopic Data for (*R*) and (*S*)-MPA Amides of Pateamine Major Fragment (**48**, **49**)

Proton	(**48**) δ ppm (*J* in Hz)	(**49**) δ ppm (*J* in Hz)	(*R*)-(*S*) Δδ ppm
H2a	2.53 (5.2, 16)	2.43 (6.5)	0.10
H2b	2.47 (5.2, 16)	2.43 (6.5)	0.04
H3	3.98	4.07	n/a
H4a	1.94	1.97	-0.03
H4b	1.84	1.89	-0.05
H5	2.76	2.99	-0.23
H7	6.30	6.89	-0.59

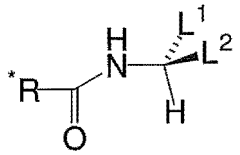

Figure 3.19 MPA Amine Assignment Diagram[31]

Substituting CH_2-4 for L^2 and CH_2-2 for L^1, the stereochemistry of C3 is assigned as (*R*).

3.5 Stereochemistry at C10

The methanolysis of the MPA amides of pateamine (**48**, **49**) resulted in an hydroxy residue at C10. This hydroxy group could be utilised in an attempt to elucidate the stereochemistry at C10. Portions of 3((*S*)-MPA)-pateamine major fragment (**49**) were each subsequently reacted with (*R*)-MTPA and (*S*)-MTPA.

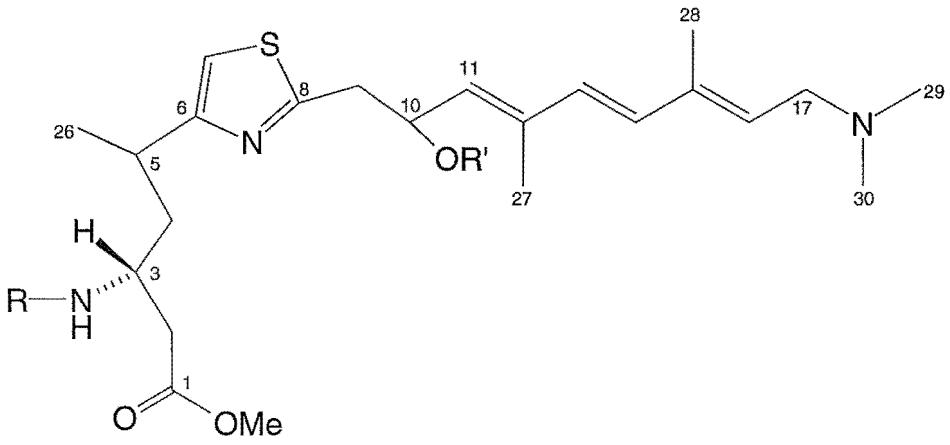

R= (*S*)-MPA R'=(*R*)-MTPA (**50**)
R= (*S*)-MPA R'=(*S*)-MTPA (**51**)

High resolution fast atom bombardment mass spectrometry of 3((*S*)-MPA)-10((*S*)-MTPA)-pateamine major fragment (**51**) gave a MH^+ parent ion at 800.3545 a.m.u. which was within experimental error of the calculated mass ($C_{42}H_{53}F_3N_3O_7S$, 800.3556 a.m.u.).

3.5.1 ^{1}H NMR Spectroscopic Assignment of 3((*S*)-MPA)-10((*S*)-MTPA)-pateamine Major Fragment (**51**)

The ^{1}H NMR spectroscopic assignment of both the 3((*S*)-MPA)-10(MTPA)-pateamine major fragments (**50**, **51**) is incomplete due to the small amount of material available. The ^{1}H NMR spectroscopic assignment of 3((*S*)-MPA)-10((*S*)-MTPA)-pateamine major fragment (**51**) started with the multiplet at δ_H 4.05 ppm. A 2D-TOCSY experiment (80 ms mixing time) revealed correlations from δ_H 4.05 ppm to δ_H 7.14, 2.94, 2.42, 2.40, and 1.26 ppm. This pattern of correlations in the 2D-TOCSY led to these resonances being assigned as NH, H5, coincident H2's, H4 and H26 respectively. The multiplet resonances at δ_H 7.67 and 7.33 ppm were assigned as the MTPA and MPA aromatic protons respectively. The resonances at δ_H 3.58, 3.54 and 3.34 ppm were assigned by comparison to previous compounds as the OMe of the MTPA, C1 methoxy ester, and MPA moieties respectively. H10 was assigned by comparison of the pattern of correlations to H9 and H11 in the 2D-TOCSY experiment to the pattern of correlations in 3((*S*)-MPA)-pateamine major fragment (**49**). For 3((*S*)-MPA)-10((*S*)-MTPA)-pateamine major fragment (**51**) the chemical shift for H10 (δ_H 6.29 ppm) was significantly downfield from that of H10 in 3((*S*)-MPA)-pateamine major fragment (**49**) (δ_H 4.94 ppm) indicating that the alcohol function at C10 had indeed been converted to an ester. A trace through H10 (δ_H 6.28 ppm) in the F2 dimension in the TOCSY experiment clearly showed correlations to both H9's (δ_H 3.41 and 3.23 ppm) and to H11 (δ_H 5.54 ppm). Similarly a trace through H10 in the F2 dimension of the TOCSY experiment on 3(*S*)-MPA-10(*R*)-MTPA pateamine major fragment (**50**) showed correlations to both H9's (δ_H 3.45 and 3.26 ppm) and to H11 (δ_H 5.39 ppm). Other resonances

were assigned by comparison of the HMQC and TOCSY experiments of pateamine (**3**), and all other MTPA and MPA derivatives.

Chemical shift data were extracted from 2D-TOCSY experiments carried out on each of the diastereoisomers produced.

Table 3.8 Selected ^{1}H NMR Spectroscopic Data for (*R*) and (*S*)-MTPA Esters of 3((*S*)-MPA)-pateamine Major Fragment (**50**, **51**)

Proton	(**50**) δ ppm (*J* in Hz)	(**51**) δ ppm (*J* in Hz)	(*R*)-(*S*) Δδ ppm
9a	3.45 (15.2, 7.3)	3.41 (14.4, 5.0)	0.04
9b	3.26 (15.2, 5.9)	3.23 (14.4, 5.0)	0.03
10	6.28	6.29	n/a
11	5.39 (9.6)	5.54 (9.3)	-0.15

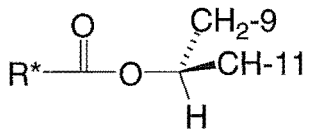

Figure 3.20 Mosher Assignment Model with L^2 and L^3 Replaced With CH-11 and CH_2-9 Respectively.

All positive Δδ values are assigned the designation L^3 and all negative Δδ were assigned L^2 (Table 3.8). Utilising the Mosher assignment diagram by substituting CH-11 for L^2 and CH_2-9 for L^3 (Figure 3.20), the chirality of position 10 can be designated as (*S*).

3.6 Stereochemistry at C5

As there is no functional group at C5 that could be derivatised with any chiral reagent, this stereocentre required a different approach. The proximity of C5 to the previously assigned C3 suggested the use of NOE experiments and coupling constants to probe the relative stereochemistry between C5 and C3.

To this end NOE experiments were carried out on various proton resonances of 3((*R*)-MPA)-pateamine major fragment (**48**) around the C2-C5-C26 spin system. Coupling constants extracted from the simulation of this fragment limited the number of conformers that needed to be considered.

Table 3.9 Coupling Constants Extracted from NMR Simulation of C3 to C5 Spin System of 3((*R*)-MPA)-pateamine Major Fragment (**48**)

Coupling between	*J* (in Hz)
$J_{5,4a}$	9.8
$J_{5,4b}$	4.5
$J_{4a,4b}$	13.6
$J_{4a,3}$	4.5
$J_{4b,3}$	10.0
$J_{3,NH}$	9.5

Table 3.10 Selected Difference NOE Enhancements (%) for 3((R)-MPA)-pateamine Major Fragment (**48**)

From/To	H2	H3	H4a	H4b	H5	H7	CH_3-26	NH
H3	2.4	-	1.6	0.6	1.5	1.9	0.2	2.6
H4a	1	2.4	-		<2[a]	1.2	0.3	
H4b		1	3.7	-	3.5		0.7	2.6
H5		1.4		0.7	-	6.5	1.8	2
CH_3-26		1	1.3	0.8	9	3	-	
NH	0.8	1.9		0.7	1.8	0.3		-

[a]This value is affected by spikes

From Table 3.9 the coupling constant between H5 and H4a ($J_{5,4a}$) is 9.8 Hz which suggests that H5 is predominantly *anti* to H4a. The coupling constant $J_{4b,3}$ is 10.0 Hz suggesting H4b is mostly *anti* to H3. These coupling constants limit the number of rotamers around the H5-H4 bond and the H4-H3 bond to four, two for 3*R*,5*R* and two for 3*R*,5*S* (Figure 3.21).

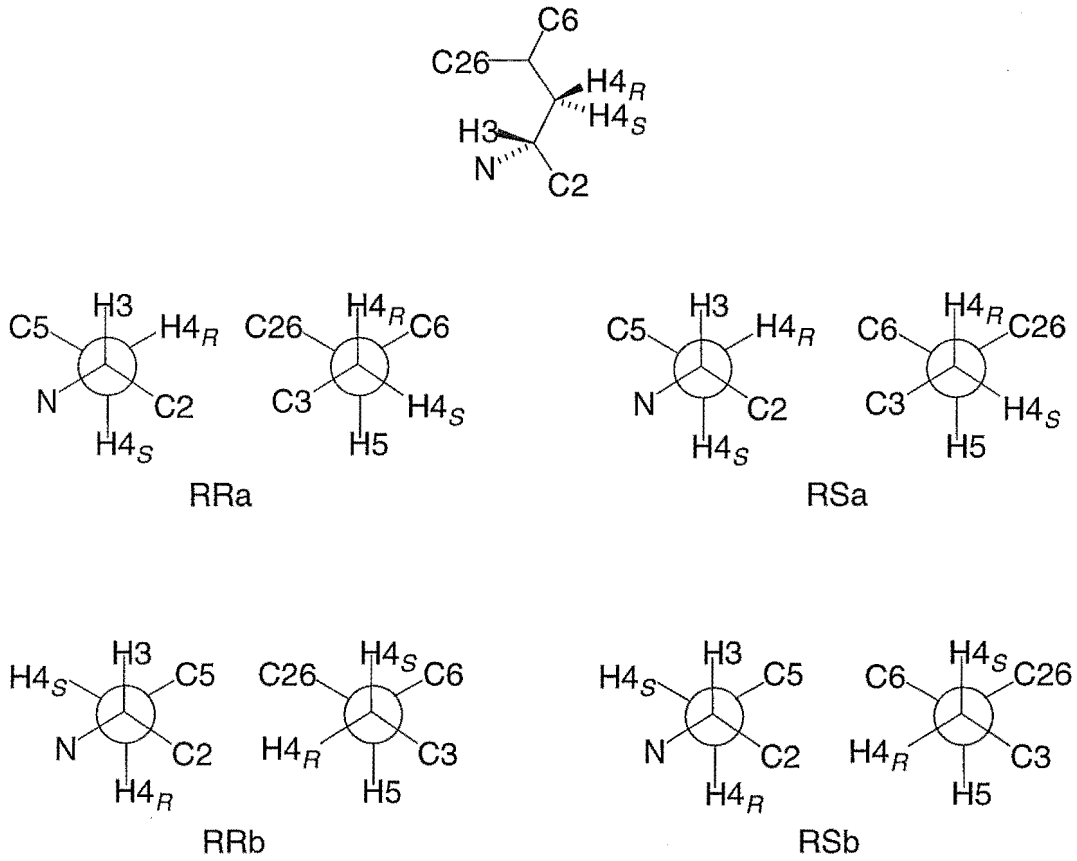

Figure 3.21 Newman Projections Along the C3-C4 and C4-C5 Bonds for the Four Possible Rotamers of C3 to C5 Spin System of 3((*R*)-MPA)-pateamine Major Fragment (**48**).

Table 3.11 Allowed and ***Disallowed*** NOE Enhancements (%) for the Four Rotamers, RSa, RSb, RRa, RRb

RSa	From/To	H2	H3	H4a	H4b	H5	H7	CH_3-26	NH
	H3	2.4	-	1.6	***0.6***	1.5	1.9	***0.2***	2.6
	H4a	1	2.4	-		***<2[b]***	1.2	0.3	
	H4b		***1***	3.7	-	3.5		0.7	2.6
	H5		1.4		0.7	-	6.5	1.8	2
	CH_3-26		***1***	1.3	0.8	9	3	-	
	NH	0.8	1.9		0.7	1.8	0.3		-

RSb	From/To	H2	H3	H4a	H4b	H5	H7	CH_3-26	NH
	H3	2.4	-	***1.6***	0.6	1.5	***1.9***	0.2	2.6
	H4a	1	***2.4***	-		<2[b]	1.2	***0.3***	
	H4b		1	3.7	-	***3.5***		0.7	2.6
	H5		1.4		***0.7***	-	6.5	1.8	***2***
	CH_3-26		1	***1.3***	0.8	9	3	-	
	NH	0.8	1.9		0.7	***1.8***	0.3		-

RRa	From/To	H2	H3	H4a	H4b	H5	H7	CH_3-26	NH
	H3	2.4	-	1.6	***0.6***	1.5	***1.9***	0.2	2.6
	H4a	***1***	2.4	-		<2[b]	1.2	0.3	
	H4b		1	3.7	-	3.5		***0.7***	2.6
	H5		1.4		0.7	-	6.5	1.8	2
	CH_3-26		1	1.3	***0.8***	9	3	-	
	NH	0.8	1.9		0.7	1.8	***0.3***		-

RRb	From/To	H2	H3	H4a	H4b	H5	H7	CH_3-26	NH
	H3	2.4	-	***1.6***	0.6	1.5	1.9	***0.2***	2.6
	H4a	1	***2.4***	-		<2[b]	***1.2***	0.3	
	H4b		1	3.7	-	***3.5***		0.7	2.6
	H5		1.4		***0.7***	-	6.5	1.8	***2***
	CH_3-26		1	1.3	0.8	9	3	-	
	NH	***0.8***	1.9		0.7	***1.8***	0.3		-

[a]Allowed NOE's are those within 3.5Å, ***Disallowed*** refers to a situation which cannot give rise to an NOE because of excessive distance

[b]This value is affected by spikes

Irradiation of H5 in the difference NOE experiment leads to an enhancement for the upfield H4 (H4b). From molecular mechanics modelling of rotamers

RRa and RSa, the enhanced H4 must be $H4_S$. Upon irradiation of the upfield H4 an enhancement of CH_3-26 is observed that, from the distances measured from MM2 results for each rotamer, indicates an allowed NOE for RSa (≈2.5 Å), but disallowed NOE for the RRa rotamer (≈3.9 Å). Distance measurements from the MM2 results exclude both the RRa and RSb rotamers as the NOE enhancement of H7 by irradiation of H3 would be due to excessive distance (4.6 Å and 5.3 Å respectively). Further evidence for the exclusion of RSb is the irradiation of H5 that leads to an NOE enhancement for the upfield H4. This must be due to $H4_R$ in RSb but the NOE enhancement of CH_3-26 observed when the upfield H4 (H4b) is irradiated, is disallowed (≈3.8 Å) due to excessive distance. Irradiation of the NH proton leads to an NOE enhancement of both H5 and the upfield H4. The NOE enhancement of H5 by irradiation of the NH proton is disallowed for both RRb or RSb due to excessive distance (5.0 Å and 4.4 Å respectively). The NOE enhancement of CH_3-26 upon irradiation of H3 cannot be explained by either RRb (≈4.4 Å) or RSa (≈4.7 Å) due to excessive distance. These NOE experiments suggest that none of the four rotamers discussed exist in solution as a sole entity.

The rotamer which allows the greatest number of significant NOE enhancements is RSa followed by the rotamer RRa. Invoking minor populations of RSb and RRb can explain all observed NOE's for both the RS and RR set of rotamers. For the RR set of rotamers however, RRb cannot be the major rotamer as the 2.4 % enhancement of H3 by irradiation of H4a and the 3.5 % enhancement of H5 by irradiation of H4b must be from the dominant rotamer. RRa is excluded from being the major rotamer by the

1.9 % enhancement of H7 by irradiation of H3 that must also be from the major rotamer. RSa has no major disallowed NOE enhancements and the minor disallowed enhancements can be assigned as due to a minor population of RSb. This evidence suggests RSa is the major rotamer.

The experimental coupling constants show intermediate values to those derived from molecular mechanics modelling of the RSa and RSb rotamers of 3((*R*)-MPA)-pateamine major fragment (**48**) (Table 3.12). This indicates that there is more than one conformer present. The experimental coupling constants are weighted in favour of the RSa rotomer, further suggesting the RSa rotamer is the major contributor.

Table 3.12 Coupling Constants for the Rotamers of 3((*R*)-MPA)-pateamine Major Fragment (**48**) from MM2 Modelling and NMR Simulation

Couplings	RSb MM2 *J* (in Hz)	RSa MM2 *J* (in Hz)	NMR *J* (in Hz)
$J_{H5,H4S}$	12.3	2.1	4.5
$J_{H5,H4R}$	2.9	12.3	9.8
$J_{H4S,H3}$	3.5	11.7	10.0
$J_{H4R,H3}$	11.7	2.0	4.5
$J_{H3,H2S}$	2.5	2.2	5.2
$J_{H3,H2R}$	4.1	4.3	5.2

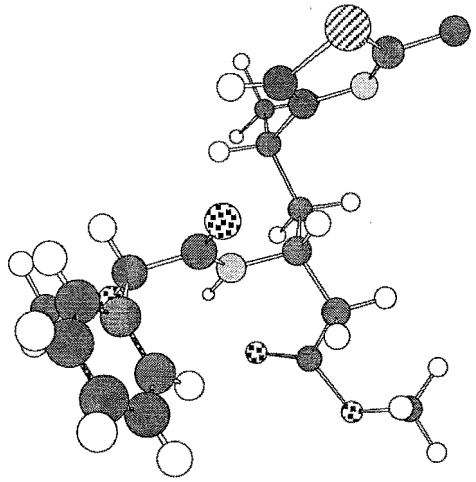

Figure 3.22 The MM2 Minimised Rotamer RSa of 3((*R*)-MPA)-pateamine Major Fragment (**48**) (C9-C17 side chain removed)

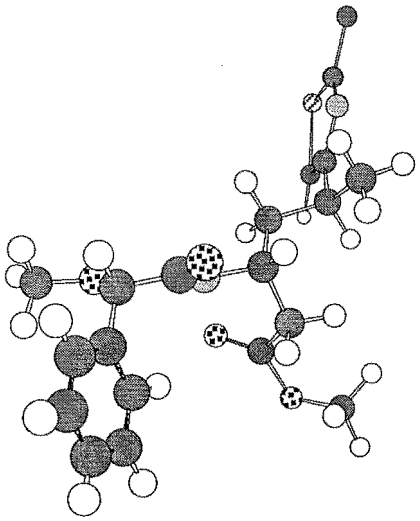

Figure 3.23 The MM2 Minimised Rotamer RSb of 3((*R*)-MPA)-pateamine Major Fragment (**48**) (C9-C17 side chain removed)

The combination of information derived from the NOE difference experiments and the coupling constants derived from the NMR simulation of the 3((*R*)-MPA)-pateamine major fragment (**48**) reveals that the major rotamer is RSa (Figure 3.22) with a minor population of RSb (Figure 3.23). The relative MM energies for RSa (23.25 kcal/mol) and RSb (25.00 kcal/mol) also support the

major rotamer as being RSa. From the RSa rotamer, H4a (downfield resonance) can be assigned as $H4_R$ and H4b (upfield resonance) can be assigned as $H4_S$. This allows the assignment of (*S*) stereochemistry to C5.

This relative stereochemistry between C3 and C5 is consistent with earlier findings based on molecular mechanics modelling for pateamine (**3**) itself, using coupling constant and NOE information determined for pateamine (**3**). This earlier work also determined that the coupling constants and NOE enhancements measured could not have arisen from a single conformer of pateamine (**3**).[50]

3.7 Other Pateamine Derivatives

3.7.1 Crystallisation Attempts

Two counter ions, PF_6^- and $ZnCl_4^{2-}$, were employed in separate experiments in the continuing attempts to obtain crystals suitable for single-crystal X-ray diffraction analysis. These attempts were unsuccessful and no pateamine (**3**) was recovered from either attempt.

3.7.2 3(*N*-Acetyl)-pateamine (**52**)

During this study of pateamine (**3**) it was noted that upon storage pateamine (**3**) degraded to give a neutral mix of compounds which were not retained on CBA cartridges. Upon methanolysis of pateamine (**3**) to extract the hydroxydiene moiety at no time could the major fragment be isolated or purified. 3(*N*-Acetyl)-pateamine (**52**) was synthesised with the view that this

may be a more stable compound than pateamine (**3**) itself, and the methanolysis of 3(*N*-acetyl)-pateamine (**52**) may lead to a more stable fragment which could then allow derivation of C10 with no chiral auxiliary present at C3.

3(*N*-Acetyl)-pateamine (**52**) was the first substituted pateamine derivative to be methanolysed. Initially attempts were made to neutralise the NaOMe with the addition of H_2O and TFA followed by trapping of the organic material on a C18 cartridge. CBA chromatographic material was considered but previous work had shown that salts had a detrimental effect on the effectiveness of this sorbent. Subsequent ^1H NMR spectroscopic analysis of the material trapped on the C18 cartridge and then eluted with MeOH showed a complex mix of compounds. As there were now no salts in the sample the material was further chromatographed on a CBA cartridge in an attempt to trap the desired basic reaction products. No material was trapped on the CBA sorbent indicating that the amine at C17 had eliminated. Due to the small amount of material available and the complexity of the mixture this section of work was discontinued.

The method of isolation of the methanolysis products employed above was abandoned in favour of size separation on LH-20 gel permeation material followed by CBA chromatography. This had the advantage of not requiring the addition of H_2O or TFA and could be carried out using dry MeOH which prevented the formation of NaOH and eliminated the risk of excessive addition of TFA. The gel permeation method was very successful and all subsequent work employed this method of isolation.

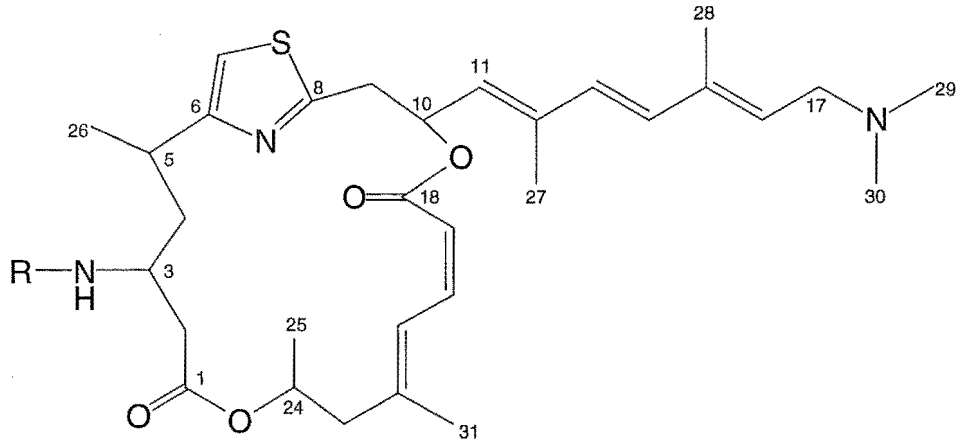

R= acetyl (**52**)
R= *p*-bromobenzoyl (**54**)

High resolution fast atom bombardment mass spectrometry (Lewis Pannell, NIDDK, NIH, U.S.A.) of 3(*N*-acetyl)-pateamine (**52**) gave a parent ion (MH^+) at 598.3306 a.m.u. which was within experimental error of the calculated mass ($C_{33}H_{48}N_3O_5S$ calc. 598.3314).

3.7.3 3(*p*-BBA)-pateamine (**54**)

Pateamine (**3**) was derivatised with *p*-bromobenzoic acid (*p*-BBA) in an attempt to obtain a single crystal which would be suitable for analysis by single crystal X-ray crystallography. The scale of the reaction precluded the formation of a crystal but the methodology was proved and with a further supply of pateamine (**3**) in the future it may be possible that this derivative will lead to an independent assignment of the stereochemistry of the four stereocentres of pateamine (**3**).

High resolution fast atom bombardment mass spectrometry gave a parent ion (MH^+) at 738.2582 a.m.u. which was within experimental error of the calculated mass ($C_{38}H_{49}N_3O_5SBr$ calc. 738.2576).

3.8 Conclusion

Through the use of a combination of degradative and derivatisation chemistry the absolute stereochemistry of pateamine (**3**) has been determined as 3*R*,5*S*,10*S*,24*S*.

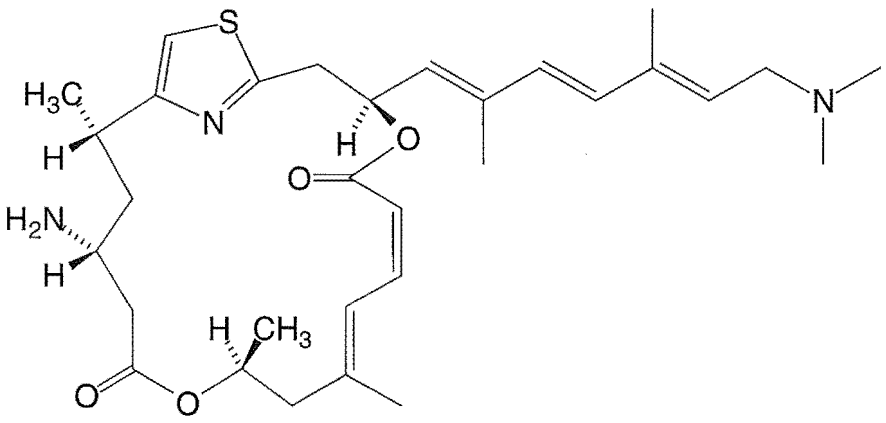

3*R*,5*S*,10*S*,24*S*-pateamine (**3**)

Chapter 4

Aplysia parvula

4.1 Introduction

Aplysia spp., subclass Opisthobranchia, order Anaspidea, family Aplysiidae are hind gilled molluscs, lacking a cephalic shield with an internal, relatively small, membranous to lightly calcified shell enclosed by parapodia, or swimming flaps. *Aplysia* are herbivorous molluscs that feed preferentially on various red algae found in the littoral zone and the lack of a protective shell makes *Aplysia* spp. potentially vulnerable to predators.[57] This lack of mechanical protection coupled with the absence of known predators suggests sea hares have a chemical defence.

Sea hares are not the only soft bodied molluscs to appear immune to predation. Other Opisthobranchia, for example the shell-less, carnivorous nudibranchs, sequester metabolites from food sources, such as sponges and tunicates, and locate them in the mantle and in mucus that they exude when disturbed.[58]

4.2 Selected Compounds Isolated from *Aplysia* spp.

A large number of compounds have been isolated from sea hares.[59] The first compounds isolated from an *Aplysia* sp. were the brominated sesquiterpenes, aplysin (**55**), debromoaplysin (**56**) and aplysinol (**57**). These were isolated from *A. kurodai* by Yamamura and Hirata in 1963.[60]

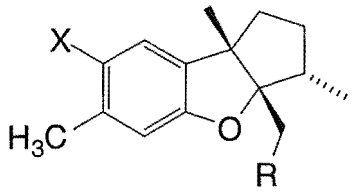

X=Br, R=H aplysin (**55**)
X=Br, R=OH aplysinol (**57**)
X=H, R=H debromoaplysin (**56**)

Irie *et al.* later isolated these compounds from the red alga *Laurencia okamurai*.[61] Irie *et al.* went on to describe laurinterol (**58**) and debromolaurinterol (**59**) from *L. intermedia*[62, 63] and demonstrated that these compounds are able to be transformed into aplysin (**55**) and debromoaplysin (**56**) respectively by treatment with *p*-toluenesulfonic acid in refluxing benzene in good yield.

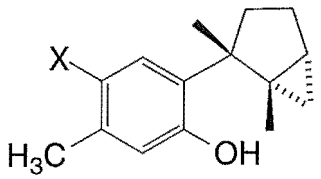

X=Br, R=H laurinterol (**58**)
X=H, R=H debromolaurinterol (**59**)

This *in vitro* transformation provided a model for the *in vivo* conversion of laurinterol (**58**), from the sea hare's diet of the red alga *Laurencia* sp. Stallard and Faulkner[64] demonstrated that sea hares are capable of chemically modifying dietary metabolites by feeding radio-labelled laurinterol (**58**) to *A. californica* and isolating radio-labelled aplysin (**55**).

Whereas aplysin (**55**) and other brominated metabolites have been claimed to be antifeedants,[65] there is no direct evidence to suggest that all

brominated metabolites are in fact antifeedant nor that the modifications carried out *in vivo* enhance any bioactivity of the sequestered metabolites.[66] The transformation of laurinterol (**58**) into aplysin (**55**) may also be purely a result of the acidity of the digestive gland of *Aplysia*.[64]

4.2.1 Antifeedant compounds from *Aplysia* spp.

Kinnel *et al.*[67] carried out extensive studies on the antifeedant properties of different parts of the sea hare's body and also several compounds isolated from the sea hare *A. brasiliana*. *Aplysia* pieces sandwiched between fillets of fish and fed to sharks were invariably spat out, while the fillet was consumed. Smaller fish also rejected *Aplysia* pieces. Two of the isolated compounds shown to have antifeedant activity were brasilenyne (**60**) and *cis*-dihydrorhodophytin (**61**).

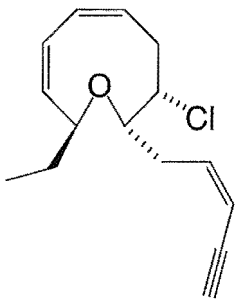

brasilenyne (**60**)

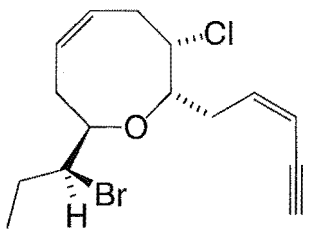

cis-dihydrorhodophytin (**61**)

These compounds were topically coated onto beetle larvae (*Tribolium confusum*) and offered, with controls, to swordtail fish (*Xiphophous helleri*). The controls were invariably eaten while the treated larvae were rejected outright or rinsed by the fish using a flow of water generated by the action of the gills. The rinsed larvae were still susceptible to being rejected. The

rinsing activity was brought about by as little as 0.1 μg of brasilenyne (**60**). These compounds are similar to chlorofucin (**62**), poiteol (**63**) and obtusenyne (**64**) which were isolated from various species of *Laurencia*.[68]

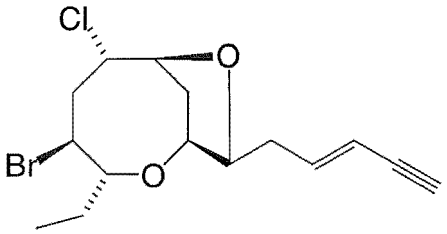

chlorofucin (**62**)

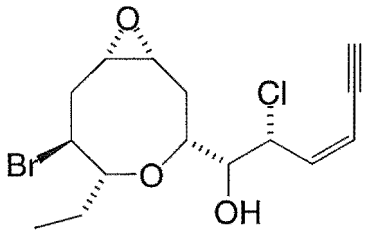

poiteol (**63**)

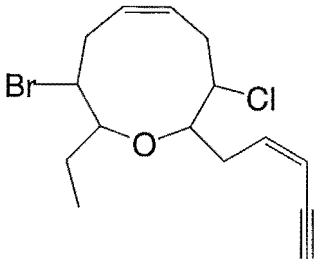

obtusenyne (**64**)

Another compound isolated from *A. brasiliana*, also reported to be an antifeedant, is the bromoallene, panacene (**65**).[69, 70]

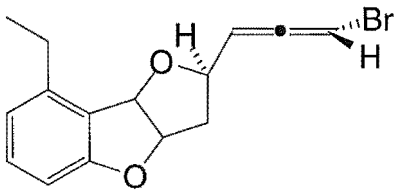

panacene (**65**)

Further experimental evidence for *Aplysia* containing antifeedants was provided by Stallard *et al.*[71] When extracts from the digestive gland of *A. brasiliana* were painted onto the shell of a juvenile crab, *Callinectes sapidus*,

this preferred prey became repulsive to the octopus, *Octopus vulgaris*. From this study *A. brasiliana* yielded two compounds, brasilenol (**66**) and *epi*-brasilenol (**67**), that are likely to be sequestered from a dietary source as they have also been isolated from the Mediterranean red alga, *L. obtusa*.[71] No experiments were conducted to prove that these compounds were the components giving rise to the antifeedant activity of the digestive gland extract.

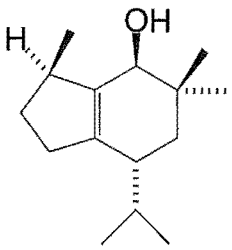

brasilenol (**66**)

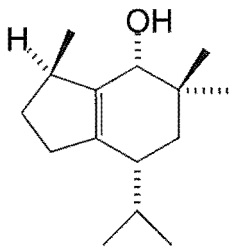

epi-brasilenol (**67**)

The function of the digestive gland has attracted much interest as it is from this organ that many of the compounds mentioned thus far are isolated. Stallard and Faulkner[72] offer two possibilities for the function of the digestive gland: the site of enzymatic digestion of polyhalogenated compounds or the storage of defensive chemicals. GCMS analysis of the non-polar oils extracted from the digestive gland of an *Aplysia* sp. fed solely *L. coccineum* var. *pacificum* revealed the presence of a large number of polyhalogenated constituents which were similar to those from the algae. Two halogenated monoterpenes isolated and identified were (3*S*,4*S*,7*S*)-3,7-dimethyl-1,8,8-tribromo-3,4,7-trichloro-1,5-octadiene (**68**) and (3*R*,4*S*,6*S*)-7-chloro-3,7-dimethyl-1,4,6-tribromo-1-octen-3-ol (**69**).[72]

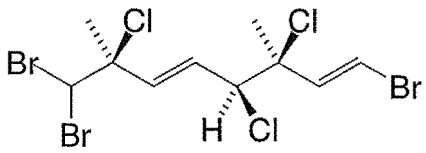

(3*S*,4*S*,7*S*)-3,7-dimethyl-1,8,8-tribromo-3,4,7-trichloro-1,5-octadiene (**68**)

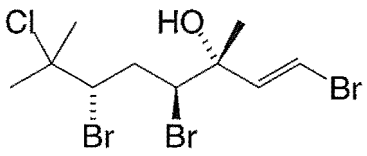

(3*R*,4*S*,6*S*)-7-chloro-3,7-dimethyl-1,4,6-tribromo-1-octen-3-ol (**69**)

However there were not the lipids present which might be considered to constitute a normal diet. This suggests, along with the antifeedant experiments, that the digestive gland is the site of storage for antifeedant compounds. Pennings and Paul[58] reported that sequestered secondary metabolites are almost exclusively stored in the digestive gland. Some authors[72, 58] have questioned how the antifeedants from the digestive glands are mobilised to effect deterrence. One explanation is that physical transportation of antifeedants need not occur as a naive generalist predator may attack what seems to be an easy meal only to discover, upon digestion of the body, that all is not as it seemed. The generalist predator thereby learns from this experience that the *Aplysia* sp. is not a desirable food source and will practice avoidance of the *Aplysia* sp. sampled, and most likely the entire genus, in the future.[73] That the individual has not benefited from the antifeedants before death is contrary to Darwinian selection where, for a trait to be selectively advantageous, the individual(s) possessing the trait must survive to reproduce at a higher rate than individuals lacking the trait. However it must be mentioned that Darwinian selection also selects out

useless traits, so the location of the sequestered secondary metabolites in the digestive gland must have some selective advantage. Specialist predators will have coevolved with the *Aplysia* and will either be immune to the antifeedants or have some mechanism to avoid their effects.

Another possibility is that the defensive chemicals are transported to the skin but are only present in amounts below the concentration at which they can be detected by spectroscopic properties.

The chemical defence exhibited by *Aplysia* spp. has been hypothesised to have allowed the sea hares to dispense with the mechanical defence of a shell.[74] The capability of sea hares for *de novo* synthesis of chemicals remains unexplored.[66]

Blunt *et al.* have previously reported the isolation of thyrsiferol (**70**),[75] a squalene-derived polyether metabolite, and a series of vinyl acetylenic chloro diols (**71**, **72**, **73**, **74**)[76, 77] from *L. thyrsifera.*

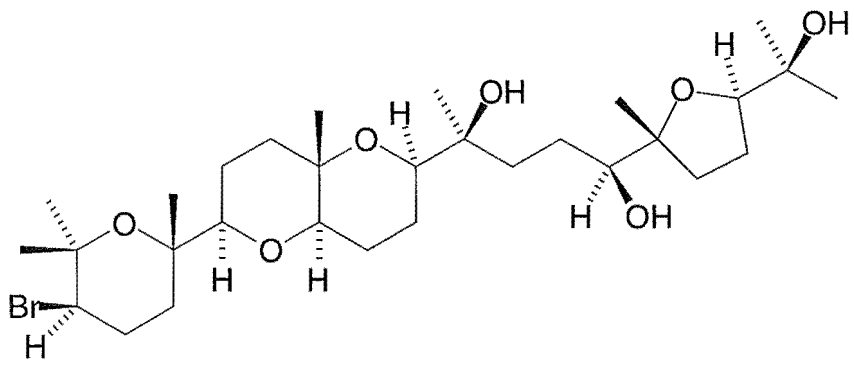

thyrsiferol (**70**)

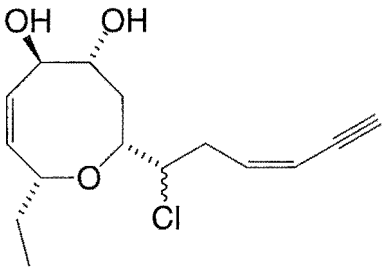

(71)

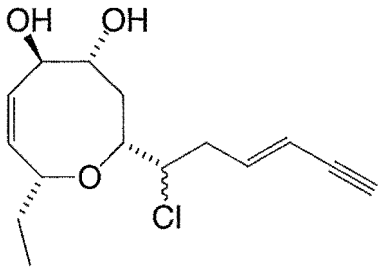

(72)

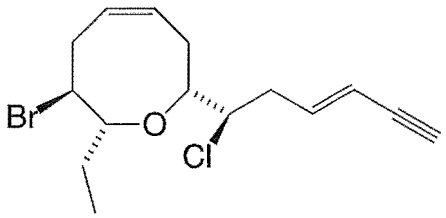

(73)

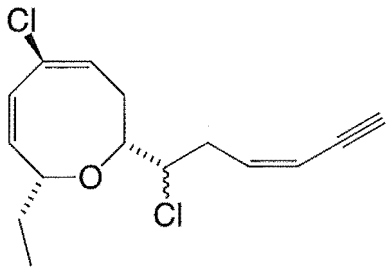

(74)

4.3 Current Work

This study was initiated to ascertain if the sea-hare *Aplysia parvula* sequesters selected metabolites from the red alga *Laurencia thyrsifera.* The animals used in this study were found grazing on inter-tidal fields of the red alga *L. thyrsifera*[78] at Seal Reef, Kaikoura on the East Coast of the South Island, the same location as the specimens of *L. thyrsifera* were collected from for the Blunt *et al.*[75, 76, 77] studies.

4.3.1 Chemical Investigation

The bodies of *Aplysia parvula* were drained, dissected and the digestive glands excised. The purple fluid given off by the animals during harvesting was collected and showed marked P388 activity. The fluid was passed down a C18 reverse-phase cartridge to trap any organic material but the trapped

material was not active. Due to the lack of organic-soluble activity, attention was focused on the bodies and excised digestive glands. The organic extract of the bodies (less digestive glands) was coated onto Celite and dry-packed on to a C18 reverse-phase column. Eleven fractions were collected from the column. Slight antimicrobial activity existed in fractions 3 (50:50 MeOH/H_2O) to 6 (80:20 MeOH/H_2O), but no P388 activity was observed in any fraction.

C18 reverse-phase chromatography of the organic extract from the digestive glands yielded 12 fractions. The fraction from the C18 column that was the most active antimicrobial fraction was rechromatographed on DIOL sorbent to yield thyrsiferol (**70**). The extended ^1H NMR spectroscopic assignment of thyrsiferol (**70**) is the subject of the following chapter.

Thyrsiferol (**70**) was initially reported to be biologically inactive.[75] However, Suzuki *et al.*[79] isolated thyrsiferol (**70**) and thyrsiferyl acetate (**75**) from *L. obtusa* and reported P388 ED_{50} values of 10 and 0.3 ng/mL respectively. In this study, thyrsiferol (**70**) returned a IC_{50} value of 1222 ng/mL in the P388 assay.

GCMS analysis of the organic fraction from the extraction of the digestive glands displayed eleven peaks in the total ion count trace. The mass spectra of these peaks revealed that the compounds present were C-12 mono-, and C14 di-unsaturated hydrocarbons, and a series of C-13, C-15, C-17, and C-19 fatty acid methyl esters with various methyl substitution patterns. None of

the mass spectra of the peaks displayed any halogen isotopic splitting patterns. The analysis was not continued beyond this stage.

4.3.2 The Egg Masses of *A. parvula*

While collecting *A. parvula*, it was noted that the bright orange egg masses conspicuously attached to rocks, usually under small overhangs, survived untouched for periods of up to 14 days. There is no obvious physical protection for the egg mass, which in principle is an ideal food source for reef predators such as the numerous starfishes (Order Asteroidea) and triplefins (Family Tripterygidae) present. Either chemical and/or microbial protection was suspected. Gil-Turnes and Fenical[80, 81] have reported microbial protection of spawned embryos of an estuarine shrimp, *Palaemon macrodactylus*, and embryos of the American lobster, *Homarus americanus*. The shrimp embryos were covered in an *Alteromonas* sp. from which 2,3-indolinedione (**76**) was isolated and the lobster embryos were covered by a Gram-negative rod-type bacteria from which 2-(4'-hydroxyphenyl)ethanol (**77**) was isolated. Both these animals are external brooders with the embryos continuously exposed to water-borne microorganisms.

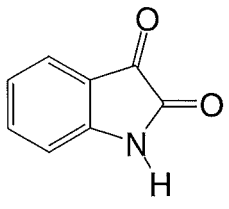

2,3-indolinedione (**76**)

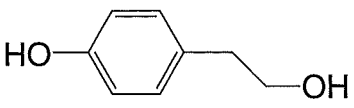

2-(4'-hydroxyphenyl)ethanol (**77**)

There is also the possibility of chemical defence of the egg masses arising from the adult animal bestowing protection in the form of chemicals which either leach into the surrounding water over time or are released by mechanical disturbance.

To test the possibility of chemical and/or microbial protection of *A. parvula* egg masses, the majority were extracted with solvent for chemical analysis with the balance used for the cultivation of microbial colonies and examination by electron microscopy.

A. parvula were collected and placed into a 200 litre sea water tank with several kilograms of fresh *L. thyrsifera*. Periodically the tank was inspected, cleaned, and newly found, wild *A. parvula* and fresh algae added. The egg masses were removed as they were found and frozen until required. The frozen eggs (280 g) were steeped in MeOH (600 mL) until thawed, sonicated for 30 minutes and then homogenised in a Waring blender. After filtering through Celite, extracts were combined and the solvent removed *in vacuo* to yield an orange viscous oil (12.5 g). The extract was coated onto Celite and chromatographed on a C18 reverse-phase column (28 mm x 400 mm, 100 g). A large amount of material (10.5 g) was eluted in the first two fractions. Some fractions showed strong antiviral activity (*Herpes simplex* type 1 virus (ATCC VR 733) and *Polio* virus type 1 (Pfiser vaccine strain)) and some antimicrobial activity (against *Bacillus subtilis* and the three species of fungi).

All fractions were compared by TLC with a genuine sample of thyrsiferol (**70**) and those with a similar R_f were partitioned between CH_2Cl_2 and H_2O, while

the remaining antimicrobial fractions were chromatographed on a DIOL column (10 mm x 140 mm, 10 g). A ^{1}H NMR spectroscopic analysis of fractions 4-9 from this column displayed only signals characteristic for triglycerides. Fraction 3 (0.4 mg) only had ^{1}H NMR resonances characteristic of terpenoid compounds. No olefinic resonances were obvious. This fraction was selected for FABMS as it contained the least amount of triglycerides. The mass spectrum revealed an ion of 640 a.m.u. but the fragmentation pattern was not amenable to analysis due to the mixture of compounds present.

Fractions 3-9 all had antimicrobial activity but the lack of other than triglyceride resonances in the ^{1}H NMR spectra suggested that the active compound was at a very low level. GCMS analysis of several of the fractions revealed that the compounds present were C-13 and C-18 saturated hydrocarbons, and a series of C-17, and C-19 fatty acid methyl esters. Neither the GCMS or the FABMS of fraction 3 displayed any bromine isotopic splitting patterns. This precludes the presence of thyrsiferol (**70**) or any of the many other brominated algal metabolites or thermally degraded products of these compounds. The lack of material remaining precluded further work in this area.

4.3.3 Investigation of Microorganisms

Fresh *Aplysia* embryos were located and removed from the substrate, rinsed and wiped over three salt water agar plates. The egg masses were then homogenised with a sterile tissue grinder and 100 µL of the homogenate streaked in a standard pattern over each of three further salt water agar

plates. The plates were incubated at room temperature for 7 days, examined daily and individual colonies lifted, cultured and restreaked until monocultures were obtained. Nine monocultures were obtained in this fashion. The successfully isolated colonies were each bulked up on several agar plates. These were each diluted with MeOH (200 μL) and sonicated for 10 minutes. The resultant solution was filtered and submitted for the P388 assay in a standard assay. Of the nine colonies isolated, four showed some level of activity in the P388 assay. Samples of the four microorganisms that returned activity in this assay were forwarded to PharmaMar (Spain) and the Abbott Chemical Company (U.S.A.) for further assessment. However, none of the microorganisms met those companies' requirements for further study.

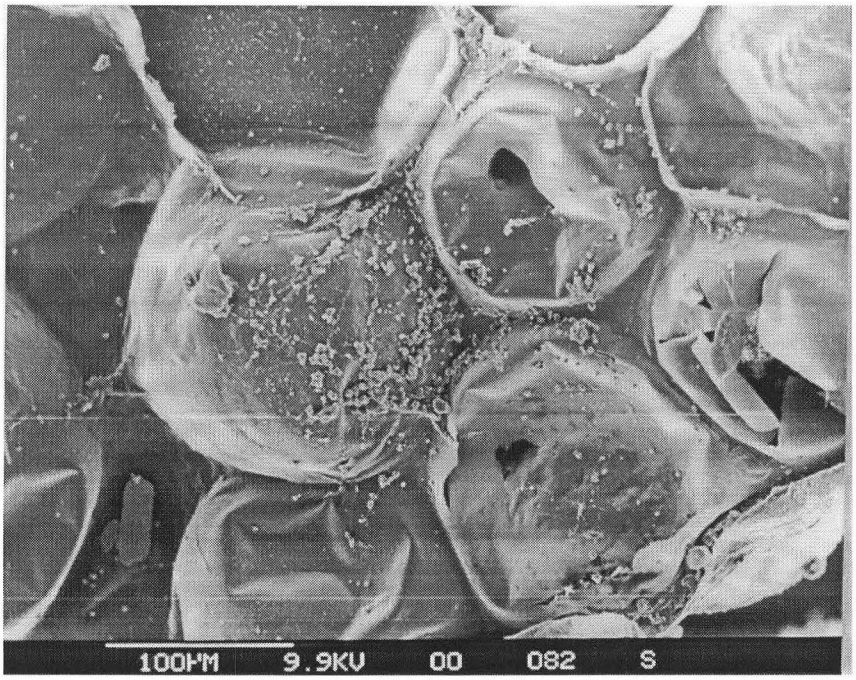

Figure 4.1 The Eggs of *Aplysia parvula*

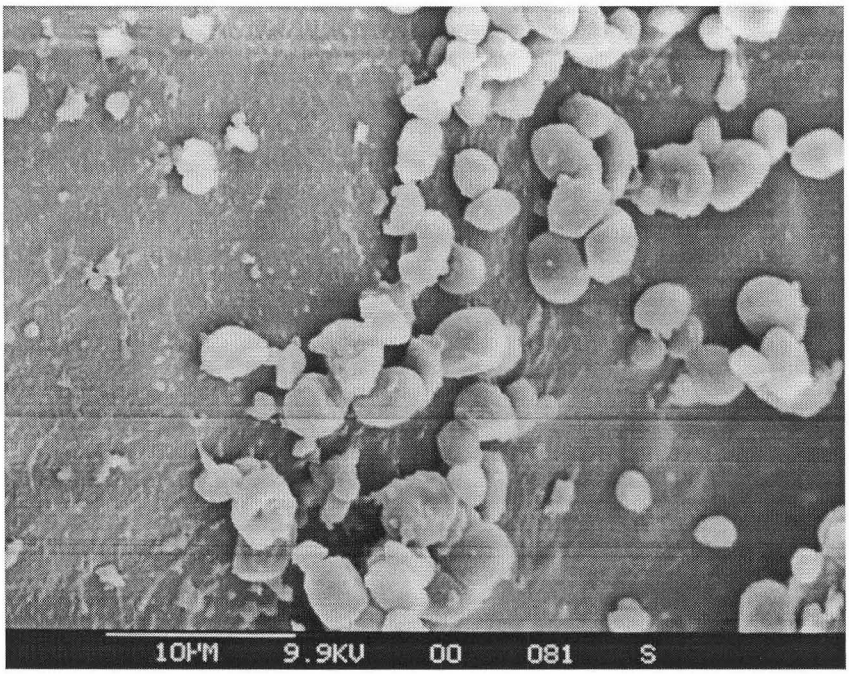

Figure 4.2 A Magnified View Showing Micro-organisms

4.4 Conclusion

The sea hare *Aplysia parvula* has been shown to store the cytotoxic metabolite thyrsiferol (**70**) in the digestive gland. This metabolite has been sequestered from the preferred food source, the red alga *Laurencia thyrsifera*. If the egg masses are indeed protected by an endowed chemical then the most likely compound for this role is thyrsiferol (**70**), supplied to the egg masses from the digestive gland of the adult. However, no evidence was found to suggest that *A. parvula* actually transfers thyrsiferol (**70**) to the egg mass.

Quite clearly there are microorganisms associated with the egg masses, but all attempts made in our laboratory to culture microorganisms producing compounds with antibiotic or cytotoxic properties were not successful. Other workers too, have found that it is difficult to cultivate all the microorganisms present in or on an organism. Kang *et al.*[82] isolated the antibiotic enterocin (**78**), previously isolated from a microbial source,[83] from a marine ascidian of the genus *Didemnum.*

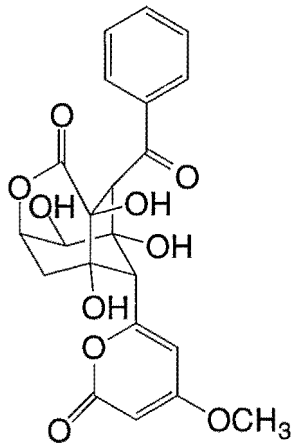

enterocin (**78**)

Microscopic examination of the tunic of the *Didemnum* sp. revealed large amounts of bacteria, thought to be *Arthrobacter* species. Twenty strains of endobacteria were isolated but none could be confirmed as the origin of the antibiotic isolated from the entire animal.

The whole area of culturing microorganisms from marine environments is a rapidly expanding field, but is one fraught with many difficulties and has a minimum requirement for an expert microbiologist experienced in the marine area. It is almost certain that success in this area will only come when that requirement is coupled with new, innovative approaches to the field. It has been estimated from extracted DNA that a typical marine source such as a sediment, or the interior of a sponge contains close to 1000 different species of microorganism, but the best efforts in the laboratory typically yield only 1-5 % of this number. Our efforts on culturing microorganisms from the surface of the egg masses of *A. parvula* are therefore fairly typical for what has been achieved to date. Clearly, a microbiological source of protection for the egg masses can not be ruled out.

In conclusion, it is suggested that the protection displayed by the egg masses of *A. parvula* is most probably biological in origin. Upon spawning the eggs would have a fixed supply of nutrients and these must be directed to cell growth processes, to allow the larvae to have the best chance of survival, rather than be used for the energetically expensive biosynthesis of defence chemicals. Consequently the embryos must either have a generous amount of antifeedants when spawned or have low levels of active material, which must be constantly renewed. The restricted volume of the eggs for the storage of defensive compounds would tend to suggest constant replacement by symbiotic microorganisms as the method of choice.

Chapter 5

Thyrsiferol

5.1 Introduction

The isolation of thyrsiferol (**70**) from *Aplysia parvula* afforded the opportunity to re-examine and extend the assignment of the NMR spectra of thyrsiferol (**70**)[75] using more modern equipment and techniques. The complete assignment of the ^{13}C and ^{1}H NMR spectra of thyrsiferyl acetate (**75**) and a partial assignment of thyrsiferol (**70**) was reported by Blunt *et al.*[84] in 1989. An X-ray crystallographic structure of the mono acetate, thyrsiferyl acetate (**75**), gave the relative stereochemistry, but the absolute configuration was not obtained unequivocally.

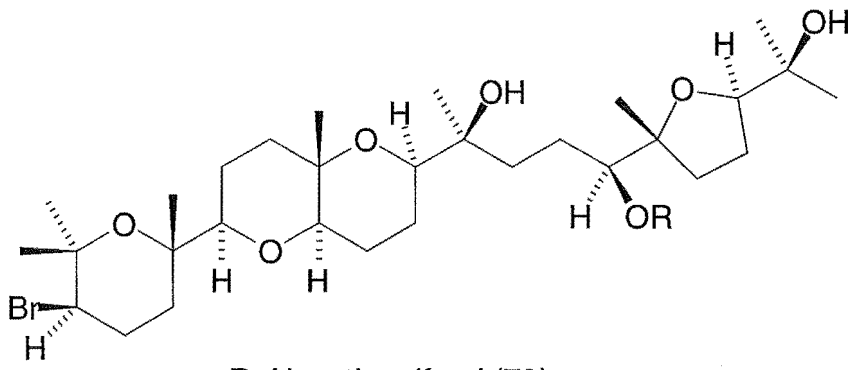

R=H thyrsiferol (**70**)
R=Ac thyrsiferyl acetate (**75**)

Venustatriol (**79**), a diastereoisomer of thyrsiferol (**70**), was isolated by Sakemi *et al.*[85] in 1986 from *L. venusta*. Venustatriol (**79**) was converted to venustatriol-18 acetate (**80**) and found by analysis of the NMR data to have the same conformation for the six membered rings (C1-C14) as thyrsiferol acetate (**75**). The substituents of the tetrahydrofuran ring had a different stereochemistry to that of thyrsiferol (**70**), which could not be determined by NMR. Consequently, venustatriol-18 acetate (**80**) was crystallised and the

absolute configuration determined by X-ray crystallography. This enabled Sakemi *et al.* to define the absolute configuration for thyrsiferyl acetate (**75**) and hence for thyrsiferol (**70**).

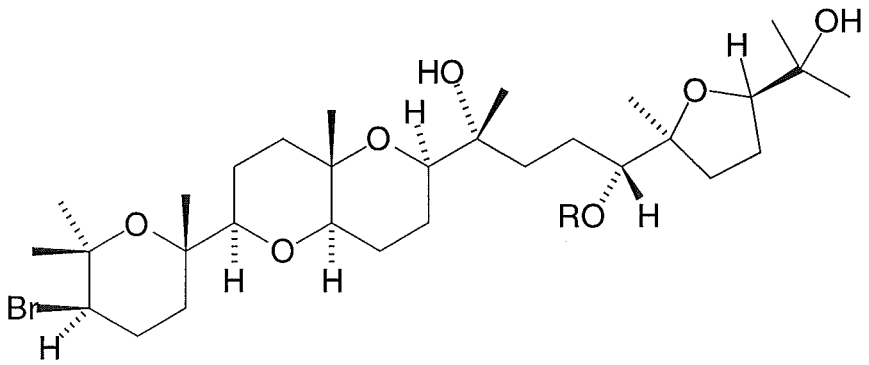

R=H venustatriol (**79**)
R=Ac venustatriol-18 acetate (**80**)

Venustatriol (**79**) was reported as having significant antiviral activity.[85]

5.2 NMR Spectroscopic Assignment of Thyrsiferol

The ^{1}H NMR spectrum of thyrsiferol (**70**) (Figure 5.1) showed much overlap in the methyl and methylene regions requiring the use of several 1D- and 2D-NMR techniques *viz.* HMQC, HMBC, TOCSY, NOE and ECOSY[86, 87, 88] NMR experiments. Distinct resonances for several ring junction protons allowed access to most of the remaining protons.

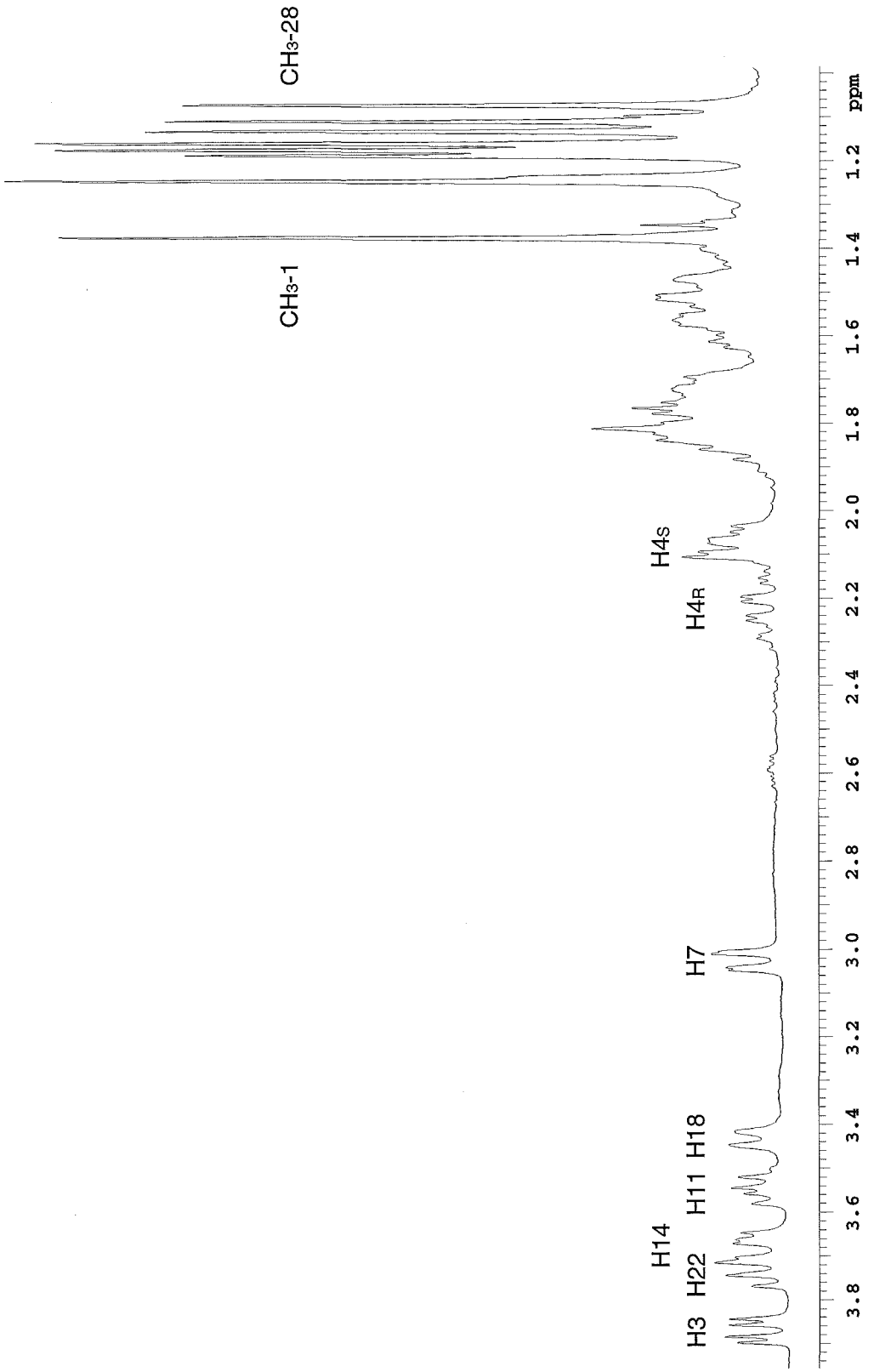

Figure 5.1 ^{1}H NMR Spectrum of Thyrsiferol

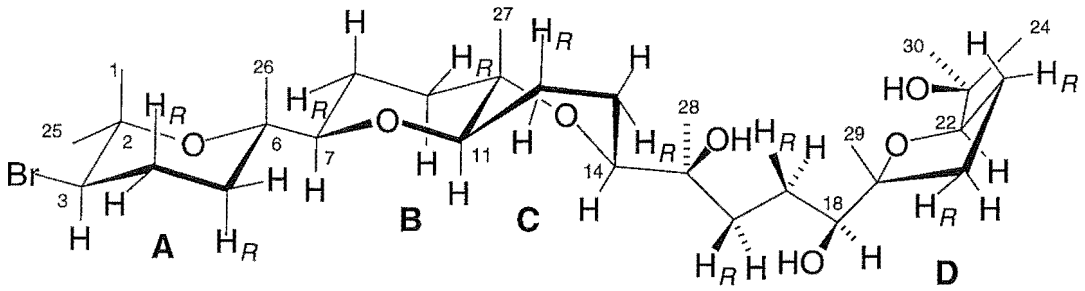

Figure 5.2 Conformational Diagram of Thyrsiferol (**70**)

Table 5.1 ^{1}H NMR Spectroscopic Data for Thyrsiferol (**70**).

Proton[a]	Literature δ ppm[84,b]	$CDCl_3$ δ ppm (*J* in Hz)	Proton[a]	Literature δ ppm[84,b]	$CDCl_3$ δ ppm (*J* in Hz)
CH_3-1	1.40	1.39	H16[d]	2.1	1.37
H3	3.89	3.89 (4,12)	H16[d]		1.81
$H4_R$	2.24	2.24 (4,13,13,13)	H17[d]		1.46
$H4_S$	2.07	2.07 (4,4,13)[c]	H17[d]		1.55
$H5_R$	1.52	1.51 (4,13)	H18	3.45	3.44 (2,10)
$H5_S$	1.79	1.78 (4,12)	$H20_R$		1.57
H7	3.04	3.04 (3,9)	$H20_S$		2.07
$H8_R$		1.71 (3)	$H21_R$	1.85	1.81
$H8_S$		1.40 (9)	$H21_S$	1.85	1.81
$H9_R$	1.78	1.76	H22	3.76	3.76 (6,9)
$H9_S$	1.53	1.51	CH_3-24	1.12	1.12
H11	3.57	3.56 (7,11)	CH_3-25	1.27	1.26
$H12_R$		1.47 (11)	CH_3-26	1.18	1.19
$H12_S$		1.87 (7)	CH_3-27	1.20	1.17
$H13_R$	1.58	1.67 (4)	CH_3-28	1.15	1.09
$H13_S$	1.58	1.82 (12)	CH_3-29	1.09	1.15
H14	3.73	3.69	CH_3-30	1.21	1.20

[a] The notation $_R$ and $_S$ represent pro-*R* and pro-*S* geminal protons respectively

[b] Literature data do not distinguish between pro-*R* and pro-*S*

[c] Coupling constants have been lifted from various NMR experiments but are incomplete

[d] Unable to assign pro-*R* and pro-*S*

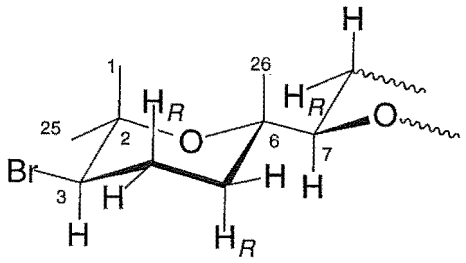

Figure 5.3 C1-C7 Fragment of Thyrsiferol (**70**)

The starting point for ring A (Figure 5.3) was the assignment of H3 (3.89 ppm) from an HMQC correlation between H3 and the unambiguously assigned halogenated C3 (58.95 ppm). ECOSY correlations from H3 to both H4 protons (Figure 5.4) combined with the conformation diagram derived from the X-ray crystallographic study[75] showing H3 to be axial, allowed the assignment of $H4_R$ (2.24 ppm, $J_{3,4R}$=13 Hz) as being axial and $H4_S$ (2.07 ppm, $J_{3,4S}$=4 Hz) as equatorial.

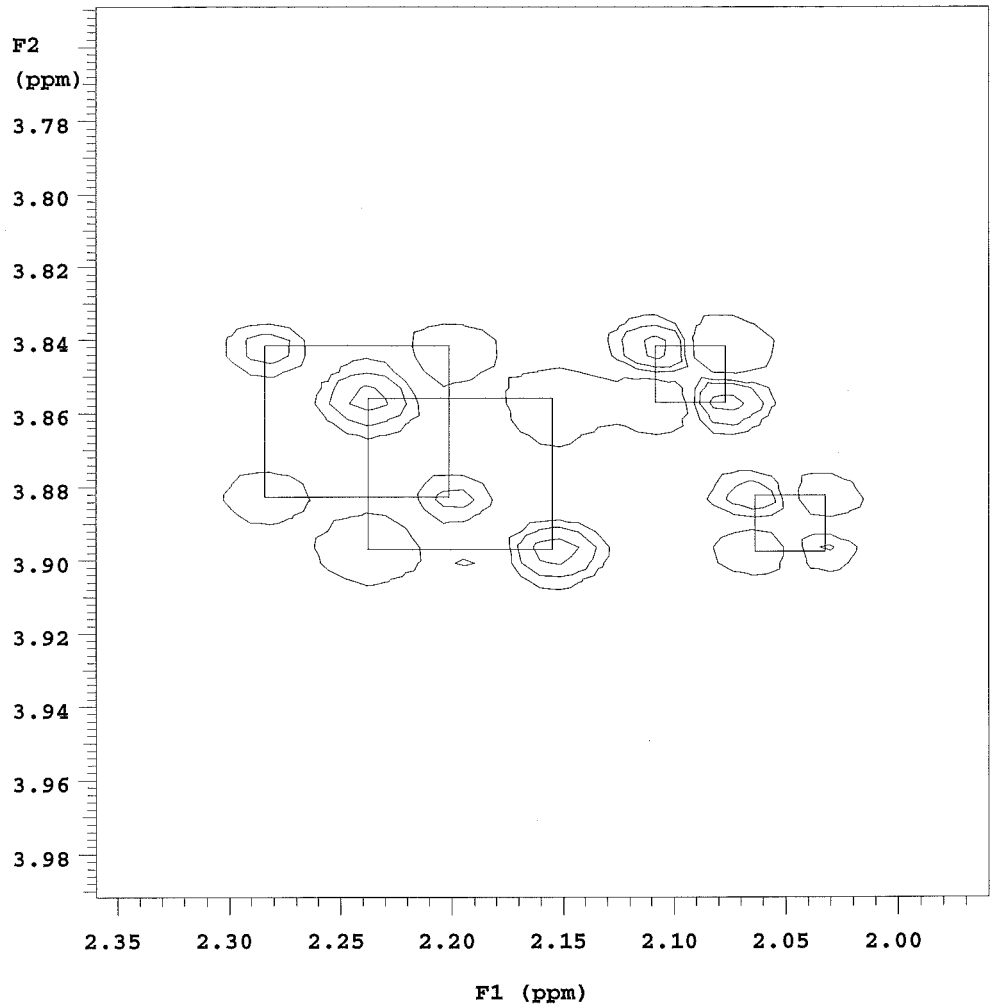

Figure 5.4 ECOSY Correlations From H3 (δH 3.89 ppm, F2 dimension) to $H4_R$ δH (2.24 ppm, $J_{3,4R}$=13 Hz, large box) and $H4_S$ (δH 2.07 ppm, $J_{3,4S}$=4 Hz, small box)

The HMQC spectrum showed correlations between $H4_R$ and $H4_S$ protons and C4 (28.19 ppm). $H4_R$ showed correlations in the ECOSY to signals for H3, $H5_R$ (1.51 ppm) and $H5_S$ (1.78 ppm). The coupling constants revealed by the ECOSY experiment showed $H5_R$ to be axial ($J_{4R,5R}$=13 Hz) and $H5_S$ to be equatorial ($J_{4R,5S}$=4 Hz). The HMQC data revealed that the two resonances due to $H5_R$ and $H5_S$ are both connected to C5 (37.02 ppm). An

HMBC trace through H3 (3.89 ppm) showed correlations to δ_C 74.92 ppm, δ_C 74.34 ppm, C5 (37.02 ppm), δ_C 30.97 ppm, C4 (28.20 ppm) and δ_C 23.65 ppm. Irradiation of $H4_R$ in an NOE experiment enhanced two methyl signals, δ_H 1.39 ppm and δ_H 1.19 ppm. A trace through δ_H 1.39 ppm in the HMBC spectrum showed correlations to δ_C 74.92 ppm, C3 (58.95 ppm) and δ_C 30.97 ppm. The HMBC correlation from δ_H 1.39 ppm to C3 (58.95 ppm) assigned δ_H 1.39 ppm to $C\underline{H}_3$-1. The HMQC experiment correlated $C\underline{H}_3$-1 (1.39 ppm) to δ_C 23.65 ppm and this resonance was assigned as $\underline{C}H_3$-1. The δ_C 74.92 ppm resonance was assigned to C2 due to its chemical shift, correlation in the HMBC experiment to $C\underline{H}_3$-1 and lack of any HMQC correlation. The δ_C 74.34 ppm correlation seen from H3 (3.89 ppm) was assigned to C6 due to its chemical shift and lack of any HMQC correlation. Although the H3 to C6 correlation is a $^4J_{CH}$, the HMBC experiment also showed a correlation from $H4_S$ (2.07 ppm) to δ_C 74.34 ppm. This left the remaining HMBC correlation from $C\underline{H}_3$-1 (1.39 ppm) to δ_C 30.97 ppm to be assigned as $\underline{C}H_3$-25. The HMQC experiment showed a correlation from $\underline{C}H_3$-25 (30.97 ppm) to δ_H 1.26 ppm ($C\underline{H}_3$-25). The remaining NOE enhancement at δ_H 1.19 ppm from irradiation of $H4_R$ (2.24 ppm) was assigned to $C\underline{H}_3$-26 as $H4_R$ and CH_3-26 are in a 1,3-diaxial conformation. The HMQC experiment showed a correlation from $C\underline{H}_3$-26 (1.19 ppm) to δ_C 20.02 ppm ($\underline{C}H_3$-26). An irradiation of H3 (3.89 ppm) in an NOE experiment enhanced $C\underline{H}_3$-25 (1.26 ppm). A 2D-TOCSY experiment showed correlations from H3 (3.89 ppm) to $H4_R$ (2.24 ppm), $H4_S$ (2.07 ppm), $H5_S$ (1.78 ppm), $H5_R$ (1.51 ppm).

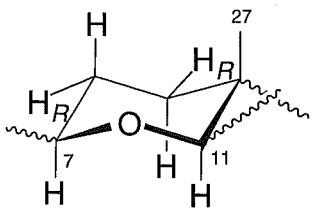

Figure 5.5 C7-C11 Fragment of Thyrsiferol (**70**)

An HMBC trace through C$\underline{H}_3$-26 (1.19 ppm) showed correlations to δ_C 86.50 ppm, C6 (74.34 ppm) and C5 (37.02 ppm). This allowed C7 to be assigned to the peak at δ_C 86.50 ppm, and thus provided the linkage between the A and B rings (Figure 5.5). An HMQC correlation between C7 and δ_H 3.04 ppm assigned H7. H7 (3.04 ppm) showed correlations in the ECOSY spectrum to H8$_R$ (1.71 ppm, $J_{7,8R}$=3 Hz, equatorial) and H8$_S$ (1.40 ppm, $J_{7,8S}$=9 Hz, axial). Both H8 protons correlated to a single carbon in the HMQC spectrum, C8 (22.96 ppm). The TOCSY experiment revealed that H7 was correlated to another proton resonating at δ_H 1.51 ppm but any other protons present were overlapping with the H8 protons. An NOE irradiation of H7 led to enhancements at δ_H 3.56 ppm and δ_H 1.51 ppm. Due to the conformation of the B ring the resonance at δ_H 3.56 ppm was assigned to H11. An HMQC correlation between H11 (3.56 ppm) and δ_C 76.26 ppm assigned C11. The NOE enhancement at δ_H 1.51 ppm was thought to be due to H5$_R$ but upon irradiation of H11, an enhancement at δ_H 1.51 ppm was also seen. This led to the conclusion that the resonance at δ_H 1.51 ppm is due also to H9$_S$ as this proton is in a 1,3-diaxial conformation with both H7 and H11. Although irradiation of H7 may enhance H5$_R$, it is coincident with any enhancement of H9$_S$. A trace through H7 (3.04 ppm) in the HMBC experiment showed correlations to C11 (76.26 ppm), C6 (74.34 ppm), δ_C 38.49 ppm, C5 (37.02 ppm), C8 (22.96 ppm) and $\underline{C}H_3$-26 (20.02 ppm). The

correlation to δ_C 38.49 ppm was assigned as being due to C9. From the HMQC data, C9 (38.49 ppm) is correlated to $H9_S$ (1.51 ppm) and another signal at δ_H 1.76 ppm which could then be assigned as $H9_R$.

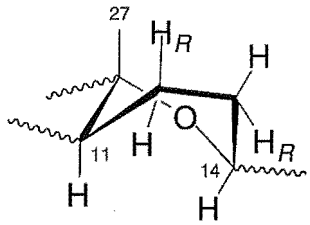

Figure 5.6 C10-C14 Fragment of Thyrsiferol (**70**)

A trace through H11 (3.56 ppm) in the HMBC spectrum revealed correlations to C7 (86.50 ppm), δ_C 71.92 ppm, C9 (38.49 ppm) and a very broad correlation to δ_C 21.30 ppm. The correlation to δ_C 71.92 ppm was assigned to C10 due to its chemical shift and lack of any HMQC correlation. The ECOSY experiment showed a correlation from H11 (3.56 ppm) to $H12_S$ (1.87 ppm, $J_{11,12S}$=7 Hz, equatorial) and $H12_R$ (1.47 ppm, $J_{11,12R}$=11 Hz, axial). Correlation in the HMQC experiment of $H12_S$ and $H12_R$ to δ_C 21.12 ppm assigned this resonance as C12. The TOCSY experiment showed further correlations from H11 (3.56 ppm) to δ_H 3.69 ppm and to δ_H 1.67 ppm. The δ_H 3.69 ppm correlation could be assigned to H14 due to the chemical shift, and the δ_H 1.67 ppm correlation must be due to one or both of the H13 protons (Figure 5.6). The HMQC experiment displayed a correlation from H14 (3.69 ppm) to C14 (76.05 ppm). The ECOSY showed a correlation from H14 (3.69 ppm) to $H13_S$ (1.82 ppm, $J_{14,13S}$=12 Hz, axial) and $H13_R$ (1.67 ppm, $J_{14,13R}$=4 Hz, equatorial). The HMQC experiment displayed a correlation from both $H13_S$ (1.82 ppm) and $H13_R$ (1.67 ppm) to δ_C 20.68 ppm

which assigned C13. An irradiation of H11 (3.56 ppm) in an NOE experiment showed an enhancement of H14 (3.69 ppm), H7 (3.04 ppm), $H12_S$ (1.87 ppm) and $H9_S$ (1.51 ppm). The enhancement of H14 by irradiation of H11 shows that the conformation of the C ring is of a boat form.

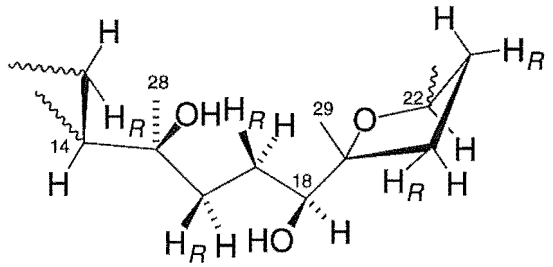

Figure 5.7 C13-C22 Fragment of Thyrsiferol (**70**)

The trace through H14 (3.69 ppm) in the HMBC experiment showed correlations to δ_C 73.21 ppm, δ_C 33.51 ppm, δ_C 22.85 ppm and C13 (20.68 ppm). An NOE enhancement of δ_H 1.09 ppm by irradiation of H14 (3.69 ppm) located $C\underline{H}_3$-28 as this is the only methyl that can adopt the correct conformation to display an enhancement (Figure 5.7). The HMQC spectrum showed a correlation between $C\underline{H}_3$-28 (1.09 ppm) and δ_C 22.85 ppm ($\underline{C}H_3$-28). A trace through $C\underline{H}_3$-28 (1.09 ppm) in the HMBC spectrum showed correlations to C14 (76.05 ppm), δ_C 73.21 ppm and δ_C 33.51 ppm. The δ_C 73.21 ppm correlation was assigned to C15 due to its chemical shift and lack of any HMQC correlation. This left the remaining HMBC correlation of δ_C 33.51 ppm still to be assigned. The HMQC spectrum showed a correlation from δ_C 33.51 ppm to δ_H 1.81 ppm and δ_H 1.37 ppm. This methylene group was assigned as C16 as no other methylene carbons showed a correlation to $\underline{C}H_3$-28 in the HMBC spectrum. Both H16 protons showed correlations in the TOCSY experiment to δ_H 3.44 ppm which in turn,

displayed a correlation to δ_C 77.60 ppm in the HMQC experiment. These were assigned to H18 and C18 respectively, due to the chemical shifts. A trace through H18 (3.44 ppm) in the HMBC experiment showed correlations to δ_C 86.01 ppm, C16 (33.51 ppm), δ_C 32.31 ppm, δ_C 25.43 ppm and δ_C 23.39 ppm. The resonance at δ_C 86.01 ppm was assigned to C19 due to its chemical shift and lack of HMQC correlation. The ECOSY experiment revealed a correlation from H18 (3.44 ppm) to δ_H 1.46 ppm and δ_H 1.55 ppm. The HMQC experiment showed a correlation from δ_C 25.43 ppm to δ_H 1.46 ppm and to δ_H 1.55 ppm and these resonances were assigned to C17 and to the H17 protons respectively. The HMQC experiment also showed a correlation from δ_C 23.39 ppm to δ_H 1.15 ppm and due to the chemical shift of these correlations these signals were assigned to C29 and C$\underline{H}_3$-29 respectively. The remaining HMBC correlation from H18 to δ_C 32.31 ppm was assigned to C20. The HMQC experiment showed a correlation from C20 (32.31 ppm) to δ_H 1.57 ppm and to δ_H 2.07 ppm, the H20 protons. The TOCSY experiment revealed correlations from both δ_H 1.57 ppm and δ_H 2.07 ppm to δ_H 3.76 ppm and to δ_H 1.81 ppm. The ECOSY experiment correlated δ_H 3.76 ppm to a lone signal at δ_H 1.81 ppm thus establishing that the H21 protons were coincident (δ_H 1.81 ppm) and that the δ_H 3.76 ppm signal was H22. The HMQC experiment showed correlations from H22 to δ_C 87.40 ppm (C22), and from the H21 protons (δ_H 1.81 ppm) to δ_C 26.57 ppm (C21). An NOE experiment irradiating C$\underline{H}_3$-29 (1.15 ppm) gave enhancement of H18 (3.44 ppm), one of the H21 protons at δ_H 1.81 ppm and the proton at δ_H 1.57 ppm (H20). H20$_R$ could now be assigned as δ_H 1.57 ppm due to the conformation of the ring, and H20$_S$ as δ_H 2.07 ppm.

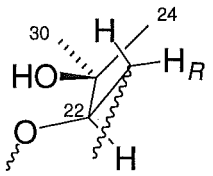

Figure 5.8 C21-C24 Fragment of Thyrsiferol (**70**)

An irradiation of H22 (3.76 ppm) in an NOE experiment showed an enhancement of one of the H21 protons at δ_H 1.81 ppm and an enhancement of two methyl signals, δ_H 1.20 ppm and δ_H 1.12 ppm. An irradiation in an NOE experiment of δ_H 1.12 ppm gave enhancements for H21 (1.81 ppm) and H22 (3.76 ppm). Irradiation of δ_H 1.20 ppm gave an enhancement for H22 (3.76 ppm) only. These NOE experiments allowed the assignment of C$\underline{H}_3$-24 as δ_H 1.12 ppm and C$\underline{H}_3$-30 as δ_H 1.20 ppm. The HMQC experiment showed correlations between C$\underline{H}_3$-24 (1.12 ppm) and δ_C 23.46 ppm, and also between C$\underline{H}_3$-30 (1.20 ppm) and δ_C 27.23 ppm, assigning $\underline{C}H_3$-24 and $\underline{C}H_3$-30 respectively (Figure 5.8).

This left CH_3-27 as the last moiety still to be assigned. The only remaining resonance is the methyl signal at δ_H 1.17 ppm which has a correlation in the HMQC experiment to δ_C 21.42 ppm. This was assigned to CH_3-27 by default. The HMBC correlations from H11 were of no use in the attempt to assign $\underline{C}H_3$-27 due to the proximity of the carbon resonances for C12 and C13.

5.3 Conclusion

This NMR study of thyrsiferol (**70**) has extended and revised the previous assignment[84] of the ^{1}H and ^{13}C NMR spectra but is still incomplete. The flexibility of the C15-C18 chain poses a challenging problem in assigning the pro-*S* and pro-*R* protons for both the H16 and the H17 protons. Several coupling constants were unable to be measured.

Experimental

General Methods

Nuclear Magnetic Resonance

All NMR spectra were recorded on a Varian Unity 300 spectrometer at 23°C, operating at 300 MHz for ^{1}H nuclei and at 75 MHz for ^{13}C nuclei. Other NMR experiments described in this thesis *viz.* 1D-TOCSY, 2D-TOCSY, ECOSY, NOE, COSY and the reverse-detected HMQC and HMBC experiments were recorded at 300 MHz. This instrument was fitted with a Nalorac Z.spec 5 mm Indirect Detection Probe, except for work described in Chapter 3, for which the data were obtained from the Varian Unity 300 spectrometer fitted with a Nalorac Z.spec MID300 3 mm Indirect Detection Probe. Chemical shifts in this thesis were described in parts per million (ppm), on the δ scale, and were referenced to the appropriate solvent peaks: $CDCl_3$ referenced to $C\mathbf{H}Cl_3$ at δ_H 7.26 ppm (^{1}H) and $\mathbf{C}HCl_3$ at δ_C 77.0 ppm (^{13}C). For Chapter 3 the $CDCl_3$ solvent had 0.01 % d_5-pyridine added to inhibit residual acidity. ^{1}H NMR spectra were recorded using an acquisition time of 2 s; ^{13}C NMR spectra were recorded using an acquisition time of 0.5 s. ECOSY experiments were recorded using an acquisition time of 0.7 s and a relaxation delay of 0.5 s. COSY experiments were recorded using an acquisition time of 0.24 s and a relaxation delay of 1 s. 2D-TOCSY spectra were recorded using an acquisition time of 0.53 s, a relaxation delay of 1 s and a mixing time of 80 ms. 1D-TOCSY spectra were recorded using an acquisition time of 2 s, a relaxation delay of 1 s and mixing times as indicated in the discussion. All HMQC and HSMQC were recorded with an acquisition time of 0.2 s, a relaxation delay of 0.4 s and $J_{X\text{-}H}$=130 Hz. HMBC experiments were recorded with an acquisition time of 0.21 s, a relaxation delay of 0.3 s, J=140 Hz and J_{NXH}=8.3 Hz.

Modelling

The simulation of spin systems described in Chapter 3 was performed on a Sun SPARCstation 2 using the spin simulation software which is part of the Varian VNMR 4.3 operating system software. The minimisation of molecular models described in Chapter 3 was performed on a VAX 6430 running VMS V5.5-2 and minimised with the MM2 option of the program MODEL version KS2.99.

Mass Spectrometry

Mass Spectrometry was performed on a Kratos MS80 Mass Spectrometer operated at 4 kV. FAB was performed with an Ion Tech ZN11FN ion gun using Xe as the reagent gas, operating at 8 kV and 2 mA with a *m*-nitrobenzyl alcohol (NOBA) matrix.

Some samples (stated) were sent to Lewis Pannell (NIDDK, NIH, U.S.A.) for HRFABMS analysis. This mass spectrometry was performed on a JEOL SX102 operated at 10 kV. FAB was performed with an JEOL FAB ion gun using Xe as the reagent gas, operating at 6 kV and 5 mA with a *m*-nitrobenzyl alcohol (NOBA) matrix.

High Performance Liquid Chromatography

Most analytical HPLC was performed on a Philips PU4100 Liquid Chromatograph equipped with a Philips PU4120 Diode Array Detector interfaced to a PC General 486 computer running Philips PU6003 Diode Array Detector System Software (V3.0) and a Hewlett Packard 7475A

Plotter. Some analytical work described in Chapter 3 was performed on a Shimadzu LC-4A instrument equipped with a Shimadzu UV Spectrophotometric Detector SPD-2AS and a Hewlett Packard 3390A integrator using a Supelcosil-LC-(*R*)-UREA column (250 mm x 4.6 mm, 5μm), eluting with propan-2-ol/hexane (1:200) at a flow rate of 750 μL/minute. H_2O was purified using a MilliQ deionising system. MeOH (J.T. Baker, HPLC reagent grade) and acetonitrile (BDH, HiPerSolv) solvents were used undistilled. All other solvent were of technical grade and were purified and re-distilled before use. All solvents were filtered through a Millipore filter apparatus equipped with a Rainin Nylon-66 filter (0.45 μm) prior to use. All samples were filtered through a syringe filter (Alltech, 0.45 μm) prior to injection.

Column Chromatography

Octadecyl (C18) reverse-phase packing used for preparative and flash column chromatography was prepared from silica gel (Davisil, 35-70 μm) using a solution of octadecyltrichlorosilane (2 % *v/v*, EGA-Chemie) in carbon tetrachloride.[89] The silica gel was stirred gently with a teflon-coated magnetic follower overnight before washing with carbon tetrachloride (x 2). Unreacted chloride groups were removed by washing with dry MeOH. A carbon tetrachloride solution of trimethylchlorosilane (2 % *v/v*, Aldrich) was used to end-cap any unreacted hydroxyl groups. The reverse-phase material was finally washed with CH_2Cl_2 (x 2) and MeOH (x 2) to remove the reagents. The C18 reverse-phase material was extensively washed with MeOH immediately before use. Small scale preparative C18 reverse-phase column chromatography was performed using either 200 mg Alltech

disposable cartridges or, more commonly, using 500 mg BondElut disposable cartridges. DIOL column chromatography was performed using either Bakerbond DIOL (40 μm APD) packing material in glass columns of stated dimensions or using 500 mg DIOL Bakerbond disposable cartridges. Carboxylic acid (CBA) column chromatography was performed using either Bakerbond CBA (40 μm APD) packing material in glass columns of stated dimensions or using 500 mg CBA BondElut cartridges. Cyano column chromatography was performed using 500 mg cyano BondElut disposable cartridges. Amino column chromatography was performed using either Bakerbond amino (40 μm APD) packing material in glass columns of stated dimensions or using 500 mg amino BondElut disposable cartridges. Celite filtration and coating was performed using diatomaceous earth (Celite Corporation). LH-20 column chromatography was performed using pre-swollen Sephadex LH-20 (Pharmacia Biotech AB) packing material in glass columns of stated dimensions.

Thin Layer Chromatography

The silica analytical TLC described in this thesis was performed using Merck silica gel 60 F_{254} plastic or aluminium-backed sheets, the silica 0.2 mm in thickness. DIOL analytical TLC was performed using Merck F_{254} glass-backed plates of 0.2 mm thickness. Whatman $MKC_{18}F$ TLC plates of 0.2 mm thickness were used for analytical C18 TLC performed in this thesis. Cyano TLC was performed on Merck F_{254} glass-backed plates of 0.2 mm thickness. Amino analytical TLC was performed on Merck F_{254} glass-backed plates of 0.2 mm thickness. Silica TLC plates containing pateamine or the major fragment of pateamine were visualised with H_2SO_4 in ethanol (1:1). All

other silica and DIOL plates were visualised initially under short-wave (λ 254 nm) light and subsequently with phosphomolybdic acid in ethanol spray (10 % phosphomolybdic acid in ethanol *w/v*).

Solvents

Technical grade solvents were distilled and dried using standard procedures. Dry methanol was distilled from freshly prepared magnesium methoxide immediately before use. Hexane was prepared from petroleum ether (10 L, b.pt. 60-70°C), nitrated with a mixture of *c.* HNO_3 (1 L) and *c.* H_2SO_4 (1 L) for two days. After this time, the nitrating mixture was removed and the organic layer washed with H_2O (20 L), and dried over $CaCl_2$ overnight. The resulting solution was filtered through activated alumina (Laporate, 100 mesh) and distilled.

Halisarca Sp.

First Extraction (90OP 18-1)

Halisarca sp. (1 kg wet weight, HSV, ?; Hcyt 3+ (10, 4); PV1, ?; Pcyt, 4+, (4); P388, 4230 10^{-6} dil; no antimicrobial activity, see appendices for an explanation of the codes for the antiviral and antimicrobial assays performed at the University of Canterbury) was steeped in MeOH (1 L) overnight at 4°C. The MeOH was decanted off and the sponge was then homogenised with MeOH (2 L) in a Waring blender and extracted overnight at 4°C. The mat was re-homogenised in MeOH/CH_2Cl_2 (3:1, 1 L), and again filtered through Celite. The solvents were removed *in vacuo* to yield a mobile yellow/green oil (40 g). The combined extracts were partitioned between H_2O (2 x 200 mL) and CH_2Cl_2 (2 x 200 mL). The solvents were removed *in vacuo* to give a white friable powder (H_2O fraction, 21.7 g, IC_{50} >25000 ng/mL) and a green/yellow gum (CH_2Cl_2 fraction, 18.6 g, 1597 ng/mL).

Chemical screening was carried out as follows (full details of the current protocol can be found in Appendix I): an aliquot (2 mg) of the active fraction was dissolved in 50:50 MeOH/H_2O and loaded onto a reverse-phase C18 cartridge. Four fractions (3 mL) were collected from a steep stepped gradient (F1, 50:50 MeOH/H_2O, 2697 10^{-6} dil; F2, 80:20 MeOH/H_2O, 181 10^{-6} dil; F3, MeOH, <97.5 10^{-6} dil; F4, 10:90 CH_2Cl_2/MeOH, <97.5 10^{-6} dil). Another aliquot of the same active fraction (3 mg) was dissolved in benzene and loaded onto a DIOL cartridge. Five fractions (3 mL) were collected from a stepped gradient (benzene 0.3 mg, >12500 ng/mL; hexane, 0.3 mg, >12500 ng/mL; 5:95 CH_2Cl_2/hexane , 1.0 mg, >12500 ng/mL; CH_2Cl_2, 0.1 mg, >12500 ng/mL; MeOH, 1.4 mg, 109.9 ng/mL). Finally,

another aliquot of the same active fraction (1.7 mg) was dissolved in MeOH and loaded onto a CBA cartridge. Three fractions (3 mL) were collected from a "pH" gradient (MeOH, 1.9 mg, 134 ng/mL; MeOH/TFA (1 drop), 0.4 mg, 134 ng/mL; MeOH/NH_3 (1 drop), 0.3 mg, >12500 ng/mL).

The CH_2Cl_2 fraction was chromatographed on a C18 reverse-phase column (28 mm x 400 mm, 100 g). The CH_2Cl_2 suspension of the fraction was mixed with C18 packing material to form a slurry and the solvents removed *in vacuo*. The coated C18 packing material was then dry packed onto the column that was equilibrated to 25:75 MeOH/H_2O. Seventeen fractions were collected from the column, which was eluted with a stepped gradient from 25:75 MeOH/H_2O through MeOH to 10:90 CH_2Cl_2/MeOH, then stripped with MeOH and CH_2Cl_2. The active material was contained in fractions 6 through 12 (F6, 70:30 MeOH/H_2O, 17.0 mg, 99.5 ng/mL; F7, 70:30 MeOH/H_2O, 18.6 mg, 134.3 ng/mL; F8, 80:20 MeOH/H_2O, 38.9 mg, 51.9 ng/mL; F9, 80:20 MeOH/H_2O, 11.4 mg, 20.0 ng/mL; F10, 90:10 MeOH/H_2O, 68.0 mg, >125 ng/mL; F11, 90:10 MeOH/H_2O, 111.9 mg, 60.3 ng/mL; F12, MeOH, 375.8 mg, 200 ng/mL).

Fractions 9, 10 and 11 were combined (191 mg) and chromatographed on a normal-phase DIOL column (12 mm x 300 mm, 12 g) equilibrated to CH_2Cl_2. Nine fractions were collected from the column, which was eluted with a gradient from CH_2Cl_2 through EtOAc to MeOH. The active material eluted early off the column (F1, CH_2Cl_2, 46.6 mg, 22 ng/mL; F2, 20:80 CH_2Cl_2/EtOAc, 40.4 mg, 232 ng/mL). Fractions 8 and 12 from the previous C18 column were combined (413 mg) and chromatographed on a larger

DIOL column (28 mm x 200 mm, 20 g) equilibrated to benzene. Ten fractions were collected from the column, which was eluted with a gradient from benzene through CH_2Cl_2 to MeOH. The active material was contained in fractions 3 through 8 (F3, 25:75 benzene/CH_2Cl_2, 24.2 mg, 27 ng/mL; F4, 50:50 benzene/CH_2Cl_2, 34.1 mg, 49.4 ng/mL; F5, 25:75 benzene/CH_2Cl_2, 20.6 mg, 63.4 ng/mL; F6, CH_2Cl_2, 15.4 mg, 66.6 ng/mL; F7, 50:50 MeOH/CH_2Cl_2, 8 mg, 221 ng/mL; F8, 25:75 MeOH/CH_2Cl_2, 71.2 mg, 49 ng/mL).

Fraction 8 from the latter DIOL column was used in an attempt to develop the chemical screening technique using amino and strong anion exchange (SAX) cartridges. The 4 amino cartridges and 1 SAX cartridge were loaded with equal aliquots of fraction 8 from the latter DIOL column and prepared and eluted with different schemes. The amino cartridge 1 was prepared with MeOH followed by 0.01 % TFA in MeOH and eluted with MeOH, 2 % NH_4OH/MeOH, 2 % TFA/MeOH; amino cartridge 2 was prepared with MeOH followed by 2 % NH_4OH/MeOH and eluted with MeOH, 0.01 % TFA/MeOH, 2 % NH_4OH/MeOH; amino cartridge 3 was prepared with MeOH and eluted with MeOH, 2 % NH_4OH/MeOH, 0.01 % TFA/MeOH; amino cartridge 4, a previously used column, was prepared by MeOH followed by 0.01 % TFA in MeOH, eluted with MeOH, 2 % NH_4OH/MeOH, 0.01 % TFA/MeOH. All amino cartridges destroyed or retained the activity. The SAX cartridge (100 mg) was prepared with MeOH and eluted with MeOH, 2 % NH_3 in MeOH and 0.01 % TFA in MeOH. All the activity was contained in fraction 1 (F1, MeOH, MeOH, 5.1 mg, 97.5 ng/mL)

The active fractions from the earlier DIOL column were chromatographed on two identical LH-20 gel permeation columns (16 mm x 300 mm, 20 g). The first column is described, but the results were identical for both. The active fraction (40 mg) was dissolved in MeOH and loaded onto the LH-20 column, which was eluted with MeOH. Eighty three fractions (20 mL) were collected after the void volume with the activity diffused throughout the first 29 fractions. All fractions from both columns showing activity were combined (43.4 mg). Analysis of this fraction by ^{1}H NMR revealed contamination by plasticiser.

The contaminated active material from both LH-20 columns was chromatographed on a normal-phase DIOL column (10 mm x 200 mm, 7 g) equilibrated to benzene. Eight fractions were collected from the column, which was eluted with a gradient from benzene through CH_2Cl_2 to MeOH. The active material eluted in fractions 4 through 7 (F4, CH_2Cl_2, 1.5 mg, 14.8 ng/mL; F5, 25:75 MeOH/CH_2Cl_2, 9.0 mg, <97.5 ng/mL; F6, 50:50 MeOH/CH_2Cl_2, 7.8 mg, 99.4 ng/mL; F7, 50:50 MeOH/CH_2Cl_2, 16.7 mg, 54.6 ng/mL).

Significant activity was lost in further attempts to develop the chemical screening technique using amino and CBA cartridges. The active fractions were combined and equal aliquots loaded onto an amino and a CBA cartridge. The amino cartridge was prepared with MeOH followed by 0.1 % TFA in MeOH, then eluted with MeOH, followed by 2 % NH_4OH/MeOH, and 2 % TFA/MeOH. The CBA cartridge was prepared with MeOH followed by 0.1 % TFA in MeOH, then eluted with MeOH, 2 % NH_4OH/MeOH. The

amino cartridge returned activity early (F1, MeOH, 1.5 mg, 97.5 ng/mL) and the CBA cartridge returned activity late (F2, 2 % NH_4OH/MeOH, 3.9 mg, 200 ng/mL).

Second Extraction of Halisarca (90OP 19-4)

Halisarca sp. (740 g wet weight, HSV, ?; Hcyt 3+ (10, 4); PV1, ?; Pcyt, 3+, (4); P388, 5432 10^{-6} dil; no antimicrobial activity) was sonicated in distilled H_2O (1 L), to remove the mucous material permeating the sponge, the resulting solution drained off and the sample re-sonicated (1 L). The two H_2O solutions were combined and freeze dried. The sponge was then homogenised with MeOH (2 L) in a Waring blender with Celite (400 g), and extracted overnight at 4°C. The resulting homogenate was filtered through Celite to give a yellow coloured filtrate. The mat was re-homogenised in CH_2Cl_2 (1 L) then again filtered through Celite. The solvents were removed *in vacuo* to yield a light brown crusty powder (16.1 g), a yellow/brown gum (14.0 g) and a brown gum respectively (1.1 g). Assays revealed that the cytotoxic material was contained in the MeOH soluble extract (H_2O soluble extract, IC_{50} >12500 10^{-6} dil; MeOH soluble extract, IC_{50} 2980 10^{-6} dil; CH_2Cl_2 soluble extract, IC_{50} >12500 10^{-6} dil).

The MeOH fraction (14.0 g) was concentrated, which resulted in formation of a precipitate that was resolubilised with the addition of CH_2Cl_2. The MeOH/CH_2Cl_2 suspension of the fraction was mixed with Celite to form a slurry and the solvents removed *in vacuo*. The coated Celite was then dry-packed onto a C18 reverse-phase column (28 mm x 400 mm, 100 g), equilibrated to 25:75 MeOH/H_2O. Twelve fractions were collected from the

column, which was eluted with a stepped gradient from 25:75 MeOH/H_2O through MeOH to CH_2Cl_2 then back to MeOH. The active material was contained in fractions 5 through 10 (F5, 85:15 MeOH/H_2O, 101.0 mg, 518 ng/mL; F6, 90:10 MeOH/H_2O, 59.8 mg, 424 ng/mL; F7, MeOH, 73.2 mg, 275 ng/mL; F8, 90:10 MeOH/CH_2Cl_2, 133.4 mg, 773 ng/mL; F9, 80:20 MeOH/CH_2Cl_2, 612.8 mg, 172 ng/mL; F10, 80:20 MeOH/CH_2Cl_2, 667.3 mg, 347 ng/mL).

Fractions 5, 6, 7, 8, and 9 (978 mg) were combined and partitioned between H_2O and CH_2Cl_2. All the activity was in the organic phase (518.4 mg, 898 ng/mL). The active material was chromatographed on an LH-20 gel permeation column (16 mm x 300 mm, 20 g). Forty one fractions were collected after the void volume, with no activity detectable in any fraction.

Fraction 10 was chromatographed on a normal-phase DIOL column (12 mm x 300 mm, 12 g) equilibrated to hexane. Nine fractions were collected from the column, which was eluted with a stepped gradient from hexane through CH_2Cl_2 to MeOH. The active material was contained solely in fraction 5 (F5, CH_2Cl_2, 14.4 mg, 127 ng/mL, 8.9 % recovery of activity).

Various HPLC profiles were used in an attempt to further purify the active component, however these attempts were unsuccessful, and the entire 14 mg of active material was consumed.

Third Extraction of Halisarca (91OP 28-2)

Halisarca sp. (800 g wet weight, no antiviral activity; P388, 8103 10^{-6} dil; no antimicrobial activity) was sonicated in distilled H_2O (1 L), the resulting solution drained off and the sample re-sonicated (1 L). The two H_2O solutions were combined and freeze dried. The sponge was then homogenised with MeOH (2 L) in a Waring blender with Celite (400 g), and extracted overnight at 4°C. The resulting homogenate was filtered through Celite to give a yellow coloured filtrate. The residue was re-homogenised in CH_2Cl_2 (1 L) then again filtered through Celite. The solvents were removed *in vacuo* to yield a white crusty powder (15.3 g), a yellow/brown gum (8.6 g) and a brown gum respectively (1.4 g). Assays revealed that the cytotoxic material was contained mainly in the MeOH soluble extract (H_2O soluble extract, IC_{50} 4914 ng/mL; MeOH soluble extract, IC_{50} <97.5 ng/mL; CH_2Cl_2 soluble extract, IC_{50} 1480 ng/mL). The MeOH extract was partitioned between H_2O (2 x 100 mL) and CH_2Cl_2 (2 x 100 mL). The solvents were removed *in vacuo* to give a brown friable powder (H_2O fraction, 7.81 g, IC_{50} 13394 ng/mL) and a green/yellow gum (CH_2Cl_2 fraction, 370 mg, 121 ng/mL). TLC showed a large amount of sterols present (Silica gel, 95:5 CH_2Cl_2/MeOH, phosphomolybdic acid spray, R_f 0.75).

The active fraction (361 mg) was chromatographed on a C18 reverse-phase column (18 mm x 270 mm, 15 g). The MeOH/CH_2Cl_2 suspension of the fraction was mixed with Celite to form a slurry, and the solvents removed *in vacuo*. The coated Celite was then dry packed onto the column, and equilibrated to 50:50 MeOH/H_2O. Thirteen fractions were collected from the column, which was eluted with a stepped gradient from 50:50 MeOH/H_2O

through MeOH to 5:95 CH_2Cl_2/MeOH, and then stripped with MeOH and CH_2Cl_2. The active material was contained in fractions 7, 8, 9, and 10 (F7, 90:10 MeOH/H_2O, 15.8 mg, <97.5 ng/mL; F8, MeOH, 15.2 mg, 134 ng/mL; F9, MeOH, 35.8 mg, 190 ng/mL; F10, MeOH, 67.7 mg, 200 ng/mL).

Fractions 7,8,9 and 10 were combined (130 mg), and then chromatographed on a normal-phase DIOL column (10 mm x 200 mm, 7 g) equilibrated to hexane. Sixteen fractions were collected from the column, which was eluted with a gradient from hexane through CH_2Cl_2 to MeOH. The active material eluted late off the column (F14, CH_2Cl_2, 32.0 mg, 17.7 ng/mL; F15, 50:50 CH_2Cl_2/MeOH, 65.8 mg, 35 ng/mL; F16, MeOH, 4.4 mg, 281 ng/mL).

F15 was re-chromatographed on a DIOL cartridge, with four fractions being collected (F1, 50:50 hexane, 24.0 mg, 89 ng/mL; F2, CH_2Cl_2, 12.4 mg, 56 ng/mL; F3, 50:50 CH_2Cl_2/MeOH, 17.3 mg, 1122 ng/mL; F4, MeOH, 0.3 mg, 1122 ng/mL).

F14 was further chromatographed on an amino cartridge, with three fractions being eluted using a stepped gradient from CH_2Cl_2 through EtOAc to MeOH. Only slight activity was recovered (F1, CH_2Cl_2, 1.7 mg, 125 ng/mL; F2, EtOAc, 4.1 mg, 354 ng/mL; F3, MeOH, 4.7 mg, 2511 ng/mL). With this result, and the other failed attempts at using this sorbent, amino was discounted for further purification of the active material.

The three active fractions from the DIOL cartridge and the two remaining active fractions from the DIOL column were combined (17.4 mg, 100 ng/mL).

This was dissolved in MeOH/acetonitrile/H_2O (1:1:1, 500 μL), filtered, and injected onto a reverse-phase C18 preparative HPLC column (Rainin Dynamax-60A, 250 mm x 21.4 mm, 55:45 ACN/H_2O, 5 mL/minute, UV detection at 200 nm). Six fractions were collected, then the column was stripped. The combined weight of the six fractions (4.7 mg) and the strip (3.8 mg) only accounted for 50 % of the mass. Assays revealed no activity remained.

Pateamine

4*S*-Hydroxy-2-pentanone (**29**)

Baker's yeast (25 g, Bluebird Foods) and table sugar (10 g) were mixed with tap water (140 mL) and stirred for 5 minutes by a magnetic follower. Acetylacetone (1.4 mL) was added, and the reaction mix isolated from the atmosphere by a non-return water trap. The mix was stirred for 5 days at room temperature. The suspension was centrifuged (4000 rpm, 15 minutes), and the supernatant decanted from the pellet. The aqueous solution was extracted with CH_2Cl_2 (3 x 100 mL), then freeze-dried to approximately half the original volume and re-extracted with CH_2Cl_2 (100 mL). All the CH_2Cl_2 extracts were combined, and the solvent evaporated to give a viscous dark brown tar (0.5 mL). Simple vacuum distillation to dryness (20 mm Hg) of the tar gave 4*S*-hydroxy-2-pentanone (**29**) (107 mg), a colourless viscous oil; ^1H NMR δ_H: 4.22 (m, 1H, H4), 2.62 (dd, 1H, J=3.4, 17.5 Hz, H3$_S$), 2.52 (dd, 1H, J=8.5, 17.5 Hz, H3$_R$), 2.15 (s, 3H, H1), 1.16 (d, 3H, J=6.4 Hz, H5) ppm.

Racemic 4-Hydroxy-2-pentanone (**30**)

Acetaldehyde (11 g, 0.25 mol) was passed as a vapour in a stream of dry nitrogen into a 250 mL round bottom flask containing acetone (94 mL), MeOH (6 mL), and potassium hydroxide (0.34 g) during 1.5 hours. Oxalic acid was added to neutralise the product, the precipitate was removed by vacuum filtration, and the residue was fractionally distilled, collecting the fraction with b. p. 65-75°C at 20 mm Hg to give racemic 4-hydroxy-2-pentanone (**30**) (20 mL), a colourless viscous oil.

Chiral Gas Chromatography on 4-Hydroxy-2-pentanone (**29**, **30**)

4*S*-Hydroxy-2-pentanone (**29**) was analysed by chiral gas chromatography (Carlo-Erba/Kratos, MSC500 HRGC, injector; 100°C) using a 30 m x 0.32 mm Cyclodex-B column (J&W, 0.25 μm film, 35°C isothermal), with He as the carrier gas and a mass spectrometer as a detector, to give a retention time of 6 minutes 17 seconds. Injection of racemic 4-hydroxy-2-pentanone (**30**) allowed the assignment of the peak with the retention time of 6 minutes 11 seconds as the (*R*) isomer. Racemic 4-hydroxy-2-pentanone (**30**) spiked with 4*S*-hydroxy-2-pentanone (**29**) enhanced the latter peak confirming that the (*S*) isomer was retained relative to the (*R*) isomer.

(*S*)-α-Methoxy-α-(trifluoromethyl)phenylacetylchloride ((*S*)-MTPACl)

The following is a representative synthesis of a number that were carried out. The reaction was scaled as necessary.

(*R*)-α-Methoxy-α-(trifluoromethyl)phenylacetic acid ((*R*)-MTPA) was added as a CH_2Cl_2 solution to a 1 mL Reactivial and taken to dryness. The (*R*)-MTPA was dissolved in hexane (0.5 mL), then DMF (9 μL) and oxalyl chloride (5 μL) were added producing copious quantities of white precipitate and generating gases. After 40 minutes reaction time extra oxalyl chloride (5 μL) was added. After a further 20 minutes the solution was filtered through an HPLC filter (0.45 μm) into a 5 mL Reactivial. Hexane (2 x 0.5 mL) was used to rinse the reaction vessel. The Reactivial was placed under vacuum (1 mm Hg) for 1 hour to yield (*S*)-MTPACl in 95 % yield (by ^{1}H NMR). ^{1}H NMR δ_H: 7.52 (m, 2H, phenyl), 7.46 (m, 3H, phenyl), 3.76 (q, 3H, F-HJ_5=1.9 Hz) ppm.

(*R*)-α-Methoxy-α-(trifluoromethyl)phenylacetylchloride ((*R*)-MTPACl)

(*R*)-MTPACl was formed in an identical manner to (*S*)-MTPACl.

4*S*-((*S*)-MTPA)-2-pentanone (**34**)

4*S*-Hydroxy-2-pentanone (**34**) (10.2 mg), triethylamine (40 μL) and N,N-dimethylaminopyridine (4.0 mg) were mixed and transferred in CH_2Cl_2 (2 x 500 μL) to a 5 mL Reactivial containing (*R*)-MTPACl (28 mg). After 22 hours the solution was blown to dryness under a stream of N_2 and taken up in benzene (1 mL). This solution was chromatographed on silica (6 mm x 30 mm, 2 g) equilibrated to benzene. Fraction 1 (F1, 5 mL benzene) gave 4*S*-((*S*)-MTPA)-2-pentanone (**34**) (5 mg) in 16 % yield. ^{1}H NMR δ_H: 7.49 (m, 2H, phenyl), 7.40 (m, 3H, phenyl), 5.56 (m, 1H, H4), 3.51 (s, 3H, MTPA-OC$\underline{H}_3$), 2.91 (dd, 1H, *J*=8.3, 17.1 Hz, H3a), 2.60 (dd, 1H, *J*=4.6, 17.1 Hz, H3b), 2.13 (s, 3H, H1), 1.31 (d, 3H, *J*=5.9 Hz, H5) ppm.

(*S*)-MTPA Esters of Racemic Hydroxyketone (**34,36**)

(*S*)-MTPA esters of racemic hydroxyketone (**34,36**) were formed in a similar but scaled down manner to 4*S*((*S*)-MTPA)-2-pentanone (**34**) to give both 4*S*-((*S*)-MTPA)-2-pentanone (**34**) and 4*R*((*S*)-MTPA)-2-pentanone (**36**) (1.5 mg) in 47 % yield. 4*R*-((*S*)-MTPA)-2-pentanone (**36**) ^{1}H NMR δ_H: 7.49 (m, 2H, phenyl), 7.40 (m, 3H, phenyl), 5.56 (m, 1H, H4), 3.55 (s, 3H, MTPA-OC$\underline{H}_3$), 2.85 (dd, 1H, *J*=7.8, 17.1 Hz, H3a), 2.60 (dd, 1H, *J*=5.1, 17.1 Hz, H3b), 2.04 (s, 3H, H1), 1.39 (d, 3H, *J*=5.1 Hz, H5) ppm.

Extraction of 94FL04-12

The following extraction procedure is a representative extraction of a number that were carried out. 150 mg of pateamine (**3**) was isolated in total.

Frozen *Mycale* sp. (2.2 kg wet weight) was thawed in MeOH (2 L) overnight and then homogenised in a Waring blender. The resultant homogenate was then filtered through Celite to give a dark brown filtrate. The mat was re-homogenised in MeOH (1 L), re-filtered then re-homogenised and soaked overnight at 4°C with 33:66 CH_2Cl_2/MeOH. The homogenate was then filtered, and the mat washed with MeOH (1 L). All filtrates were combined, concentrated and re-filtered through Celite. The solvents were removed *in vacuo* to give a green/brown gum (58.6 g). The gum was homogenised by sonification in MeOH (600 mL) and diluted to 50:50 MeOH/H_2O. This homogenate was loaded onto a reverse-phase C18 column (170 mm x 70 mm, 1 kg). 14 fractions (1 L) were collected from the column, which was eluted with a stepped gradient from 50:50 MeOH/H_2O to CH_2Cl_2 and back to MeOH. Assays revealed that fractions 9 through 14 contained all of the activity (F9, 10:90 CH_2Cl_2/MeOH, 1.16 g, <97.5 ng/mL; F10, 20:80 CH_2Cl_2/MeOH, 970 mg, <97.5 ng/mL; F11, 50:50 CH_2Cl_2/MeOH, 400 mg, <97.5 ng/mL; F12, CH_2Cl_2, 230 mg, <97.5 ng/mL; F13, 50:50 CH_2Cl_2/MeOH, 220 mg, <97.5 ng/mL; F14, MeOH, 1 g, <97.5 ng/mL).

Fractions 9 through 14 were combined (4.23 g) and then chromatographed on a CBA column (28 x 300 mm, 100 g) equilibrated to 0.05 % trifluoroacetic acid (TFA)/MeOH. 32 fractions (20 mL) were collected from the column, which was eluted with a gradient from 0.05 % TFA/MeOH through MeOH,

and then with 0.05 % NH_4OH/MeOH, to 2 % NH_4OH/MeOH. Assays revealed that fractions 3 through 15 were active, as was the final fraction. Silica TLC (2 % NH_4OH/MeOH, 50:50 *c.* H_2SO_4/EtOH, heat) showed that all the active fractions contained yellow spots at R_f 0.2 and 0.3. These yellow charring spots have previously been found to correspond to the pateamine family of compounds.[90] Fraction 32 (84.6 mg) showed much pateamine character (by ^1H NMR) and was dissolved in MeOH (1 mL) then chromatographed on an amino cartridge (500 mg) equilibrated to MeOH. Two fractions (5 mL) were collected, with the yellow charring material occuring in fraction 1 (MeOH, 68 mg).

Fraction 1 was dissolved in CH_2Cl_2 (1 mL) and chromatographed on a normal-phase DIOL column (10 x 230 mm, 8 g) equilibrated to CH_2Cl_2. Four fractions were collected from the column, which was eluted with a gradient from CH_2Cl_2 to acetone containing a trace of TFA. The yellow charring material was contained in fraction 3 (MeOH, 38 mg).

Fraction 3 was dissolved in MeOH (1 mL) and re-chromatographed on a CBA column (20 mm x 40 mm, 5 g) equilibrated to MeOH. Two fractions were collected, with the yellow charring material eluting off in fraction 2 (2 % NH_4OH/MeOH, 25.4 mg). Fraction 2 was not totally soluble in CH_2Cl_2, so the material was filtered through an HPLC filter (0.45 μm) to give pateamine (**3**) (22 mg).

24*S*-Hydroxydienoate (**37**)

Pateamine (**3**, 10 mg) was added to a sodium methoxide solution (5 mL; Na (0.86 g) in dry MeOH (20 mL)) at room temperature. After 4 hours, the solution was diluted with H_2O (10 mL), neutralised by the addition of TFA and the products trapped onto a reverse-phase C18 cartridge (Alltech; 200 mg) equilibrated to H_2O. The C18 phase was washed with H_2O (10 mL), before being stripped with MeOH (2 mL). The MeOH was removed under a stream of N_2, and the resultant yellow gum triturated with CH_2Cl_2 to give crude 24*S*-hydroxydienoate (**37**). Crude 24*S*-hydroxydienoate (**37**) was further purified by passage through a CBA cartridge (Analytichem; 300 mg) in MeOH in order to remove traces of unreacted pateamine (**3**), to give (**37**) (2.2 mg) in 67 % yield and a trace (by ^{1}H NMR) of (**38**). ^{1}H NMR (**37**) δ_H: 7.23 (br d, 1H, *J*=11.7 Hz, H4), 6.88 (t, 1H, *J*=11.7 Hz, H3), 5.63 (d, 1H, *J*=11.7 Hz, H2), 4.02 (m, 1H, H7), 3.72 (s, 3H, OC$\underline{H}_3$), 2.32 (d, 2H, *J*=6.3 Hz, H6), 1.89 (d, 3H, *J*=1.4 Hz, H9), 1.23 (d, 3H, *J*=6.3 Hz, H8) ppm; ^{1}H NMR (**38**) δ_H: 7.57 (dd, 1H, *J*=11.2, 11.7 Hz, H3), 6.06 (br d, 1H, *J*=11.7 Hz, H4), 5.83 (d, 1H, *J*=15.6 Hz, H2), 4.03 (m, 1H, H7), 3.75 (s, 3H, OC$\underline{H}_3$), 2.27 (d, 2H, *J*=6.8 Hz, H6), 1.93 (d, 3H, *J*=1.4 Hz, H9), 1.22 (d, 3H, *J*=5.3 Hz, H8) ppm.

Attempt at Osmylation of (*S*)-Hydroxydienoate (**37**)

A CH_2Cl_2 solution of (*S*)-hydroxydienoate (1 mg) was taken to dryness in a 1 mL Reactivial and dissolved in ether (100 µL). OsO_4 (2 mg) was transferred to the Reactivial in ether (40 µL), then pyridine (30 µL) was added, the reaction capped with a septa, and left for 3 hours at RT. A solution of $Na_2S_2O_5$ (9 mg in 260 µL H_2O) was added, and the resulting mix extracted with CH_2Cl_2 (3 x 1 mL) and the solvent removed. $NaIO_4$ (5 mg in 200 µL

H_2O) was added, a triangular magnetic follower placed in the Reactivial and the reaction left stirring for 48 hours. The solution was extracted with CH_2Cl_2 (3 x 500 µL). ^1H NMR spectra showed no (*S*)-hydroxydienoate or 4*S*-hydroxy-2-pentanone.

24*S*((*R*)-MTPA)-hydroxydienoate (Synthetic) (**39**)

24*S*-Hydroxydienoate (**37**) (1 mg), triethylamine (4 µL) and N,N-dimethylaminopyridine (approx. 0.1 mg) were mixed and transferred in CH_2Cl_2 (2 x 100 µL) to a 1 mL Reactivial containing (*S*)-MTPACl. After 1 hour the solution was blown to dryness under a stream of N_2 and taken up in benzene (200 µL). This solution was chromatographed on silica (6 mm x 20 mm, 1.5 g) equilibrated to benzene. Fraction 1 and 2 (F1, 1 mL benzene, 0.5 mg; F2, 1 mL CH_2Cl_2, 0.8 mg) were combined to give 24*S*((*R*)-MTPA)-hydroxydienoate (**39**) in 57 % yield. ^1H NMR (pateamine numbering) δ_H: 7.49 (m, 2H, phenyl), 7.36 (m, 3H, phenyl), 7.14 (d, 1H, *J*=11.7 Hz, H21), 6.76 (t, 1H, *J*=11.7 Hz, H20), 5.60 (d, 1H, *J*=11.7 Hz, H19), 5.37 (m, 1H, H24), 3.70 (s, 3H, $OC\underline{H}_3$), 3.53 (d, 3H, *J*=1.0 Hz, MTPA-$OC\underline{H}_3$), 2.52 (dd, 1H, *J*=7.8, 13.7 Hz, H23a), 2.36 (dd, 1H, *J*=5.6, 13.9 Hz, H23b), 1.77 (bs, 3H, H31), 1.36 (d, 3H, *J*=6.4 Hz, H25) ppm.

24*S*((*R*)-MTPA)-hydroxydienoate (Pateamine Derived) (**39**)

24*S*((*R*)-MTPA)-hydroxydienoate (**39**) derived from pateamine was formed in an identical manner to synthetic 24*S*((*R*)-MTPA)-hydroxydienoate (**39**) in 24 % yield (0.9 mg). ^1H NMR (pateamine numbering) δ_H: 7.49 (m, 2H, phenyl), 7.36 (m, 3H, phenyl), 7.14 (d, 1H, *J*=12.2 Hz, H21), 6.76 (t, 1H, *J*=11.5 Hz, H20), 5.60 (d, 1H, *J*=11.7 Hz, H19), 5.37 (m, 1H, H24), 3.70 (s, 3H, $OC\underline{H}_3$),

3.53 (d, 3H, *J*=1.0 Hz, MTPA-OC$\underline{H}_3$), 2.52 (dd, 1H, *J*=8.0, 14.0 Hz, H23a), 2.36 (dd, 1H, *J*=5.1, 14.0 Hz, H23b), 1.77 (d, 3H, *J*=1.0 Hz, H31), 1.36 (d, 3H, *J*=6.3 Hz, H25) ppm.

24*S*((*S*)-MTPA)-hydroxydienoate (synthetic) (**40**)

Synthetic 24*S*-hydroxydienoate (**37**) (1.0 mg) was reacted with (*R*)-MTPACl in an identical manner to (*S*)-MTPACl, as previously described, to give 24*S*((*S*)-MTPA)-hydroxydienoate (**40**) (0.9 mg) in 41 % yield. ^{1}H NMR (pateamine numbering) δ_H: 7.49 (m, 2H, phenyl), 7.36 (m, 3H, phenyl), 7.23 (d, 1H, *J*=11.7 Hz, H21), 6.84 (t, 1H, *J*=11.5 Hz, H20), 5.64 (d, 1H, *J*=11.2 Hz, H19), 5.38 (m, 1H, H24), 3.71 (s, 3H, OC$\underline{H}_3$), 3.53 (d, 3H, *J*=1.5 Hz, MTPA-OC$\underline{H}_3$), 2.59 (dd, 1H, *J*=8.0, 14.0 Hz, H23a), 2.40 (dd, 1H, *J*=5.4, 14.0 Hz, H23b), 1.87 (d, 3H, *J*=1.5 Hz, H31), 1.28 (d, 3H, *J*=6.4 Hz, H25) ppm.

3((*R*)-MTPA)-pateamine (**41**)

A CH_2Cl_2 solution of pateamine (**3**) (1.4 mg) was placed in a 1 mL Reactivial and taken to dryness. 1-Hydroxybenzotriazole (HOBT) (0.5 mg, in CH_2Cl_2, 2 x 250 µL), and (*R*)-MTPA (4 mg, in CH_2Cl_2, 2 x 250 µL) were transferred to the Reactivial. The solution was stirred with a magnetic follower and the vial cooled in an ice/water bath. N,N'-dicyclohexylcarbodiimide (DCC) (0.8 mg) was added, and the reaction was allowed to return to room temperature as the ice melted (12 hours). MeOH (3 mL) was added to the reaction mix, and the solution was chromatographed on a CBA cartridge. The cartridge was washed with MeOH and stripped with 2 % NH_4OH/MeOH. Fraction 2 contained (by ^{1}H NMR) 3((*R*)-MTPA)-pateamine (**41**) (1.5 mg) in 80 % yield. ^{1}H NMR δ_H: 7.51 (m, 2H, phenyl), 7.38 (m, 3H, phenyl), 7.00 (d, 1H, *J*=11.5

Hz, H21), 6.85 (d, 1H, *J*=7.2 Hz, NH), 6.80 (s, 1H, H7), 6.69 (t, 1H, *J*=12.0 Hz, H20), 6.40 (d, 1H, *J*=15.9 Hz, H14), 6.26 (m, 1H, H10), 6.22 (d, 1H, *J*=15.9 Hz, H13), 5.64 (t, 1H, *J*=7.6 Hz, H16), 5.54 (d, 1H, *J*=9.0 Hz, H11), 5.45 (d, 1H, *J*=11.7 Hz, H19), 5.05 (m, 1H, H24), 3.67 (m, 1H, H3), 3.39 (m, 3H, MTPA-OC$\underline{H}_3$), 3.20 (d, 1H, *J*=3.8 Hz, H9), 3.05 (d, 1H, *J*=7.3 Hz, H17), 2.89 (m, 1H, H5), 2.65 (dd, 1H, *J*=11.3, 16.6 Hz, H2a), 2.36 (dd, 1H, *J*=3.8, 16.6 Hz, H2b), 2.29 (dd, 1H, *J*=2.9, 13.3 Hz, H23a), 2.24 (s, 3H, H29), 2.24 (s, 3H, H30), 2.12 (d, 1H, *J*=13.3 Hz, H23b), 1.99 (d, 3H, *J*=1.1 Hz, H27), 1.97 (m, 2H, H4), 1.80 (d, 3H, *J*=0.97 Hz, H28), 1.79 (d, 3H, *J*=1.2 Hz, H31), 1.23 (d, 3H, *J*=6.7 Hz, H25), 1.23 (d, 3H, *J*=6.7 Hz, H26) ppm; ^{13}C NMR δ_C: 170.1 (C1), 140.8 (C20), 132.5 (C14), 131.5 (C13), 129.3 (C16), 128.4 (phenyl), 128.1 (phenyl), 126.2 (C11), 124.1 (C21), 115.2 (C19), 113.7 (C7), 69.0 (C10), 67.8 (C24), 56.3 (C17), 54.9 (MTPA-O$\underline{C}H_3$), 47.5 (C23), 46.6 (C3), 44.1 (C29), 44.1 (C30), 42.0 (C4), 38.8 (C2), 38.7 (C9), 33.7 (C5), 22.0 (C26), 20.7 (C25), 17.3 (C31), 13.4 (C27), 12.8 (C28) ppm; HRFABMS (Lewis Pannell, NIDDK, NIH, U.S.A.) MH^+ 772.3622 ($C_{41}H_{53}F_3N_3O_6S$ calc. 772.3607).

3((*S*)-MTPA)-pateamine (**42**)

Pateamine (**3**) (1.0 mg) was reacted with (*S*)-MTPA, HOBT and DCC in an identical manner to (*R*)-MTPA, as described above, to give 3((*S*)-MTPA)-pateamine (**42**) (1.0 mg) in 72 % yield. ^{1}H NMR δ_H: 7.56 (m, 2H, phenyl), 7.39 (m, 3H, phenyl), 6.97 (d, 1H, *J*=11.7 Hz, H21), 6.83 (d, 1H, *J*=8.6 Hz, NH), 6.72 (s, 1H, H7), 6.67 (t, 1H, *J*=11.2 Hz, H20), 6.37 (d, 1H, *J*=16.7 Hz, H14), 6.23 (m, 1H, H10), 6.22 (d, 1H, *J*=16.7 Hz, H13), 5.64 (t, 1H, *J*=6.7 Hz, H16), 5.53 (d, 1H, *J*=9.0 Hz, H11), 5.41 (d, 1H, *J*=11.2 Hz, H19), 5.02 (m,

1H, H24), 3.70 (m, 1H, H3), 3.36 (m, 3H, MTPA-OC$\underline{H}_3$), 3.23 (dd, 1H, *J*=3.4, 14.5 Hz, H9a), 3.14 (dd, 1H, *J*=10.4, 14.5 Hz, H9b), 3.11 (d, 2H, *J*=8.7 Hz, H17), 2.80 (m, 1H, H5), 2.58 (dd, 1H, *J*=11.2, 16.6 Hz, H2a), 2.40 (dd, 1H, *J*=3.8, 16.6 Hz, H2b), 2.27 (s, 3H, H30), 2.27 (s, 3H, H29), 2.00 (d, 3H, *J*=1.2 Hz, H27), 1.98 (m, 2H, H4), 1.81 (d, 3H, *J*=1.0 Hz, H28), 1.79 (d, 3H, *J*=1.0 Hz, H31), 1.27 (d, 3H, *J*=7.2 Hz, H26), 1.15 (d, 3H, *J*=6.6 Hz, H25) ppm; HRFABMS (Lewis Pannell, NIDDK, NIH, U.S.A.) MH^+ 772.3605 ($C_{41}H_{53}F_3N_3O_6S$ calc. 772.3607).

3((*S*)-MPA)-pateamine (**44**)

A CH_2Cl_2 solution of pateamine (**3**) (10 mg) was placed in a 5 mL Reactivial and taken to dryness. HOBT (2.6 mg, in N,N-dimethylformamide (DMF), 2 x 100 μL), and (*S*)-α-methoxyphenylacetic acid ((*S*)-MPA), (3.2 mg, in CH_2Cl_2, 2 x 150 μL) were transferred to the Reactivial. The solution was stirred with a magnetic follower, and the vial cooled in an ice/water bath. DCC (4 mg) was added, and the reaction allowed to return to room temperature as the ice melted (9 hours). MeOH (3 mL) was added to the reaction mix, and the solution was chromatographed on a CBA cartridge. The cartridge was washed with MeOH and stripped with 2 % NH_4OH/MeOH. Fraction 2 contained (by ^1H NMR) 3((*S*)-MPA)-pateamine (**44**) (8.3 mg) in 66 % yield. ^1H NMR δ_H: 7.35 (m, 5H, phenyl), 6.99 (d, 1H, *J*=11.5 Hz, H21), 6.81 (s, 1H, H7), 6.81 (d, 1H, *J*=7.2 Hz, NH), 6.69 (t, 1H, *J*=11.5 Hz, H20), 6.37 (d, 1H, *J*=15.5 Hz, H14), 6.24 (d, 1H, *J*=15.5 Hz, H13), 6.24 (m, 1H, H10), 5.64 (t, 1H, *J*=7.1 Hz, H16), 5.55 (d, 1H, *J*=8.9 Hz, H11), 5.44 (d, 1H, *J*=11.5 Hz, H19), 4.95 (m, 1H, H24), 4.56 (s, 1H, MPA-$\underline{H}$), 3.65 (m, 1H, H3), 3.34 (s, 3H, MPA-OC$\underline{H}_3$), 3.24 (m, 2H, H17), 3.15 (m, 2H, H9), 2.83 (m, 1H, H5), 2.61

(dd, 1H, *J*=10, 16 Hz, H2a), 2.34 (dd, 1H, *J*=3, 16 Hz, H2b), 2.31 (s, 3H, H29), 2.31 (s, 3H, H30), 2.20 (t, 1H, *J*=11.3 Hz, H23a), 2.04 (d, 1H, *J*=14.4 Hz, H23b), 1.99 (s, 3H, H27), 1.96 (bt, 2H, *J*=5.7 Hz, H4), 1.82 (s, 3H, H28), 1.78 (s, 3H, H31), 1.21 (d, 3H, *J*=6.9 Hz, H26), 1.19 (d, 3H, *J*=6.5 Hz, H25) ppm; HRFABMS MH^+ 704.3750 ($C_{40}H_{54}N_3O_6S$ calc. 704.3733).

3((*R*)-MPA)-pateamine (**43**)

Pateamine (**3**) (10.0 mg) was reacted with (*R*)-MPA, HOBT and DCC in an identical manner to (*S*)-MPA described above, to give 3((*R*)-MPA)-pateamine (**43**) (5.7 mg) in 45 % yield. ^1H NMR δ_H: 7.35 (m, 5H, phenyl), 7.01 (dd, 1H, *J*=1.0, 10 Hz, H21), 6.76 (d, 1H, *J*=5.8 Hz, NH), 6.72 (s, 1H, H7), 6.72 (t, 1H, *J*=11.5 Hz, H20), 6.37 (d, 1H, *J*=14 Hz, H14), 6.25 (d, 1H, *J*=16 Hz, H13), 6.24 (m, 1H, H10), 5.66 (dt, 1H, *J*=1.0, 7 Hz, H16), 5.57 (d, 1H, *J*=10 Hz, H11), 5.46 (d, 1H, *J*=12 Hz, H19), 5.07 (m, 1H, H24), 4.55 (s, 1H, MPA-H), 3.69 (m, 1H, H3), 3.32 (s, 3H, MPA-OCH$_3$), 3.19 (m, 2H, H9), 3.19 (m, 2H, H17), 2.81 (m, 1H, H5), 2.49 (dd, 1H, *J*=12, 16 Hz, H2a), 2.34 (s, 3H, H29), 2.34 (s, 3H, H30), 2.30 (t, 1H, *J*=12.5 Hz, H23a), 2.29 (d, 1H, *J*=12 Hz, H2b), 2.12 (d, 1H, *J*=16.6 Hz, H23b), 2.00 (s, 3H, H27), 1.94 (m, 2H, H4), 1.92 (s, 3H, H28), 1.82 (s, 3H, H31), 1.21 (d, 3H, *J*=6.2 Hz, H25), 1.20 (d, 3H, *J*=6 Hz, H26) ppm; ^{13}C NMR δ_C: 170.4 (C1), 165.3 (C8), 161.0 (C6), 145.5 (C22), 140.9 (C20), 138.0 (C12), 137.3 (C15), 133.7 (C14), 129.1 (C13), 128.9 (C11), 128.5 (phenyl), 128.3 (C16), 127.2 (phenyl), 123.9 (C21), 115.1 (C19), 113.2 (C7), 83.8 (MPA-CH), 68.9 (C10), 67.6 (C24), 56.9 (C17), 56.4 (MPA-OCH$_3$), 47.6 (C23), 46.0 (C3), 44.5 (C29), 44.5 (C30), 41.4 (C2), 41.3 (C4), 38.8 (C9), 33.8 (C5), 22.3 (C26), 20.9 (C25), 17.1 (C31), 13.4 (C27), 12.8 (C28) ppm; HRFABMS MH^+ 704.3748 ($C_{40}H_{54}N_3O_6S$ calc. 704.3733).

3((*S*)-MPA)-pateamine Major Fragment (**49**)

3((*S*)-MPA)-pateamine (**44**) (8.3 mg) was dissolved in dry MeOH (200 μL) and placed in a dry 1 mL Reactivial. Sodium methoxide solution (500 μL; Na (0.120 g) in dry MeOH (3 mL)) was added to the 3((*S*)-MPA)-pateamine (**44**) at room temperature. After 2.5 hours the MeOH solution was chromatographed on an LH-20 gel permeation column (5 mm x 200 mm, 800 mg) equilibrated to MeOH. ^{1}H NMR revealed fractions 2 and 3 contained the major fragment.

Fractions 2 and 3 were combined, dissolved in MeOH (5 mL) and chromatographed on a CBA cartridge equilibrated to MeOH. Fraction 2 (2 % NH_4OH/MeOH) contained (**49**) (5.4 mg) in 78 % yield. ^{1}H NMR δ_H: 7.34 (m, 5H, phenyl), 7.13 (d, 1H, *J*=9 Hz, NH), 6.89 (s, 1H, H7), 6.29 (d, 1H, *J*=16 Hz, H14), 6.21 (d, 1H, *J*=16 Hz, H13), 5.62 (m, 1H, H16), 5.57 (d, 1H, *J*=6.1 Hz, H11), 4.94 (dt, 1H, *J*=5.9, 8.3 Hz, H10), 4.57 (s, 1H, MPA-H), 4.07 (m, 1H, H3), 3.55 (s, 3H, ester-OCH_3), 3.35 (s, 3H, MPA-OCH_3), 3.11 (d, 2H, *J*=5.8 Hz, H9), 3.05 (d, 2H, *J*=6.2 Hz, H17), 2.98 (m, 1H, H5), 2.43 (d, 2H, *J*=6.5 Hz, H2), 2.24 (s, 3H, H29), 2.24 (s, 3H, H30), 1.92 (m, 2H, H4), 1.84 (d, 3H, *J*=1.2 Hz, H27), 1.79 (d, 3H, *J*=1.0 Hz, H28), 1.30 (d, 3H, *J*=7.0 Hz, H26) ppm; HRFABMS MH^+ 584.3156 ($C_{32}H_{46}N_3O_5S$ calc. 584.3158).

3((*R*)-MPA)-pateamine Major Fragment (**48**)

3((*R*)-MPA)-pateamine (**43**) (5.7 mg) was reacted with NaOMe/MeOH in an identical manner to 3((*S*)-MPA)-pateamine, as previously described, to give 3((*R*)-MPA)-pateamine fragment (**48**) (1.9 mg) in 40 % yield. ^{1}H NMR δ_H: 7.38 (m, 5H, phenyl), 7.14 (d, 1H, *J*=9.5 Hz, NH), 6.30 (s, 1H, H7), 6.28 (d,

1H, *J*=8.7 Hz, H14), 6.23 (d, 1H, *J*=8.7 Hz, H13), 5.64 (d, 1H, *J*=7.5 Hz, H16), 5.57 (d, 1H, *J*=6.6 Hz, H11), 4.90 (m, 1H, H10), 4.57 (s, 1H, MPA-H), 3.98 (m, 1H, H3), 3.66 (s, 3H, ester-OCH$_3$), 3.38 (s, 3H, MPA-OCH$_3$), 3.13 (d, 2H, *J*=7.5 Hz, H17), 3.06 (dd, 2H, *J*=1.5, 6.8 Hz, H9), 2.75 (m, 1H, H5), 2.53 (dd, 1H, *J*=5.3, 15.8 Hz, H2a), 2.48 (dd, 1H, *J*=5.3, 15.8 Hz, H2b), 2.29 (s, 3H, H29), 2.29 (s, 3H, H30), 1.94 (m, 2H, H4), 1.82 (d, 3H, *J*=1.2 Hz, H27), 1.80 (d, 3H, *J*=1.0 Hz, H28), 1.21 (d, 3H, *J*=6.5 Hz, H26) ppm; HRFABMS MH$^+$ 584.3145 ($C_{32}H_{46}N_3O_5S$ calc. 584.3158).

3((*S*)-MPA)-10((*S*)-MTPA)-pateamine Major Fragment (**51**)

A CH_2Cl_2 solution of 3((*S*)-MPA)-pateamine major fragment (**49**) (2.4 mg) was taken to dryness in a 1 mL Reactivial. (*R*)-MTPACl (11 mg) was transferred into the Reactivial in pyridine (3 x 10 µL). The solution was cooled in an ice/water bath, and allowed to react for 20 minutes. H_2O (1 mL) was added to the solution, and the products trapped onto a reverse-phase C18 cartridge equilibrated to H_2O. The column was stripped with MeOH. The stripped fraction contained 3((*S*)-MPA)-10((*S*)-MTPA)-pateamine major fragment (**51**) in 50 % yield (1.6 mg). ^{1}H NMR δ_H: 7.67 (m, 2H, phenyl), 7.33 (m, 3H, phenyl), 7.14 (d, 1H, *J*=9.2 Hz, NH), 6.86 (s, 1H, H7), 6.29 (d, 1H, *J*=14.2 Hz, H10), 6.27 (s, 1H, H13), 6.27 (s, 1H, H14), 5.62 (m, 1H, H16), 5.54 (d, 1H, *J*=9.3 Hz, H11), 4.57 (s, 1H, MPA-H), 4.05 (m, 1H, H3), 3.72 (d, 2H, *J*=7.7 Hz, H17), 3.58 (s, 3H, MTPA-OCH$_3$), 3.54 (s, 3H, ester-OCH$_3$), 3.41 (dd, 1H, *J*=14.4, 5.0 Hz, H9a), 3.34 (s, 3H, MPA-OCH$_3$), 3.23 (dd, 1H, *J*=14.4, 5.0 Hz, H9b), 2.94 (m, 1H, H5), 2.69 (s, 3H, H29), 2.69 (s, 3H, H30), 2.42 (d, 2H, *J*=5.5 Hz, H2), 2.40 (d, 2H, *J*=4.0 Hz, H4), 1.86 (s, 3H, H28),

1.83 (s, 3H, H27), 1.26 (d, 3H, *J*=7.5 Hz, H26) ppm; HRFABMS MH^+ 800.3545 ($C_{42}H_{53}F_3N_3O_7S$ calc. 800.3556).

3((*S*)-MPA)-10((*R*)-MTPA)-pateamine Major Fragment (**50**)

3((*S*)-MPA)-pateamine major fragment (**49**) (5.7 mg) was reacted with (*S*)-MTPACl in pyridine and chromatographed in an identical manner to that previously described to give 3((*S*)-MPA)-10((*R*)-MTPA)-pateamine major fragment (**50**). ^1H NMR δ_H: 7.68 (m, 2H, phenyl), 7.33 (m, 3H, phenyl), 6.90 (s, 1H, H7), 6.28 (m, 1H, H10), 5.39 (d, 1H, *J*=9.6 Hz, H11), 4.05 (m, 1H, H3), 3.45 (dd, 1H, *J*=15.2, 7.3 Hz, H9a), 3.26 (dd, 1H, *J*=15.2, 5.9 Hz, H9b), 2.96 (m, 1H, H5), 2.69 (s, 3H, H29), 2.69 (s, 3H, H30), 1.90 (m, 2H, H4), 1.26 (s, 3H, H26) ppm.

Attempt at Crystallisation of Pateamine (**3**) with $ZnCl_2$

Pateamine (**3**) (10 mg) was dissolved in MeOH (0.5 mL). $ZnCl_2$ (9.8 mg) was dissolved in MeOH (10 mL), and *c.* HCl added until the pH was approximately 5. The vial was covered with a plastic film and stored at room temperature in the dark for 5 days. After this time, some solution was removed (5 mL) and placed in another vial without any cover, and the original vial was resealed with a perforated plastic film. After 1 month, both solutions had dried to a brown gum which showed no crystalline character, and attempts made to recover the pateamine (**3**) were unsuccessful.

Attempt at Crystallisation of Pateamine (**3**) with $NaPF_6$

Pateamine (**3**) (10 mg) was dissolved in MeOH (5 mL). $NaPF_6$ (12 mg) was dissolved in MeOH (5 mL), and TFA added until the pH was approximately 5. The vial was covered with a plastic film and stored at room temperature in the dark for 5 days. After this time, an aliquot of solution was removed (5 mL) and placed in another vial without any cover, and the original vial was resealed with a perforated plastic film. After 1 month, both solutions had dried to a brown gum which showed no crystalline character, and attempts made to recover the pateamine (**3**) were unsuccessful.

3(*N*-Acetyl)-pateamine (**52**)

Pateamine (**3**) (10.0 mg) was reacted with acetic acid (1.3 mg), HOBT and DCC, as previously described with the MPA enantiomers, to give 3(*N*-acetyl)-pateamine (**52**) (4.8 mg) in 45 % yield. ^{1}H NMR δ_H: 7.05 (d, 1H, 1H, *J*=11.5 Hz, H21), 6.76 (t, 1H, *J*=11.5 Hz, H20), 6.38 (s, 1H, H7), 6.38 (s, 1H, H13), 6.38 (s, 1H, H14), 6.22 (m, 1H, H10), 5.66 (t, 1H, *J*=7.7 Hz, H16), 5.65 (d, 1H, *J*=8.2 Hz, H11), 5.54 (d, 1H, *J*=11.1 Hz, H19), 5.10 (m, 1H, H24), 3.80 (d, 2H, *J*=7.6 Hz, H17), 3.72 (m, 1H, H3), 3.20 (d, 2H, *J*=6.6 Hz, H9), 3.03 (m, 1H, H5), 2.79 (s, 3H, H29), 2.79 (s, 3H, H30), 1.99 (s, 3H, H27), 1.91 (s, 3H, *N*-acetyl), 1.89 (s, 3H, H28), 1.85 (s, 3H, H31), 1.26 (d, 3H, *J*=7.1 Hz, H26), 1.24 (d, 3H, *J*=6.4 Hz, H25) ppm; HRFABMS (Lewis Pannell, NIDDK, NIH, U.S.A.) MH^+ 598.3306 ($C_{33}H_{48}N_3O_5S$ calc. 598.3314).

Attempted Methanolysis of 3(*N*-Acetyl)-pateamine (**52**)

3(*N*-Acetyl)-pateamine (**52**) was reacted with NaOMe/MeOH in an identical manner to 3((*S*)-MPA)-pateamine, as previously described, except for the method of attempted isolation. The methanolysis was quenched by addition of 25 mL of H_2O and 10 µL TFA. The organic material was then trapped on a C18 cartridge and washed with 10 mL of H_2O. The trapped material was eluted with MeOH (3 mL) to give a complex reaction mixture (by ^1H NMR). Further chromatography on a CBA cartridge yielded no 3(*N*-acetyl)-pateamine major fragment (**53**) or starting material.

3(*N*-*p*-bromobenzoyl)-pateamine (**54**)

Pateamine (**3**) (2.2 mg) was reacted with *p*-bromobenzoic acid (*p*-BBA) (0.9 mg), HOBT and DCC, as previously described, with the MPA enantiomers to give 3(*N*-*p*-BBA)-pateamine (**54**) (0.6 mg) in 21 % yield. ^1H NMR δ_H: 7.61 (d, 3H, *J*=8.6 Hz, phenyl), 7.54 (d, 2H, *J*=8.6 Hz, phenyl), 7.05 (d, 1H, *J*=11.5 Hz, H21), 6.84 (s, 1H, H7), 6.71 (t, 1H, *J*=11.5 Hz, H20), 6.39 (d, 1H, *J*=16 Hz, H13), 6.30 (d, 1H, *J*=6 Hz, NH), 6.27 (d, 1H, *J*=16 Hz, H14), 6.20 (m, 1H, H10), 5.68 (t, 1H, *J*=7.2 Hz, H16), 5.57 (d, 1H, *J*=8.7 Hz, H11), 5.54 (d, 1H, *J*=11.5 Hz, H19), 5.05 (m, 1H, H24), 3.89 (m, 1H, H3), 3.33 (d, 1H, *J*=7.5 Hz, H17), 3.19 (d, 1H, *J*=5.6 Hz, H9), 3.03 (m, 1H, H5), 2.61 (dd, 1H, *J*=10.5, 15.6 Hz, H2a), 2.43 (s, 3H, H29), 2.43 (s, 3H, H30), 2.41 (d, 1H, *J*=12.7 Hz, H2b), 2.29 (dd, 1H, *J*=10.5, 17 Hz, H23a), 2.11 (d, 1H, *J*=14 Hz, H23b), 2.09 (m, 2H, H4), 1.97 (s, 3H, H27), 1.83 (s, 3H, H28), 1.79 (s, 3H, H31), 1.28 (d, 3H, *J*=7 Hz, H26), 1.16 (d, 3H, *J*=6.3 Hz, H25) ppm; HRFABMS MH^+ 738.2582 ($C_{38}H_{49}N_3O_5SBr$ calc. 738.2576).

Extraction of *Aplysia parvula* (92K11-04)

Isolation of Thyrsiferol (**70**)

Thirty nine *Aplysia parvula* (300 g wet weight) were washed in acetone (500 mL) and allowed to drain. The purple fluid exuded by the animals after capture was assayed (<97.5 ng/mL) then passed down a C18 cartridge to trap any organic material. The activity was found solely in the H_2O wash of the C18 column (262 mg, <97.5 ng/mL) and none in the C18-trapped material (7.7 mg, >12500 ng/mL). Due to the lack of organic soluble activity, attention was focused on the bodies and excised digestive glands.

The digestive glands were excised (200 g) from the bodies (100 g) and the latter were extracted with MeOH and CH_2Cl_2. The solvents were removed *in vacuo* to yield a yellow gum (7.8 g, 79621 ng/mL, slight antimicrobial activity). The gum was dissolved in MeOH and CH_2Cl_2, and coated onto Celite. The coated Celite was dry-packed onto a C18 reverse-phase column. Eleven fractions were collected from the column, which was eluted with a stepped gradient from 20:80 MeOH/H_2O through MeOH to CH_2Cl_2. The slight antimicrobial activity was contained in fractions 3 to 6, but no P388 activity was observed.

The excised digestive glands were homogenised in H_2O (100 mL) with a Virtis (super 30, Gardner) and filtered through Celite (50 g). The mat was washed with H_2O (2 x 250 mL), MeOH (2 x 100 mL), and then CH_2Cl_2 (2 x 100 mL). The MeOH and CH_2Cl_2 extracts were combined. The solvents were removed *in vacuo* to yield a brown friable powder (10.8 g) and a yellow gum (2.17 g) respectively. Activity was found solely in the combined

MeOH/CH_2Cl_2 extract (10.8 g, 79621 ng/mL in the P388 assay, some antimicrobial activity against *B. sub*, *C. alb* and *C. res*).

The organic-soluble material was chromatographed on a reverse-phase C18 column (25 mm x 300 mm, 100 g) equilibrated to 20:80 MeOH/H_2O. The organic-soluble material was dissolved in MeOH/CH_2Cl_2, coated onto Celite (5 g) and then dry packed onto the column. Nine fractions were collected from the column, which was eluted with a stepped gradient from 20:80 MeOH/H_2O to 5:95 MeOH/CH_2Cl_2.

The most active fraction (F6, 10:90 H_2O/MeOH, 16146 ng/mL, 450 mg) was dissolved in benzene (1 mL) and loaded onto a DIOL column (18 mm x 200 mm, 10 g). Twelve fractions were collected from the column, which was eluted with a stepped gradient from 30:70 benzene/hexane through CH_2Cl_2 to 20:80 MeOH/CH_2Cl_2. Analysis of the fractions by ^{1}H NMR revealed thyrsiferol (**70**) in fractions F8, CH_2Cl_2, 40.1 mg; F9, 1:99 MeOH/CH_2Cl_2, 27.8 mg; F11, 10:90, MeOH/CH_2Cl_2, 43.1 mg) were combined (111 mg) and re-chromatographed on the same DIOL column. Ten fractions were collected from the column, which was eluted using a gradient elution from hexane through CH_2Cl_2 to EtOAc. Fraction 6 (90:10 CH_2Cl_2/hexane) gave pure thyrsiferol (**70**) (16.7 mg) ^{1}H NMR δ_H: 3.89 (dd, 1H, *J*=4, 12 Hz, H3), 3.76 (dd, 1H, *J*=6, 9 Hz, H22), 3.69 (m, 1H, H14), 3.56 (dd, 1H, *J*=7, 11 Hz, H11), 3.44 (dd, 1H, *J*=2, 10 Hz, H18), 3.04 (dd, 1H, *J*=3, 9 Hz, H7), 2.24 (dq, 1H, *J*=4, 13, 13, 13 Hz, $H4_R$), 2.07 (m, 1H, $H4_S$), 2.07 (m, 1H, $H20_S$), 1.87 (m, 1H, $H12_S$), 1.82 (m, 1H, $H13_S$), 1.81 (m, 1H, H16a), 1.81 (m, 2H, $H21_{R\&S}$), 1.78 (m, 1H, $H5_S$), 1.76 (m, 1H, $H9_R$), 1.71 (m, 1H, $H8_R$), 1.67 (m,

1H, H13$_R$), 1.57 (m, 1H, H20$_R$), 1.55 (m, 1H, H17a), 1.51 (m, 1H, H5$_R$), 1.51 (m, 1H, H9$_S$), 1.47 (m, 1H, H12$_R$), 1.46 (m, 1H, H17b), 1.40 (m, 1H, H8$_S$), 1.39 (s, 3H, CH_3-1), 1.37 (m, 1H, H16b), 1.26 (s, 3H, CH_3-25), 1.20 (s, 3H, CH_3-30), 1.19 (s, 3H, CH_3-26), 1.17 (s, 3H, CH_3-27), 1.15 (s, 3H, CH_3-29), 1.12 (s, 3H, CH_3-24), 1.09 (s, 3H, CH_3-28) ppm; ^{13}C NMR δ_C: 87.4 (C22), 86.5 (C7), 86.01 (C19), 77.6 (C18), 76.3 (C11), 76.1 (C14), 74.9 (C2), 74.3 (C6), 73.2 (C15), 71.9 (C10), 58.9 (C3), 38.5 (C9), 37.0 (C5), 33.5 (C16), 32.3 (C20), 31.0 (C25), 28.2 (C4), 27.2 (C30), 26.6 (C21), 25.4 (C17), 23.7 (C1), 23.4 (C29), 23.0 (C8), 22.8 (C28), 21.4 (C27), 21.1 (C12), 20.7 (C13), 20.0 (C26) ppm. Thyrsiferol (**70**) returned an IC_{50} value of 1222 ng/mL in the P388 assay.

GCMS Analysis of Digestive Glands

The organic fraction of the extraction of the digestive glands was analysed by GCMS (Carlo-Erba/Kratos, MSC500 HRGC, injector; 260°C) using a 30 m x 0.25 mm DB-1 column (J&W, 0.25 μm film, 50°C initial column temperature, held for 1 minute, then 5°C minute^{-1} to 250°C), with He as the carrier gas. Eleven peaks were visible in the total ion count chromatographic trace. The mass spectra of these peaks revealed that the compounds present were C-12 mono-, and C14 di-unsaturated hydrocarbons, and a series of C-13, C-15, C-17, and C-19 fatty acid methyl esters with various methyl substitution patterns.

Extraction of Egg Masses

Approximately 50 *A. parvula* were collected from April to June 1996. These were placed into a 200 litre tank with several kilograms of fresh *Laurencia thyrsifera*. Fresh sea water was run through the tank continuously. Every two weeks the tank was searched for egg masses, which were removed and stored at -18°C until required. Newly found wild *Aplysia* were added after the tank was cleaned and fresh algae added. At the end of June no wild *L. thyrsifera* could be found, and the *A. parvula* were kept until all had starved, by which time 260 g of egg masses had been collected. The frozen eggs were steeped in MeOH (600 mL) until thawed, then sonicated for 30 minutes. The eggs and solution were homogenised in a Waring blender, and the resultant homogenate filtered through Celite. The mat was rehomogenised with CH_2Cl_2 in the Waring blender and refiltered. All extracts were combined and the solvent removed *in vacuo* to yield an orange viscous oil (12.5 g). The extract was taken up in CH_2Cl_2 and MeOH, and dried onto Celite, then packed onto a C18 reverse-phase column (28 mm x 400 mm, 100 g) equilibrated to 80:20 H_2O/MeOH. Eleven factions were collected from the column, which was eluted with a gradient from H_2O/MeOH (80:20) to MeOH (F1, 80:20 H_2O/MeOH, 7.6 g; F2, 80:20 H_2O/MeOH, 2.9 g; F3, 50:50 H_2O/MeOH, 75.4 mg; F4, 40:60 H_2O/MeOH, 16.6 mg; F5, 30:70 H_2O/MeOH, 43.9 mg; F6, 20:80 H_2O/MeOH, 45.9 mg; F7, 10:90 H_2O/MeOH, 67.6 mg; F8, 5:95 H_2O/MeOH, 78 mg; F9, MeOH, 178.5 mg; F10, 5:95 CH_2Cl_2/MeOH, 137.7 mg), then stripped with CH_2Cl_2 and MeOH (605 mg). Fractions 3-5 showed strong antiviral activity (*Herpes simplex* type 1 virus (ATCC VR 733) and *Polio* virus type 1 (Pfiser vaccine strain)) and some antimicrobial activity (against *Bacillus subtilis* and three species of fungi).

Comparison by TLC of the fractions from the C18 column with a genuine sample of thyrsiferol (**70**) revealed that fraction 3 had material at a similar R_f ($R_f \approx 0.4$, silica, 95:5 CH_2Cl_2/MeOH). Fraction 3 (75.4 mg) was partitioned between CH_2Cl_2 (1 mL) and H_2O (2 mL), and the solvents removed *in vacuo* to yield a yellow oil (4 mg). ^1H NMR analysis revealed no thyrsiferol (**70**) in the organic phase.

The remaining active fractions (52.9 mg) were combined and dissolved in petroleum ether (500 μL) and MeOH (one drop) and loaded onto a DIOL column (10 mm x 140 mm, 10 g). Nine fractions were collected from the column, which was eluted with a stepped gradient from pet ether through EtOAc and CH_2Cl_2 to MeOH (F3, 50:50 pet ether/CH_2Cl_2, 0.4 mg; F4, 70:30 pet ether/CH_2Cl_2, 3.1 mg; F5, 90:10 pet ether/CH_2Cl_2, 1.8 mg; F6, CH_2Cl_2, 1.4 mg; F7, 20:80 EtOAc/CH_2Cl_2, 2.1 mg; F8, 50:50 EtOAc/CH_2Cl_2, 2.2 mg; F9, MeOH, 25.9 mg). ^1H NMR analysis of fractions 4-9 from this column overwhelmingly displayed the characteristic signals for triglycerides. Fractions 3-9 all had antimicrobial activity suggesting that the active compound was at a very low level. The minute masses of the material remaining after the fractions were assayed precluded further work in this area.

^1H NMR analysis of all fractions from all columns showed no thyrsiferol (**70**) was present in any sample.

GCMS Analysis of Selected Fractions

Selected fractions from the extraction of the egg masses were analysed by GCMS (Carlo-Erba/Kratos, MSC500 HRGC, injector; 260°C) using a 30 m x 0.25 mm DB-1 column (J&W, 0.25 μm film, 50°C initial column temperature, held for 1 minute, then 5°C $minute^{-1}$ to 250°C), with He as the carrier gas. No chromatographic peaks of any fraction displayed any bromine isotopic splitting patterns in the mass spectrum.

Culturing of Microorganisms

Fresh *Aplysia* egg masses were located and removed from the substrate with sterile tweezers. The egg masses were then rinsed in sterile sea water and wiped over three sterile salt water agar plates (16.5 g 'Bacto' agar, 0.5 g peptone, 0.5 g yeast extract, 750 mL filtered sea water, mixed then autoclaved for 15 minutes at 121°C). The egg masses were then homogenised with a sterile tissue grinder and a drop of the homogenate thinly spread over three more salt water agar plates. The microorganisms were cultured until sizeable colonies formed, then restreaked over fresh plates. This process was carried out until the colonies were a monoculture. Nine distinct species were isolated. The isolated colonies were bulked up on several agar plates until approximately 200 μL of microorganisms were collected. These were diluted with MeOH (200 μL), then placed into small vials (1 mL) and sonicated for 10 minutes. The resultant solution was filtered through a syringe filter (Alltech, 0.22 μm) prior to mixing with P388 (murine leukaemia) cells in a standard assay. Four colonies of interest, i.e. those in which the P388 cells metabolized the MTT stain to a level less than 5 % of

the controls, were cultured on slants and forwarded to PharmaMar (Spain) and the Abbott Chemical Company (U.S.A.) for further study. Initial testing at both these establishments revealed no samples were deemed, by these companies requirements, to warrant further work.

References

1 Colegate, S.M.; Molyneux, R.J.; In: *Bioactive Natural Products: Detection, Isolation and Structural Determination*, **1993**, Colegate, S.M. and Molyneux, R.J. (ed.s), CRC Press Ltd., Boca Raton, 1-3.

2 Williams, D.H.; Stone, M.J.; Hauck, P.R.; Rahman, S.K.; *J. Nat. Prod.*, **1989**, 52, 1189-1208.

3 der Marderosian, A.J.; *J. Pharm. Sci.*, **1969**, 58, p1.

4 Pers. Comm.; Dr. Peter Murphy, Australian Institute of Marine Sciences, to Dr. Murray Munro, University of Canterbury, April 1992.

5 Wessells, N.K.; Hopson, J.L.; *Biology*, **1988**, Random House Inc., New York, 569-571.

6 Wessells, N.K.; Hopson, J.L.; *Biology*, **1988**, Random House Inc., New York, 597-601.

7 Boyd, M.R.; *Principles and Practice of Oncology*, **1989**, 3, p1.

8 Marston, A; Décosterd, L.A.; Hostettmann, K.; In: *Bioactive Natural Products: Detection, Isolation and Structural Determination*, **1993**, Colegate, S.M. and Molyneux, R.J. (ed.s), CRC Press Ltd., Boca Raton, p222.

9 Perry, N.B.; Blunt, J.W.; Munro, M.H.G.; Pannell, L.K.; *J. Am. Chem. Soc.*, **1988**, 110, 4850-4851.

10 Perry, N.B.; Blunt, J.W.; Munro, M.H.G.; Thompson, A.M.; *J. Org. Chem.*, **1990**, 55, 223-227.

11 Pers. Comm.; Dr. Glynn Faircloth, PharmaMar USA to Dr. Murray Munro, University of Canterbury, dated 24-04-94.

12 Northcote, P.T.; Blunt, J.W.; Munro, M.H.G.; *Tet. Lett.*, **1991**, 32, 6411-6414.

13 Perry, N.B.; Blunt, J.W.; Munro, M.H.G.; *Tetrahedron*, **1988**, 44, 1727-1734.

14 Perry, N.B.; Blunt, J.W.; McCombs, J.D.; Munro, M.H.G.; *J. Org. Chem.*, **1986**, 51, 5476-5478.

15 Uemura, D.; Takahashi, K.; Yamamoto, T.; Katayama, C.; Tanaka, J.; Okumura, Y.; Hirata, Y.; *J. Am. Chem. Soc.*, **1985**, 107, 4796-4798.

16 Hirata, Y.; Uemura, D.; *Pure & Appl. Chem.*, **1986**, 58, 701-710.

17 Parker, D.; *Chem. Rev.*, **1991**, 91, 1441-1457.

18 Pers. comm.; Dr. Murray Munro, University of Canterbury.

19 Brown, J.M.; Davies, S.G.; *Nature*, **1989**, 342, 631.

20 Schurig, V.; Nowotny, A.P.; *Angew. Chem. Int. Ed. Engl.*, **1990**, 29, 939-1076.

21 Allenmark, S.G.; *Chromatographic Enantioseparation: Methods and Applications*, **1988**, Ellis Horwood, Chichester.

22 Harada, N.; Nakanishi, K.; *Accounts Chem. Res.*, **1972**, 5, 257-263.

23 Dale, J.A.; Mosher, H.S.; *J. Am. Chem. Soc.*, **1972**, 95, 512-519.

24 Dale, J.A.; Dull, D.L.; Mosher, H.S.; *J. Org. Chem.*, **1969**, 34, 2543-2549.

25 Sullivan, G.R.; Dale, J.A.; Mosher, H.S.; *J. Org. Chem.*, **1973**, 38, 2143-2147.

26 Ohtani, I.; Kusumi, T; Ishitsuka, M.O.; Kakisawa, H.; *Tet. Lett.*, **1989**, 30, 3147-3150.

27 Kusumi, T; Ohtani, I.; Inouye, Y.; Kakisawa, H.; *Tet. Lett.*, **1988**, 29, 4731-4734.

28 Riguera, R.; *8th International Symposium on Marine Natural Products, Tenerife, September*, **1995**, 63-64.

29 Latypov, S.H.; Seco, J.M.; Quiñoá, E.; Riguera, R.; *J. Org. Chem.*, **1995**, 60, 504-515.

30 Seco, J.M.; Latypov, S.H.; Quiñoá, E.; Riguera, R.; *Tetrahedron Asymmetry*, **1995**, 6, 107-110.

31 Trost, B.M.; Bunt, R.C.; Pulley, S.R.; **1994**, 59, 4202-4205.

32 Latypov, S.H.; Seco, J.M.; Quiñoá, E.; Riguera, R.; *J. Org. Chem.*, **1995**, 60, 1538-1545.

33 Ohtani, I.; Kusumi, T; Kashman, Y.; Kakisawa, H.; *J. Org. Chem.*, **1991**, 56, 1296-1298.

34 Kusumi, T; Fujita, Y.; Ohtani, I.; Kakisawa, H.; *Tet. Lett.*, **1991**, 32, 2923-2926.

35 Bergquist, P.R.; *Sponges*, **1978**, Hutchinson and Co., London.

36 MarinLit; A marine literature database maintained by, and available from, Blunt, J.W. and Munro, M.H.G., Marine Chemistry Group, University of Canterbury, Christchurch, New Zealand.

37 Cardellina, J.H.; Munro, M.H.G.; Fuller, R.W.; Manfredi, K.P.; McKee, T.C.; Tishler, M.; Bokesch, H.R.; Gustafson, K.P.; Beutler, J.A.; Boyd, M.R.; *J. Nat. Prod.*, **1993**, 56, 1123-1129.

38 Cardellina, J.H.; *J. Nat. Prod.*, **1983**, 46, 196-199.

39 Unpublished results of Dr. N. Perry, University of Canterbury.

40 Schmitz, F.J.; Gunasekera, S.P.; Yalamanchili, G.; Hossain, M.B.; van der Helm, D.; *J. Am. Chem. Soc.*, **1984**, 106, 7251-7252.

41 McCombs, J.D.; Ph.D. Thesis, University of Canterbury, 1989.

42 Unpublished results of Dr. L. Ettouati, University of Canterbury.

43 Pettit, G.R.; Cichacz, Z.A.; Herald, C.L.; Gao, F.; Boyd, M.R.; Schmidt, J.M.; Hamel, E.; Bai, R.; *J. Chem. Soc. Chem. Commun.*, **1994**, 1605-1606.

44 Pettit, G.R.; *Prog. Chem. Org Nat. Prod.*, **1991**, 57, 153-195.

45 Legrand, A.M.; Litaudon, M.; Genthon, J.N.; Bagnis, R.; Yasumoto, T.; *J. Appl. Phycol.*, **1989**, 1, 183-188.

46 Pettit, G.R.; Rideout, J.A.; Hasler, J.A.; *J. Nat. Prod.*, **1981**, 44, 588-592.

47 Murakami, Y.; Oshima, Y.; Yasumoto, T.; *Nippon Suisan Gakkaishi*, **1982**, 48, 549-552.

48 Hirata, Y.; Uemura, D.; *Pure & Appl. Chem.*, **1986**, 58, 701-710.

49 Unpublished results of Dr. M. Litaudon, University of Canterbury.

50 Blincoe, S.; M.Sc. Thesis, University of Canterbury, 1994.

51 Ohta, H.; Ozaki, K.; Tsuchihashi, G.; *Agric. Biol. Chem.*, **1986**, 50, 2499-2502.

52 Tanabe, T.; *Bull. Chem. Soc. Japan*, **1973**, 46, 2233-2234.

53 August, R.; McEwen, I.; Taylor, R.; *J. Chem. Soc. Perk. Trans. 2*, **1987**, 1683-1689.

54 D'Auria, M.V.; Debitus, C.; Paloma, L.G.; Minale, L.; Zampella, A.; *J. Am. Chem. Soc.*, **1994**, 116, 6658-6663.

55 Ward, D.E.; Rhee, C.K.; *Tet. Lett.*, **1991**, 32, 7165-7166.

56 Rzasa, R.M.; Romo, D.; Stirling, D.J.; Blunt, J.W.; Munro, M.H.G.; *Tet. Lett.*, **1995**, 36, 5307-5310.

57 Kandel, E.R.; *Behavioral Biology of Aplysia*, **1979**, W. H. Freeman and Company, San Francisco.

58 Pennings, S.C.; Paul, V.J.; *Mar. Biol.*, **1993**, 117, 535-546.

59 Faulkner, D.J.; *Nat. Prod. Rep.*, **1984**, 251-280.

60 Yamamura, S.; Hirata, Y.; *Tetrahedron*, **1963**, 19, 1485-1496.

61 Irie, T.; Suzuki, M.; Hayakawa, Y.; *Bull. Chem. Soc. Japan*, **1969**, 42, 843-844.

62 Irie, T.; Suzuki, M.; Kurosawa, E; Masamune, T.; *Tet. Lett.*, **1966**, 1837-1840.

63 Irie, T.; Suzuki, M.; Masamune, T.; *Tetrahedron*, **1970**, 26, 3271-3277.

64 Stallard, M.O.; Faulkner, D.J.; *Comp. Biochem. Physiol.*, **1974**, 49B, 37-41.

65 Nemoto, H.; Nagamochi, M.; Ishibashi, H,; Fukumoto K.; *J. Org. Chem.*, **1994**, 59, 74-79.

66 Garson, M.J.; *Chem. Rev.*, **1993**, 93, 1699-1733.

67 Kinnel, R.; Dieter, R.K.; Meinwald, J.; Van Engen, D.; Eisner, T.; Stallard, M.O.; Fenical, W.; *Proc. Nat. Acad. Sci. U.S.A.*, **1979**, 76, 3576-3579.

68 Howard, B.M.; Schulte, G.R.; Fenical, W.; Solheim, B.; Clardy, J.; *Tetrahedron*, **1980**, 36, 1747-1751.

69 Kinnel, R.; Duggan, A.J.; Eisner, T.; Meinwald, J.; *Tet. Lett.*, **1977**, 3913-3916.

70 Feldman, K.S.; Mechem, C.C.; Nader, L.; *J. Am. Chem. Soc.*, **1982**, 104, 4011-4012.

71 Stallard, M.O.; Fenical, F.; Kittredge, J.S.; *Tetrahedron*, **1978**, 34, 2077-2081.

72 Stallard, M.O.; Faulkner, D.J.; *Comp. Biochem. Physiol.*, **1974**, 49B, 25-35.

73 Pennings, S.C.; Carefoot, T.H.; *Comp. Biochem. Physiol. C. Comp. Pharmaco.*, **1995**, 111, 249-256.

74 Faulkner, D.J.; Ghiselin, M.T.; *Mar., Ecol., Prog., Ser.*, **1983**, 13, 295-301.

75 Blunt, J.W.; Hartshorn, M.P.; McLennan, T.J.; Munro, M.H.G.; Robinson, W.T.; Yorke, S.C.; *Tet. Lett.*, **1978**, 69-72.

76 Blunt, J.W.; Lake, R.J.; Munro, M.H.G.; Yorke, S.C.; *Aust. J. Chem.*, **1981**, 34, 3393-3400.

77 Blunt, J.W.; Lake, R.J.; Munro, M.H.G.; *Aust. J. Chem.*, **1984**, 37, 1545-1552.

78 Identified by Dr. M.J. Parsons, Landcare Research New Zealand Ltd.

79 Suzuki, T.; Suzuki, M.; Furusaki, A.; Matsumoto, T.; Kato, A.; Imanaka, Y.; Kurosawa, E.; *Tet. Lett.*, **1985**, 26, 1329-1332.

80 Gil-Turnes, M.S.; Fenical, W.; *Biol. Bull.*, **1992**, 182, 105-108.

81 Gil-Turnes, M.S.; Hay, M.E.; Fenical, W.; *Science*, **1989**, 246, 116-118.

82 Kang, H.; Jensen, P.R.; Fenical, W.; *J. Org. Chem.*, **1996**, 61, 1543-1546.

83 Seto, H.; Sato, T.; Urano, S.; Uzawa, J.; Yonehara, H.; *Tet. Lett.*, **1976**, 4367-4370.

84 Blunt, J.W.; McCombs, J.D.; Munro, M.H.G.; Thomas, F.N.; *Magn. Reson. Chem.*, **1989**, 27, 792-795.

85 Sakemi, S.; Higa, T.; Jefford, C.W.; Bernardinelli, G.; *Tet. Lett.*, **1986**, 27, 4287-4290.

86 Griesinger, C.; Sorensen, O.W.; Ernst, R.R.; *J. Am. Chem. Soc.*, **1985**, 107, 6394-6396.

87 Griesinger, C.; Sorensen, O.W.; Ernst, R.R.; *J. Chem. Phys.*, **1986**, 85, 6837-6852.

88 Norwood, T.J.; Jones, K.; *J. Magn. Reson.*, **1993**, 104A, 106-110.

89 Evans, M.B.; Dale, A.D.; Little, C.J.; *Chromatographia*, **1980**, 13, 5-10

90 Unpublished results of Dr. P. Northcote, University of Canterbury.

Appendices

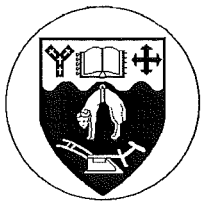

Marine Chemistry Group
University of Canterbury

Summary of assays currently in use.

THE ANTIMICROBIAL ASSAYS.

Bacteria or fungi at a known concentration are mixed with Mueller Hinton or Potato dextrose agar and poured into petri dishes so that after incubation a 'lawn' of bacteria/fungi will grow over the dish

Samples of interest are pipetted onto 6 millimetre diameter filter paper disks and their solvents evaporated.

These are then placed onto the above prepared seeded agar dishes (with appropriate solvent and positive controls) and incubated.

If the samples show any activity against the bacteria/fungi (i.e. are antimicrobial) there will be zones of inhibition outside the disk. This is measured in millimetres as the radius of inhibition and is recorded for each bacteria/fungi. A "-" in the column means no inhibition (antimicrobial activity) was detected for that bacteria/fungi.

The six organisms we currently test against are:

Bacteria-*Escherichia coli (G-ve), Bacillus subtilis (G+ve), Pseudomonas aeruginosa (G-ve).*

Fungi-*Candida albicans, Trichophyton mentagrophytes, Cladosporium resinae.*

B. subtilis and *T. mentagrophytes* are our most sensitive organisms.

THE ANTIVIRAL ASSAY

Samples of interest are pipetted onto 6 millimetre diameter filter paper disks and their solvents evaporated.

These are then placed directly onto BSC-1 cells (African Green Monkey kidney), infected with either *Herpes simplex* type 1 virus (ATCC VR 733) or *Polio* virus type 1 (Pfiser vaccine strain), then incubated.

Assays are examined after 24 hours, using an inverted microscope, for the size of antiviral (ie viral inhibition) and or cytotoxic zones, and the type of cytotoxicity.

The following scale is used for the antiviral (HSV and PV) and cytotoxicity (zone, Hcyt and Pcyt) results for *Herpes simplex* type 1 virus or *Polio* virus type 1 respectively. eg HSV, ? (Unknown due to cytotoxicity); Hcyt 3+ (10, 4 (type)); PV1, ?; Pcyt, 4+, (4).

? Unknown antiviral activity due to cytotoxicity

ND no discernible antiviral or cytotoxic effects

+- minor effects located under the disc

\+ antiviral or cytotoxic zone 1-2 mm excess radius from the disc (25 % zone)

2+ antiviral or cytotoxic zone 2-4 mm excess radius from the disc (50 % zone)

3+ antiviral or cytotoxic zone 4-6 mm excess radius from the disc (75 % zone)

4+ antiviral or cytotoxic zone over the whole well (100 % zone)

As you can imagine, sometimes it is very difficult to interpret the results when both cytotoxicity and viral effects are present in the same test well in which case a "?" is noted.

THE ANTITUMOUR ASSAY (P388)

The antitumour assay is our most sensitive assay for cytotoxicity, being up to 100 times more sensitive than the BSC-1 cells used in the antiviral assay.

For the antitumour assay a 2 fold dilution series of the sample of interest is incubated for 72 hours with P388 (Murine Leukaemia) cells. The concentration of sample required to reduce the P388 cell growth by 50 % (comparative to control cells) is determined using the absorbance values obtained when the yellow dye MTT tetrazolium is reduced by healthy cells to the purple colour MTT formazan.

The result is expressed as an IC_{50}, in ng/mL if a sample concentration has been supplied or as dilution factor

($*10^{-6}$) if a sample concentration has not been supplied. Results containing a < or > sign indicate the result is off scale and the sample needs to be retested at a lower or higher concentration.

SAMPLES FOR ASSAY

Please supply samples well labelled, in screw capped vials, either dried or in solution, with weights or concentrations listed, with solvents soluble in or the solvent used listed.

Marine samples are normally tested at 2 mg/mL, whereas some plant extracts need to be tested at 100 mg/mL.
A few samples may need to be tried to find the appropriate levels to test at.
Antimicrobial assays require a minimum of 360 µL for testing against all 6 organisms, antiviral assays require 80 µL, and antitumour assays require 40 µL.
Therefore a minimum of 500 µL at the preferred concentration is required for testing in all our assays.
1 mL or equivalent weight would be preferable to allow extra sample if assays need to be repeated etc.

For more information or to send samples please contact me.

G. Barns
Chemistry Department
University of Canterbury
Private Bag
Christchurch 1
New Zealand
Phone: (03) 3667001 ext 7416
Fax: (03) 3642110

March 92, Gill Barns

PROTOCOLS
for
CHEMICAL SCREENING

M H G Munro
Currently on leave from the University of Canterbury at the Laboratory for Drug Discovery, Research and Development (LDDRD), NCI, Frederick MD, USA.

PREAMBLE

Just as certain criteria have to be met before an extract is judged active in the initial screening, those same extracts should, in turn, be critically examined from a chemical perspective before selection for further study. Chemical screening is the chemical equivalent of biological screening and describes the process by which the physical, chromatographic and stability properties of an extract can be assessed. Chemical screening (CS) has been used routinely and very successfully for the dereplication of aqueous extracts.[37] Every effort should be made to keep procedures as simple as possible

INTRODUCTION

The POLARITY, CHARGE and SIZE of an active component in an extract can be explored by selecting sorbent phases such as C18 or DIOL, CBA or PEI and LH-20 or G-25. Depending on the choice these phases can be used with organic extracts, or with71if the selection used was C18, CBA and LH-20 then it would be possible to dispense directly from a solution of the crude extract in methanol. This avoids coating of the crude extract onto Celite with a considerable saving of time. In a similar vein, use of C18, CBA or PEI and G-25 could be used directly with aqueous solutions.

GENERAL PROCEDURE

I. Organic Samples

Preparation of Primary Standard

About 50 mg of extract are weighed out precisely and made up to 1000 µL in methanol. Withdraw 200 µL as the **primary standard.**

Preparation of Cartridges

Each cartridge needs to be pre-equilibrated with an appropriate solvent. For C18 and CBA this is by first passing 3 column volumes (3 mL) of methanol through the cartridge followed by 10 mL of the initial eluting solvent (see below). This preparation can be done under vacuum using the "Vac-Elut" system, but do not allow the cartridges to dry out. The size separation cartridges contain LH-20 and are prepared by adding 1.5 g of LH-20 to a blank cartridge, adding 4 mL of methanol, capping and shaking for a minute of two. A frit can be inserted under the liquid and pushed into place on top of the column with a glass rod. Do not trap air under the frit. Allow to drain under gravity into a vial. Wash with at least another 5 mL of methanol. Do not let the gel permeation cartridges dry out once prepared.

Loading of Cartridges

1. Carefully pipette 200 µL of the prepared solution on to the frits of the prepared LH-20 cartridge. Allow the solvent to drain under gravity for the LH-20 into the vial for the first fraction from that cartridge.
2. For the C18 first add the 200 µL of water followed by a "dollop" (~50 mg) of Celite and the 200 µL of the solution. Allow the solvent to drain under gravity into the vial for the first fraction.
3. For CBA add 200 µL of the solution followed rapidly by 80 µL of 0.05 M ammonium acetate. Allow the mixture to drain under gravity into the vial for the first fraction.

Elution of Cartridges

Add 3 mLs of the initial eluting solvent (see below) for the C18 and CBA cartridges and pull the solvent gently through the cartridge into fresh 7.4 mL vials in the "Vac-Elut". Allow the vacuum to pull the last solvent off the cartridge, but do not allow the cartridge to dry out. Repeat with each of the required solvent systems (see below) using fresh vials for each solvent change. As **ion-exchange** cartridges do not equilibrate as rapidly as the other types the slow passage of solvent is essential.

V_0 in the LH-20 **size separation** cartridge is about 2 mL. When adding the solvent, especially if you do not have a frit in place, try not to disturb the surface of the LH-20. Collect the first sample starting from the addition of the 200 µL aliquot to the top of the column. Collect 3.3 mL. (The best method is to add the sample, allow it to go on to the column, gently wash it on with 2 x 200 µL of methanol and then add

the balance of the methanol for the first fraction (2.7 mL)). The second fraction is 1.0 mL and the third is 4 mL. Even at this point there may still be colour (material?) eluting off the column. Collect a 4th fraction of 4 mL if necessary. Collect all fractions under gravity, not vacuum.

Solvent Systems

C18: 1:1 methanol/water, methanol, 1:1 CH_2Cl_2/methanol.

CBA: 4:1 methanol/ aqueous 0.05M ammonium acetate, 4:1 methanol/ 2% aqueous ammonia, 4:1 methanol/ aqueous 0.05% TFA.

LH-20: methanol.

Alternative Phases

Alternative, or additional cartridges that could be used are DIOL and Amino. For the DIOL cartridge the system is activated with CH_2Cl_2 and eluted with CH_2Cl_2, ethyl acetate and methanol. For the amino or PEI column activate with methanol as for CBA. Use the same initial solvent (4:1 methanol/ aqueous 0.05M ammonium acetate) and simply reverse the elution order of the ammonia and TFA containing solvent systems.

Removal of Solvents

Fractions can be evaporated to dryness under a stream of N_2, on a rotary evaporator, or, if available, on a vacuum concentrator (preferable). Note it is desirable to neutralise the methanolic 0.1% TFA solution by the addition of an aliquot of the methanolic 2% ammonia solution **BEFORE** concentration.

Preparation for Analysis

Each fraction is dissolved in 200 µL of methanol and assayed along with the primary standard. Suggested solvents are: C18/1; CBA/1; CBA/2; CBA/3 and LH-20/1 in 70% MeOH/water: C18/2; C18/3; LH-20/2 and LH-20/3 in MeOH. Store balance of fractions for subsequent analysis (see below).

Analysis of Results

At the LDDRD laboratory at the NCI a protocol has been developed for testing of CS fractions for anti-HIV activity. In this assay 2 µL of each fraction is submitted along with the standard in a "Sarstedt" vial. The 9 fractions and the primary standard are assayed on 1 plate over a 7 x 1:2 dilution range following an initial 1:200 dilution. This gives a top concentration of 250 µg/µL for the primary standard and as each sample has been made back up to 200 µL the "equivalent" concentration is used for each of the fractions. Dilutions are made directly into the submission vial. The results are scored by the assay lab by visual observation after a 6 day incubation and cytopathic effects as well as protection are noted using a ++, + +-, - scoring system.

Alternatively, each CS fraction could be analysed in the regular 2-drugs/plate assay. If this option is used then for each fraction that offers protection in the anti-HIV screen (EC_{50} was reached) record a +ve result. For those fractions where there was protection, but the EC_{50} was not reached, the result could be recorded as +-. For no protection note a -ve result.

Calculation of the recovery of activity in each fraction could be as follows:

$$\%\ \text{Recovery in fraction X} = \frac{100 \times EC_{50}\ \text{for primary standard}}{EC_{50}\ \text{for fraction X}}$$

At the University of Canterbury, each fraction is submitted to the P388 (murine leukaemia) assay as outlined in Appendix I.

II. Aqueous Chemical Screening

The following procedure is additional to the initial aqueous chemical screening carried out by LDDRD in the dereplication of aqueous extracts.[37] The initial procedure uses C18, a wide-pore C4 and G-25 to explore POLARITY and SIZE. The following procedure repeats the C18 chromatography and explores CHARGE by using CBA and NH_2 phases.

Preparation of Primary Standard

About 50 mg of extract are weighed out precisely and made up to 1,000 µL in water. Withdraw 200 µL as the **primary standard**.

Preparation of Cartridges

Each cartridge needs to be pre-equilibrated with an appropriate solvent. For C18, CBA and NH_2 this is done by first passing 3 column volumes (3 mL) of methanol through the cartridge followed by 10 mL of the initial eluting solvent (see below). This preparation can be done under vacuum using the "Vac-Elut" system, but do not allow the cartridges to dry out.

Loading of Cartridges

1. For the C18 first add 200 µL of the solution. Allow the solvent to drain under gravity into the vial for the first fraction.
2. For both CBA and NH_2 add 200 µL of the solution followed rapidly by 80 µL of 0.05 M ammonium acetate. Allow the mixture to drain under gravity into the vial for the first fraction.

Elution of Cartridges

Add 3 mLs of the initial eluting solvent (see below) for the C18 (aq.), CBA and NH_2 cartridges and EITHER let the solvent drain through under gravity OR pull the solvent gently through the cartridge into fresh 7.4 mL vials in the "Vac-Elut". Allow the vacuum to pull the last solvent off the cartridge, but do not allow the cartridge to dry out. Repeat with each of the required solvent systems (see below) using fresh vials for each solvent change. As **ion-exchange** cartridges do not equilibrate as rapidly as the other types the slow passage of solvent is essential.

Solvent Systems

C18: water, 1:1 water/methanol, methanol.

CBA: 0.05M ammonium acetate, 2% aqueous ammonia, 1:1 methanol/.05% aqueous TFA.

NH_2: 0.05M ammonium acetate, aqueous 0.05% TFA, 1:1 methanol/.05% aqueous TFA.

Alternative Phases

Alternative, or additional cartridges that could be used are PEI. Activate with methanol as for NH_2. Use the same initial solvent and use the same solvents as for NH_2.

Removal of Solvents

Fractions can be evaporated to dryness under a stream of N_2, by freeze-drying, on a rotary evaporator or if available on a vacuum concentrator (preferable). Note it is desirable to neutralise the methanolic 0.1% TFA solution by the addition of an aliquot of the methanolic 2% ammonia solution **BEFORE** concentration.

Preparation for Analysis

Each fraction is re-dissolved in 200 µL of an appropriate solvent and assayed along with the primary standard. Suggested solvents are: C18/1, CBA/1, and NH_2/1 in water; C18/2, C18/3, NH_2/2, NH_2/3, CBA/2 and CBA/3 in MeOH:water (1:1). Store balance of fractions for other, subsequent analyses. Each fraction and the primary standard are submitted as a 200 µL solution in a "Sarstadt" vial and assayed as noted for the organic protocol.

Analysis of Results

As for Organic Chemical Screening.

Interpretation of Results

The bioactivity data from chemical screening is most conveniently displayed as a matrix. For example:

	C18	CBA	LH-20
I			+
II	+	+	
III			

This profile established that the bioactivity was retained during chromatography and processing. Furthermore, the bioactive component(s) were cationic (retained on CBA, fraction II), of medium polarity (eluted off C18 in fraction II) and with MW >750 (fraction I off LH-20). This profile immediately indicates the best methods to approach isolation work on this extract as well as giving an insight into the chemical properties of the bioactive compound.

As a dereplication tool this combination of techniques is simple and relatively quick. Although it is ideally suited to compounds with distinctive chromophores, it can still be applied to situations where end-absorption only is observed.

An example is given below and is based on the bioactive sponge *Lamellomorpha strongylata*, worked on at the University of Canterbury. The plots shown are isoplots of the HPLC traces of the bioactive fractions from the chemical screening experiment on the extract from *Lamellomorpha strongylata*.

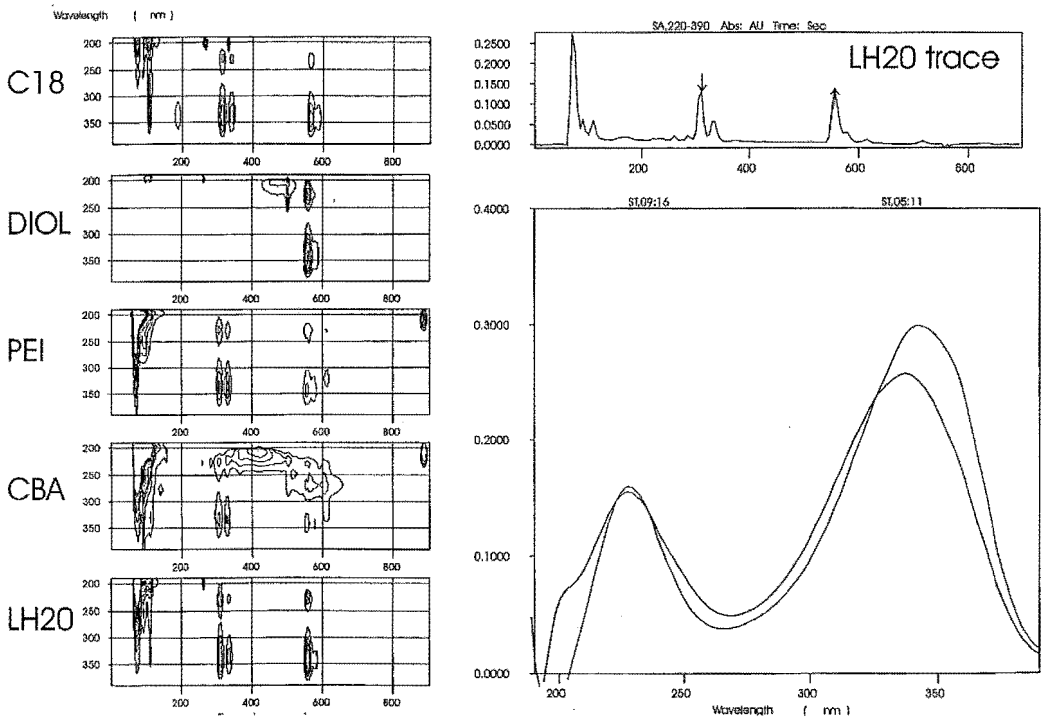

By examining the isoplots the active components (ie the components in common to all active fractions) can be located at around 300 and 600 seconds. The UV profiles are shown as is the "normal" HPLC presentation for the active fraction of the LH-20 cartridge. The UV profile allowed the active components to be quickly characterised.

Secondary Chemical Screening

In the first instance chemical screening establishes something of the chromatographic properties of a crude extract and the stability of the active(s). As shown above:

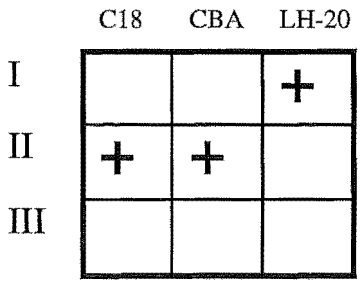

A variation on the chemical screening approach (secondary chemical screening) makes further use of the information given by the "matrix". The refinement is to passage one or more of the "active" fractions through the appropriate cartridges as indicated below.

Take an ACTIVE fraction, say C18/2 and passage it through the CBA and then take the appropriate cut (CBA/2) and passage that in turn through LH-20.

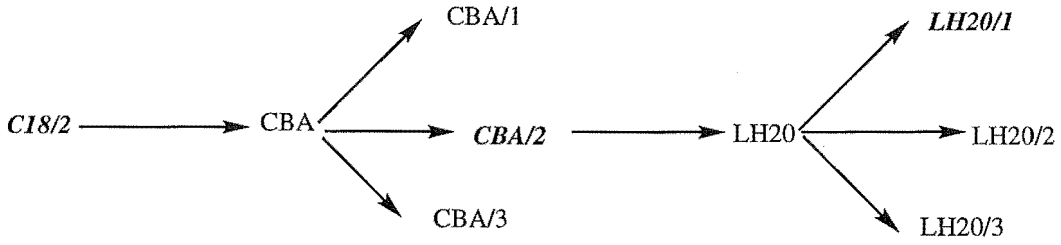

The derived fraction (LH-20/1) should be considerably "purer" and more amenable to HPLC analysis (see above). Further purification, to rapidly obtain small quantities of the active material, at a sufficient state of purity for further biological evaluation, is a distinct possibility.

Once a peak in the HPLC of an extract has been identified as the likely bioactive compound, LC/MS can be used to garner molecular weight and molecular formula data.

The emphasis at this point is NOT purification of a compound for structural elucidation, but purification to a sufficient state of purity to allow decisions to be made on the biological uniqueness of the active component.